INFORMATION TO USERS

The most advanced technology has been used to photograph and reproduce this manuscript from the microfilm master. UMI films the original text directly from the copy submitted. Thus, some dissertation copies are in typewriter face, while others may be from a computer printer.

In the unlikely event that the author did not send UMI a complete manuscript and there are missing pages, these will be noted. Also, if unauthorized copyrighted material had to be removed, a note will indicate the deletion.

Oversize materials (e.g., maps, drawings, charts) are reproduced by sectioning the original, beginning at the upper left-hand corner and continuing from left to right in equal sections with small overlaps. Each oversize page is available as one exposure on a standard 35 mm slide or as a 17″ × 23″ black and white photographic print for an additional charge.

Photographs included in the original manuscript have been reproduced xerographically in this copy. 35 mm slides or 6″ × 9″ black and white photographic prints are available for any photographs or illustrations appearing in this copy for an additional charge. Contact UMI directly to order.

Accessing the World's Information since 1938

300 North Zeeb Road, Ann Arbor, MI 48106-1346 USA

Order Number 8801705

Resonance Raman studies of visual pigments & bacteriorhodopsin

Deng, Hua, Ph.D.

City University of New York, 1987

U·M·I
300 N. Zeeb Rd.
Ann Arbor, MI 48106

PLEASE NOTE:

In all cases this material has been filmed in the best possible way from the available copy. Problems encountered with this document have been identified here with a check mark __✓__.

1. Glossy photographs or pages _____
2. Colored illustrations, paper or print _____
3. Photographs with dark background _____
4. Illustrations are poor copy _____
5. Pages with black marks, not original copy __✓__
6. Print shows through as there is text on both sides of page _____
7. Indistinct, broken or small print on several pages __✓__
8. Print exceeds margin requirements _____
9. Tightly bound copy with print lost in spine _____
10. Computer printout pages with indistinct print _____
11. Page(s) _____ lacking when material received, and not available from school or author.
12. Page(s) _____ seem to be missing in numbering only as text follows.
13. Two pages numbered _____. Text follows.
14. Curling and wrinkled pages _____
15. Dissertation contains pages with print at a slant, filmed as received _____
16. Other _____

_____

_____

RESONANCE RAMAN STUDIES OF VISUAL PIGMENTS & BACTERIORHODOPSIN

by

HUA DENG

A dissertation submitted to the Graduate Faculty in Physics in partial fulfillment of the requirements for the degree of Doctor of Philosophy, The City University of New York.

1987

The manuscript has been read and accepted for the Graduate Faculty in Physics in satisfaction of the dissertation requirement for the degree of Doctor of Philosophy.

Aug 31, 1987
Date

Chairman of Examining Committee

Aug 31, 1987
Date

Executive Officer

Prof. R. Sloan
Prof. T. Strekas
Prof. B. Honig

Supervisory Committee

The City University of New York

Abstract

RESONANCE RAMAN STUDIES OF
VISUAL PIGMENTS & BACTERIORHODOPSIN

by

Hua Deng

Adviser: Professor R. H. Callender

We have obtained the resonance Raman spectra of bovine rhodopsin, bathorhodopsin, and isorhodopsin for a series of isotopically labeled retinal chromophores. The specific substitutions are at retinal's protonated Schiff base moity and include $HC=NH^+$, $HC=ND^+$, $H^{13}C=NH^+$, and $H^{13}C=ND^+$. Apart from the doubly labeled retinal, we find that the protonated Schiff base frequency is the same, within experimental error, for rhodopsin and bathorhodopsin for all the substitutions measured here and elsewhere. We develop a force field which accurately fits the observed ethylenic (C=C) and protonated Schiff base stretching frequencies of rhodopsin and labeled derivatives. Using MINDO/3 quantum mechanical procedures, we investigate the response of the force field, and the ethylenic and Schiff base stretching frequencies, to the placement of charges close to retinal's Schiff base moiety. Specifically, we find that the Schiff base frequency should be measurably affected by a 3.0 to 4.5 angstroms movement of a negatively charged counter-ion from the positively charged protonated Schiff base moiety. That there is no experimentally discernible difference in the Schiff base frequency between rhodopsin and bathorhodopsin suggests that models for the efficient conversion of light to chemical energy in the rhodopsin to bathorhodopsin photoconversion based soly on salt bridge separation of the protonated Schiff base and its counter-ion, are probably incorrect. We discuss various alternative

models and the role of electrostatics in the rhodopsin to bathorhodopsin primary process.

We have also studied the 'Schiff base mode' in doubly labeled ($H^{13}C$=ND+) retinal chromophore in rhodopsin and bathorhodopsin in more detail. In both resonance Raman and FTIR difference spectra, the 'Schiff base mode' has different band positions in rhodopsin and bathorhodopsin, however, the two kinds of spectra suggest just the opposite assignments for this mode. We have carried out Raman and IR intensity calculations to show that both rhodopsin and bathorhodopsin have these two modes which give opposite intensity patterns in Raman and IR spectra. The intensity patterns is more sensitive to the change of the environment than the normal mode frequencies. Thus, we have a consistent interpretation for the resonance Raman and FTIR data in doubly labeled rhodopsin and bathorhodopsin, and for the data in unlabeled or singly labeled species.

We have also studied bacteriorhodopsin, which is in many ways similar to rhodopsin. The works on bacteriorhodopsin include: 1.the proton-deuteron exchange time in bacteriorhodopsin under various conditions. Our results show that the two different exchange time obtained by two different groups before probably due to different aggregation state of the sample. The effect of the aggregation suggests that this reaction is most likely diffusion controlled. 2. deionized form of bacteriorhodopsin. Our results suggest that the ion binding influences 13-cis retinal more than all-trans retinal. 3. The effort to obtain spectrally distinguishable M412 intermediate from bacteriorhodopsin has been unsuccessful. This implies that the two possible M species have their difference mainly in the protein environment.

Finally, we have probed the possibility to use SERS (Surface Enhanced Raman Spectroscopy) to study bacteriorhodopsin. We have shown that in our experiments, the electromagnetic effect in theoretical formulation of SERS is the main factor. Based on that, several possible applications are discussed.

ACKNOWLEDGEMENTS

To Professor Robert Callender the author wishes to express his sincere appreciation for the direction, valuable suggestions and encouragement given in the preparation of this thesis. His ideas have been a central and essential part of these experiments.

In addition I would like to express my special thanks to Professor J. Gersten for his valuable discussion and to Dr. C. Pande and Dr. T. Yue for their help in preparing this thesis.

The support of the entire staff of the machine shops the Department of Physics and Mr. H. Schimatz of the glass blowing shop of the Department of Chemistry have been invaluable during the course of this work.

Finally, I would like to thank my wife, Tang, Dan, for her support in preparation of this work and patience over the years.

Table of Contents

List of Tables

List of Figures

Introduction

Visual pigments and bacteriorhodopsin are two chromophore containing biological systems which have been intensively studied by resonance Raman spectroscopy (reviewed in Callender & Honig, 1977; Warshel, 1977; Mathies, 1979). During these studies several special experiment techniques have been developed such as pump-probe (Oseroff & Callender 1974), flowing and rotating cell (Callender et al., 1976; Mathies et al., 1976; Terner et al., 1978; Stockburger et al., 1979), continuous flow mixing (Doukas et al., 1981; Ehrenberg et al., 1980). These techniques combined with the isotope substitute artificial chromophore studies (Eyring et al., 1980; Curry et al., 1982; Smith et al., 1983,1984) have provided a quite good picture of the chromophore of the two systems and enhanced our knowledge about them.

The purpose of this work is to extend the resonance Raman spectroscopy to the study of the visual pigments and purple membrane systems in some more detail. As a supplementary work, the possibility of using the surface enhanced Raman spectroscopy on these systems will also be discussed.

Section I. Theoretical Background

Raman effects

In the Raman effect, the frequency of the light scattered from the sample is shifted relative to the frequency of the incident light by amounts corresponding to the molecular normal mode vibrational frequencies. Two patterns are observed, one on each side of the incident light frequency. The pattern of lines on the low-frequency side of the excitation light is termed Stokes while the pattern on the high-frequency side is termed anti-Stokes. When the incident light is in resonance with an absorption center, e. g. a chromophore of a protein, Raman effect is known as resonance Raman. The Raman cross-sections are greatly enhanced for normal modes associated with this absorption center over other protein normal modes. Thus, only Raman scattering arising from the absorption center is observed.

Since the discovery of the Raman effect (Raman and Krishnan, 1928) a considerable amount of theoretical work has been done on the Raman and resonance Raman spectroscopy (Van Vleck, 1929; Placzek, 1934; Rea 1960; Albrecht, 1961; Peticolas et al., 1970; Tang and Albrecht, 1968, 1970; Mingardi and Siebrand, 1973, 1974, 1975; Johnson and Peticolas, 1976). As the result of these works, we are able to describe the Raman and resonance Raman spectroscopy qualitatively in a simple picture shown in Fig 1.

Despite the success of the theoretical work on Raman and resonance Raman spectroscopy, a precise quantitative description is still not available today. However, several semi-empirical methods, like normal mode and their relative Raman and IR intensities calculations , have been developed to analyze the resonance Raman spectra (e.g. Tavan et al., 1985; Curry et al., 1986; Garriga et al., 1986; Kakitani et al., 1983).

In this work, the method adapted in our analysis of resonance Raman spectra of

retinal is basically from Kakitani et al (1983).The method to estimate the changes of the force field by the environment is from Rodman et al (1986).

Normal mode and internal coordinate

The most convenient terms used in the normal mode calculation are so called 'internal coordinates'. They are well defined, geometrically localized basis coordinates of Wilson et al. (1955), and are referred as C=C, C-C, C-H stretching, CCC , CCH bending, etc. Each internal coordinate is considered to have an intrinsic force constant. Couplings among such coordinates produce normal modes the normal coordinates can be expressed as the linear combination of the internal coordinates. Thus, the problem of calculating frequencies reduces to finding an appropreiate set of force constants.

Here, normal mode calculations are carried out with the force field basically adapted from that developed for polyenes by Gavin and Rice (1971), with some modifications to fit our experimental data of retinal. In order to estimate the influence of the environment on the retinal normal frequencies, MINDO/3 (modified intermediate neglect of differential overlap) is employed. This method is known for its good estimations on several aspects of real molecular systems, especially the force field of small molecules (Pullman, 1976). However, since the theoretical background is out of the range of this thesis, it is not discussed in detail here.

Raman Intensity

The total Raman intensity for the transition from an initial vibronic state m to a vibronic state n is given by

$$I_{m,n} = \frac{8\pi}{9c^4} I_0 \omega^4 \sum_{\rho\sigma} | \alpha_{m,n}^{\rho\sigma} |^2$$

where $I_{m,n}$ is the intensity of the incident light n is the frequency of the scattered light and $\alpha^{\rho\sigma}_{m,n}$ the component of the polarizability tensor. Within the Born-Oppenheimer approximation and in the resonance case, $\alpha^{\rho\sigma}_{m,n}$ is expressed by

$$\alpha^{\rho\sigma}_{m,n} = \frac{1}{h} \sum_{v} \frac{\langle gi|\mu^{\sigma}|ev\rangle\langle ev|\mu^{\rho}|gf\rangle}{\nu_{gi,ev} - \nu_0 + i\Gamma_{ev}}$$

where vibronic state $|ev\rangle$ denotes the vth vibrational level in the eth excited electronic state resonanced with the incident light, $\nu_{gi,ev}$ is the frequency difference between the indicated vibronic levels *gi* and *ev* , ν is the frequency of the incident light, Γ_{ev} the damping factor and μ the electronic dipole moment operator. The summation runs over all vibrational states on the eth electronic state.

Both theoretical and experimental works have shown that the so called Albrecht A-term is predominant term in the Raman tensor in the resonance case for retinal chromophore (Warshel and Dauber. 1975).

$$A^{\rho\sigma} = \frac{1}{h} \sum_{v} \frac{R^{ge}_{\sigma} R^{eg}_{\rho}}{\nu_{gi,ev} - \nu_0 + i\Gamma_{ev}} \langle i|v\rangle\langle v|f\rangle$$

where R is the electronic transition moment between states g and e evaluated at the equilibrium nuclear configuration of the ground electronic state and <ilv> etc represent the Franck-Condon factors.

It has been shown (Kakitani, 1979) that in a near resonance case in which the damping factor Γ can be neglected, the relative Raman intensity *I* of two modes s and t can be expressed as:

$$\frac{I_s}{I_t} \doteq \left(\frac{\Delta_s \nu_s}{\Delta_t \nu_t}\right)^2$$

where Δ_i is proportional to the equilibrium geometry shift upon excitation of the normal mode i and n_i is its vibrational frequency.

$$\Delta = 2p\,(n / h)^{1/2} dQ$$

The normal mode coordinates **Q** are given by a linear combination of internal coordinates **R** by the relation

$$\mathbf{Q} = \mathbf{LR}$$

Assuming the same transformation matrix **L** in both the ground and excited states (i. e., neglecting the Duschinsky effect), then

$$\mathbf{dQ} = \mathbf{L}\,\mathbf{dR}$$

This is the relation to be used in the Raman intensity calculations in our analysis of the resonance Raman spectra of retinal.

IR Intensity

Recently developed time-resolved and Fourier transform IR techniques have provided an additional important source of vibrational information (Bagley et al.,1982; Rothschild et al.,1983; Siebert et al., 1982). In order to understand the molecular vibration better it is desirable to compare the Raman spectra with FTIR spectra.

It is possible to measure the integrated absorption coefficient defined by

$$\int \kappa(\nu) d\nu$$

where κ is defined in

$$-dI = \kappa I\, dl$$

for the energy absorbed per unit area in unit time by a layer of infinitesimal thickness dl. The decrease in intensity of the beam, -dI, can also be expressed in terms of the Einstein coefficients B_{12} and B_{21}. The net rate of transition in unit volume from state 1 to state 2 is

$(B_{12}N_1 - B_{21}N_2)\rho(\nu) = B_{12}\rho(\nu)(N_1 - N_2)$

Each such transition reduces the energy of the radiation beam by $h\nu_{12}$ so that the decrease in intensity for a length dl with unit cross sectional area is given by

$-dI = h\nu_{12} B_{12} \rho(\nu)(N_1 - N_2)\, dl$

The radiation flux intensity and density are related by

$I = c\rho$

And B_{12} can be expressed in terms of dipole moment by (Pauling and Wilson, 1935)

$$B_{12} = B_{21} = \frac{8\pi}{3h^2}\left[|\langle 1|P_x|2\rangle|^2 + |\langle 1|P_y|2\rangle|^2 + |\langle 1|P_z|2\rangle|^2 \right.$$

Assuming the rotational and vibrational energies are separable, an summation over the rotational components leads to the following expression of the vibrational band intensity in harmonic oscillator approximation (Pauling and Wilson, 1935; Wilson et al., 1955):

$$I_k = \frac{N\pi}{3c}\left[\left(\frac{\partial P_x}{\partial Q_k}\right)^2 + \left(\frac{\partial P_y}{\partial Q_k}\right)^2 + \left(\frac{\partial P_z}{\partial Q_k}\right)^2 \right].$$

The relative IR intensity of two normal modes s and t is then given by the formula

$I_s / I_t = (\partial p/\partial Q_s)\bullet(\partial p/\partial Q_s) / (\partial p/\partial Q_t)\bullet(\partial p/\partial Q_t)$

Where **p** is the dipole moment of the molecule.

dR and charge distribution used in the Raman and IR intensity calculations can be obtained by PPP method with the parameterization developed for the retinal (Honig et al., 1976).

Surface Enhanced Raman spectroscopy (SERS)

The recent discovery of the surface enhanced Raman effects (For a review see M.

Moskovits 1985) provides a new method to look at the part of the colored system which could not be seen in resonance Raman spectroscopy. Very briefly, SERS refers to the observation that for certain molecules adsorbed on specially prepared metal surfaces a Raman spectrum is observed whose intensity exceeds by a factor of 10^5 or more than what one expects on the basis of simple calculations. Since the discovery of the SERS effect (Fleischmann et al.,1974), various explanations have been proposed to interpret the phenomena. One explanation about the phenomena which is in fairly good agreement with experiment is classical electronic theory. According to this theory, the Raman enhancement factor G after rotational averaging for molecules adsorbed on metal spheres is (McCall et al,1980; Gersten, 1980; Gersten & Nitzan, 1980, 1981; Kerker et al., 1980; Wang et al., 1980):

$$G_n = |(1 + 2g)(1 + 2g_0)|^2$$

$$G_t = |(1 - g)(1 - g_0)|^2$$

where G_n is the enhancement factor for the normal configuration (molecular dipole perpendicular to the sphere surface), and G_t is the enhancement factor for the tangential configuration (molecular dipole is parallel to the sphere surface.

$$g = \frac{\epsilon(\omega) - \epsilon_0}{\epsilon(\omega) + 2\epsilon_0}\left(\frac{R}{a}\right)^3$$

$$g_0 = \frac{\epsilon(\omega_0) - \epsilon_0}{\epsilon(\omega_0) + 2\epsilon_0}\left(\frac{R}{a}\right)^3$$

where ε_0 is the dielectric constant of the surrounding medium. ω_0 is the frequency of the incident light, ω is the frequency of the scattered light. R is the radius of the metal sphere and a is the distance of the molecular dipole from the center of the sphere.

Section II. Biological systems studied in this work

Visual pigments

The visual pigments are located in the retina of the eye, they are known as rods and cones because of their external shape. The rod consists of an inner segment that contains the nucleus and mitochondria and an outer segment (ROS) attached by a number of small fibrils. The length of the outer segment is 10-50μm and the diameter 1-6μm. Rhodopsin is located in the outer segment on the membrane of the disks. The disk membrane is composed of 40% lipid and 60% protein. Most of the protein is rhodopsin (Daemen, 1973; Papermaster and Dryer, 1974). The rhodopsin molecules have considerable freedom of rotational (Brown, 1972; Cone, 1972)and translational (Poo and Cone, 1974) movement which is temperature dependent (Blasie and Worthington, 1969). Rhodopsin is a glycoprotein of molecular weight 36000 daltons. It consists of a chromophore 11-cis retinal covalently bound to a protein called opsin via a Schiff base linkage (Lews et al., 1973; Oseroff and Callender, 1974).The protein contains a single polypeptide chain. The amino acids composition and the primary structure (amino acid sequence of rhodopsin) of the bovine opsin are known (Ovchinnikov, 1982). Some secondary structure has been proposed based on the structure of bacteriorhodopsin (Ovchinnikov, 1982).

The 11-cis retinal (Fig 2c) is the chromophore of the rhodopsin. It has an absorption band centered at 498nm. Absorption of a photon isomerizes the chromophore (Wald, 1968), and initiates a series of intermediates (Fig. 3) leading to the detachment of chromophore from the opsin. This process is called bleaching because pigments absorb in the visible while the final product, retinal and opsin, absorb in the UV. An artificial pigment, called isorhodopsin, which contains 9-cis retinal (Fig 2d) as a chromophore follows the same bleaching sequence upon absorption of light.

The first intermediate bathorhodopsin (also known as prelumirhodopsin; Yoshizawa and Wald, 1969), is formed photochemically from rhodopsin in less than 6psec (Busch et al, 1972; Monger et al, 1979). Bathorhodopsin (λmax =543nm) is red shifted from rhodopsin (λmax = 497nm). At temperature lower than 130K, rhodopsin, isorhodopsin and bathorhodopsin can be photochemically converted to each other (Yoshizawa and Wald, 1969). Low temperature calorimetry has shown that 60% of the incident photon energy (about 35 kcal/mole)is stored in bathorhodopsin (Cooper, 1979).

The primary photochemical event in vision, the photochemical formation of bathorhodopsin, is commonly believed to involve a cis-trans isomerization of the retinal chromophore, based on the liquid nitrogen temperature absorption studies (Hubbard and Kropf, 1958; Yoshizawa and Wald, 1963) and supported by the resonance Raman studies (Callender and Honig, 1977; Aton et al., 1980; Eyring et al., 1980). The Raman data suggests that the all-trans retinal (Fig 2a) chromophore in bathorhodopsin could be twisted.

One of the interesting questions related with the primary event is how to interpret the energy storage and the red shift of the absorption in the transition by a self-consistent model.One of the model suggests that isomerization of the chromophore is a concerted rotation about two double bonds, the 11-12 and 15-16, in a 'bicycle pedal' motion (Warshel, 1976). This model, however, predicts that the energy of bathorhodopsin is only 5 kcal/mole above that of rhodopsin, rather than 35 kcal/mol observed. Additionally, it predicts an efficient photochemical path from isorhodopsin to rhodopsin and allows the reverse process. Neither reaction is known to occur since it is well established that both interconversions occur only via bathorhodopsin as a common photointermediate (Yoshizawa and Wald, 1963).

Another model is that the steric constraints due to the opsin force the retinal in

bathorhodopsin into a conformation that is twisted about one or more double bonds (Kakitani and Kakitani 1975). Since the intrinsic barrier to isomerization about double bonds is about 25kcal/mole (Hubbard,1960), such mechanism could account for large part of the energy stored in bathorhodopsin. Furthermore since twisting about double bonds is known to produce red shifts (Honig et al., 1976; Kakitani and Kakitani 1975), it also results in the required red absorption shift. The difficulty of this model is that to conceive of a stable conformer that is significantly twisted, even at low temperature. The analysis of Raman spectra of bathorhodopsin suggests only small angle twists (Erying et al., 1980), which can contribute only part of the 35kcal/mole energy.

Finally, a point charge model suggests that C11=C12 isomerization flips the C=NH+ moity away from its protein counterion into a hydrophobic region of the chromophore binding site (Honig et al., 1979). The estimated energy storage as electrostatic energy could be more than 20 kcal/mole. The separation of the counterion also cause the proper red shift based on the PPP calculation (Kakitani et al., 1985). However, this model would intuitively require that the Schiff base (C=N) mode frequency would change significantly upon separation of the counterion from the Schiff base moity in the rhodopsin-bathorhodopsin transition. Raman data shows that the C=N bands are at about the same position in rhodopsin and bathorhodopsin Raman spectra (Erying and Mathies., 1979; Aton et al., 1980). An important theme in this work is to explore the question both experimentally and theoretically.

After bathorhodopsin formation, lumirhodopsin, metarhodopsin I and metarhodopsin II are formed thermally, this is shown in Fig.3. Very little is known about lumirhodopsin. Resonance Raman studies indicate that the Schiff base linkage remains protonated in the metarhodopsin I intermediate, and that the proton is released during the meta I - meta II conversion and the retinal chromophore in meta I is relaxed all

trans (Doukas et al., 1978; Aton et al., 1980). The study of kinetics of meta I - meta II conversion shows a large change of entropy (Matthews et al., 1963). Such facts have been correlated with the neural activity.

Bacteriorhodopsin

Halobacterium halobium is one of a number of halophilic bacteria that is stable in a highly saline environment (for a general review, see Stoeckenius and Bogomolni, 1982). When the oxygen supply to the organism is cut off, it synthesizes purple patches on its normally red membrane. By lowering the ambient salt concentration from 4.3M (the growth concentration), the cells can be fragmented and the purple membrane can be isolated (Becher and Cassim, 1975).

The bacterium itself is rod-shaped, about .5μm in diameter and 5μm long. The purple patches can account for up to 50% of its red membrane under anaerobic conditions. X-ray studies have shown that the purple membrane is a locally differentiated but nevertheless contiguous part of the cell membrane (Blaurock and Stoeckenius, 1971). The red color of the oxygenated bacterium is due to the presence of carotenoid bacterioruberin. The purple color of the sythesized patches is caused by a retinal chromophore covelantly linked to the sole protein on the purple membrane. Because a similar chromophore is found in the visual pigment rhodopsin, the protein on the purple membrane has acquired the name bacteriorhodopsin.

X-ray diffraction and electron microscopy studies reveal that each purple membrane patch consists of a rigid, highly ordered, two-dimentional hexagonal lattice structure of about 10^5 molecules with a 63 angstroms cell dimension. The protein molecules, known as bacterio-opsin, are arranged as trimers clustered about a symmetry axis in the unit cell (Blaurock and Stoeckenius, 1971; Henderson, 1975). A hexagonal arrangement is considered to be the most efficient way to closely pack helical molecules with regard to space. The bacterio-opsin is composed of 248 amino acids with a molecular weight of 26000 daltons, arranged in 7 α-helical segments that span the width of the membrane (Herderson and Unwin, 1975). The amino acid sequence of bacterio-opsin has also been

determined (Ovchinnikov et al., 1977,1979; Khorana et al., 1979).

The retinal chromophore is located within the hydrophobic interior of the protein (Kouyama et al., 1983)attached to the ε-amino group of lysine 216 (Rothschild et al., 1982) via a protonated Schiff base linkage (Lews et al., 1974). The retinal chromophore exists in two forms in the purple membrane, as evidenced from absorption spectra and chemical extraction. The dark-adapted form of bacteriorhodopsin contains a 1:1 mixture of all-trans and 13-cis retinal and has absorption maximum 558nm.When it is illuminated with green-yellow light, the dark adapted form converts to light adapted form which contains only all-trans retinal and has absorption maximum 568nm (Sperling et al., 1977; Ohno et al., 1977; Maeda et al., 1977).

When the light adapted form of purple membrane absorbs a photon, it goes through a series of intermediate stages before cyclically returning to its original form (Fig 3). The first product of this photoreaction, called K, is formed on a picosecond scale photochemically, while the whole cycle is completed thermally in about 10msec (Lozier et al., 1975). Associated with the absorption of light is the pumping of a proton across the cell membrane which is used in ATP phosphorylation and for other energy related cell functions (Oesterhelt and Stoeckenius, 1973; Oesterhelt, 1972; Danon and Stoeckenius, 1974). Most biological pumps are multicomponent systems with complex structure (Stoeckenius et al., 1979). Bacteriorhodopsin is a notable exception. A detailed understanding of the structure of the intermediates in the bR cycle would contribute a great deal towards the understanding of membraneous pumps.

Of all the known intermediates in the photocycle, M412 is the only species which contains an unprotonated Schiff base linkage to the protein (Lews et al., 1974; Aton et al., 1977). The conversion from L-> M species has also been associated with the pumping of proton (s) (Lozier et al., 1975; Li et al., 1984). Flashphotolysis studies of

bacteriorhodopsin have shown that the decay of M412 is biphasic (Hess and Kuschmitz, 1977; Ort and Parson, 1978).

Other intermediates like K and L contain protonated Schiff base linkage and have 13-cis chromophore conformation (Pande et al., 1981; Brainman and Mathies, 1982; Argade and Rothschild, 1983; Smith et al., 1984). The intermediate after M is O, which has an all trans conformation and is protonated Schiff base (Smith et al., 1983). These observations as well as the theoretical studies lead to the suggestion that there should be two different unprotonated Schiff base species with different chromophore conformations. However, there is no explicit experimental evidence to support this suggestion.

Recently, it has been discovered that 3-4 Ca^{++} and Mg^{++} are bound to bacteriorhodopsin. When these cations are removed from purple membrane by any of a variety of methods, the membrane turns blue with the absorption maximum of about 600nm (Kimura et al., 1984; Chang et al., 1985). The photocycle of the blue membrane is not the same as purple membrane, and its function as a proton pump also stops.

Section III Experimental Techniques

Photolability Problem and special methods

The use of resonance Raman spectroscopy on these two biological systems has a major complication. Since the exciting light is in resonance with a particular color center, the sample absorbs almost all of the light. For example, it has been reported that the Raman scattering cross-section of the most intense Raman line of rhodopsin (the C=C ethylenic mode) measured with the 568.2nm line of the krypton laser is about 8×10^{-26} cm^2/mol-sr (Callender et al., 1976). This is more than eight orders of magnitude smaller than the absorption cross-section at the same wavelength. Thus, under typical conditions of a few milliwatts of laser light focused on the sample, each pigment complex absorbs a photon every millisecond or less, while the Raman measurements take several minutes even hours to complete. Since light initiates a series of temperature dependent transformations of the pigment, the very attempt at taking a Raman spectrum of a pigment immediately causes replacement of the pigment with a quasi-photostationary mixture of several different species. Special techniques, therefore, must be used to permit Raman work on such photolabile systems.

'Pump and probe' method.

At 130K or below, however, laser irradiation produces a photostationary state containing only of rhodopsin, isorhodopsin, and bathorhodopsin in visual pigment or bacteriorhodopsin and K in purple membrane. The relative concentration of the components depend on the wavelength of the incident illumination. The first experiment to control the effect of photolability of visual pigments was that of Osceroff and Callender (1974) in their study of bovine rod outer segment vesicles at liquid nitrogen

temperatures. Two laser beams were used simultaneously, one acting as a 'pump' to modify the photostationary state of the sample and the second at a different wavelength and weaker in intensity acting as a 'probe' to excite the Raman scattering, The exact sample composition of rhodopsin, isorhodopsin and bathorhodopsin for each pump wavelength was assayed by using well developed techniques of absorption spectroscopy. Thus, all factors, including the resonance enhancement factors for various Raman lines, were held constant, except, of course, for sample composition. This technique was used to obtain rhodopsin, isorhodopsin and bathorhodopsin with natural or artificial chromophore in this work. A more detailed discussion of using this method will be given in experiments section.

Flowing sample and spinning cell.

Another method which eliminates problems associated with photolability for samples in solution was independently developed by Mathies et al. (1976) and Callender et al. (1976). The method involves flowing the sample through the irradiating laser beam so fast that a molecule traveling through the beam has little chance of absorbing a photon and, hence, of initiating any photochemistry, The sample in the laser beam absorbs light and thus becomes 'bad' sample, but this is swept out and replaced by starting sample, before it has an opportunity to accumulate to the extent it becomes an appreciable component of material in the laser interaction area. One draw back of the flow technique is that it requires a substantial amount of sample in the system and hence this method was not routinely used. An alternative method, the spinning cell, was used for many experiments in this work since the essential goal of flowing sample is to move sample in and out of the laser beam quickly. However, the experimental conditions must be such that sample, after its photochemistry is initiated in the laser interaction area, has

completed one cycle and in its original form when it arrives at the laser interaction area again. Therefore, the spinning cell technique is ideal for the study of bacteriorhodopsin and its intermediates (Ref. Fig 4).

Kinetics of Mixed reactants.

The time evolution of two reacting systems, for example, the exchange of a proton of the protonated Schiff base for a deuteron, can be monitored by Raman spectroscopy. Two reactants are mixed rapidly via two jets meeting at a mixing chamber. The mixed sample exits through a capillary tube, the exit flow speed and the position of the focused Raman exciting laser beam control the time at which the reaction is monitored after the reaction begins.

Instruments

The Raman spectra were obtained with one or the other of two spectrometers. One spectrometer consists of a 1401 Spex double monochromator, a cooled RCA 31034 photomultiplier tube and a photo counting electronic apparatus interfaced to a LSI-11 computer. The double monochromator was controlled by a CD2A control board (Spex) which was also interfaced to LSI-11 computer. The other spectrometer consists of a triplemate spectrometer (Spex 1877) and a cooled solid state detector (EG & G Princeton Applied Research Model 1420-2) with a multichannel detector controller (EG & G Princeton Applied Research Model 1218). This multichannel Raman system, interfaced to LSI-11 computer, can collect data simultaneously in about 700 pixels. The data are obtained by using the operating system developed in this lab and stored on the floppy disks.

The absorption spectra were obtained with a GCA Mcphersoon UV-VIS spectrometer, which is interfaced with a PDP-8e computer for data collection. The data were then transferred to LSI-11 computer for manipulation and storage.

A Coherent Radiation model CR2000 and a 52B krypton ion laser and a Spectra-Physics model 165 argon ion laser were used to produce the monochromatic excitation of the samples. The available wavelengths span the range from the UV (323.7nm) to the red (676.4nm). The laser beam was diffracted on a grating to separate the discharge lines and the first order diffracted beam was used to excite the sample. A right angle scattering geometry was used. Power levels were measured before the sample with a calibrated thermopile (Eppley Laboratories, Newport, R. I.).

Low temperature Raman spectra were taken using a home-built nitrogen cold finger dewar connected to the end of a flexible nitrogen/helium transfer line LT-3-110 (Air Products and Chemicals, Allentown, Pa.). The sample was deposited in a concave

depression in a temperature controlled copper sample holder arranged for 90 degree scattering from the surface of the sample. The holder was cooled by a continuous stream of liquid nitrogen or the gas evaporated from it. Temperature in the holder could be set between 80K to 273K and maintained within 1K of the set temperature, which was monitored with a thermistor.

The double monochromator was calibrated with the known krypton or argon laser lines. The wavenumber scales of the spectra obtained from triplemate spectrometer were calibrated against the known Raman lines from toluene. The accuracy of the line assignments and the resolution of the spectra were different for each experiment and in the range of 2-3 cm^{-1} for accuracy and 6-11 cm^{-1} for resolution.

Section IV . Raman experiments

1. A Schiff Base Study of Bovine rhodopsin and Bathorhodopsin.

When rhodopsin, the visual pigment protein, absorbs a photon, a species called bathorhodopsin is formed photochemically. About two-thirds of the photon's energy is converted to chemical energy in the rhodopsin to bathorhodopsin conversion (Cooper, 1979). A model was proposed (Honig et al., 1979) to understand the energy conversion as well as the red shift of the absorption maximum and the 11-cis to all-trans retinal chromophore isomerization (see Section II for more detail). The essential feature of this model was the movement of the positively charged Schiff base through space against an electrostatic field. Specifically proposed was the separation of the positively charged protonated Schiff base moiety from a nearby hydrogen bonded negatively charged counter-ion. This charge separation was presumed to be the consequence of retinal's photoisomerization. Taking Coulomb's law and assuming reasonable values for the partial charges on the Schiff base and its counterion and the separation distance that could occur between the protonated Schiff base and its counter-ion in an 11-cis to all-trans isomerization, it was shown that a large fraction of the absorbed photon's energy could be converted to chemical energy in this mechanism.

The results of resonance Raman spectroscopy, aside from confirming and characterizing the retinal 11-cis to all-trans photoisomerization, is that the stretching frequency of the protonated Schiff base moiety, -HC=NH+, is essentially the same for rhodopsin and bathorhodopsin and their deuterated derivatives. These results suggest, qualitatively, that the environment of the protonated Schiff base is similar in rhodopsin and bathorhodopsin. This appears to be inconsistent with a simple charge separation model since it might be expected that the protonated Schiff base counter-ion charge

separation would affect substantially the frequency of the protonated Schiff base stretching frequency.

The goal of this study is to examine such qualitative concepts more thoroughly, both experimentally and theoretically. To probe whether or not rhodopsin's and bathorhodopsin's Schiff base mode is "accidentally" at the same frequency, we have obtained the resonance Raman spectra of bovine rhodopsin, bathorhodopsin, and isorhodopsin for a series of isotopically labeled retinals. The retinals used in this study are labeled at retinal's protonated Schiff base moiety and include -HC=NH+, -HC=ND+, -H^{13}C=NH+, and -H^{13}C =ND+. Apart from the doubly labeled retinal, we find that the Schiff base frequency is the same for both rhodopsin and bathorhodopsin.

In order to assess which factors play a role in determining the position of the protonated Schiff base stretching frequency, we develop a force field which fits the observed ethylenic (C=C) and protonated Schiff base stretching frequencies of rhodopsin and its labeled derivatives. Apart from the doubly labeled derivatives, the protonated Schiff base mode is shown to be fairly well localized to the Schiff base moiety. It is composed principally of C=N stretch and C=N-H bending motions. Thus, the protonated Schiff base frequency should be sensitive to the changes around this end of the retinal chromophore.

By using previously developed (Rodman et al., 1987) quantum mechanical procedures, we estimate the changes on our force field produced by moving a counterion away from the protonated Schiff base moiety from 3.0 to 4.5 angstroms. The 3.0 angstroms separation corresponds to the charge separation at the protonated Schiff base in rhodopsin as given in Honig et al. (1979), and the 1.5 angstroms change has been calculated to be capable of yielding the observed change in absorption maximum of rhodopsin to bathorhodopsin. We find that a protonated Schiff base counter-ion charge

separation from 3.0 to 4.5 angstroms would have certainly measurable effects on the frequency of the Schiff base mode. That no change occurs in the Schiff base stretching frequency when rhodopsin transforms to bathorhodopsin thus suggests that the simplest electrostatic model for energy transformation in visual pigments is probably incorrect.

Methods

Bovine rod outer segments were prepared according to the method of Papermaster and Dreyer (1974), and the opsin was prepared according to the method of Ebrey (1982). The ^{13}C substituted C15 11-cis retinal and the regenerated pigment were prepared according to the method of Bragley et al. (1985). These samples were provided by Nakanishi's group in Columbia University. Deuteration of the Schiff base nitrogen was achieved by concentrating the appropriate visual pigment to a pellet by centrifugation and resuspension in D_2O.

The low temperature set up was used for this experiment. The resonance Raman spectra were recorded by the multichannal detector described earlier. As described in detail by Oseroff and Callender (1974), and Aton et al. (1980), the essential feature of the experimental procedure is to stimulate the Raman scattered light with a fixed single wavelength (the 'probe' beam), while simultaneously irradiating the sample with a second spatially overlapping laser beam (the 'pump' beam), whose wavelength and power can be varied. Below 130K, irradiating with visible light drives the sample to a photostationary mixture of rhodopsin, isorhodopsin and bathorhodopsin. The equilibrium composition is determined by the irradiating light frequency. The probe beam used was 488.0nm line from an argon ion laser. The pump beams were 568.2nm and 647.1nm lines from a kripton ion laser. For each sample, three Raman spectra were taken. The first was a probe only spectrum; the second was a probe with 568.2 nm

pump with a pump/probe ratio of 30:1; and the third was a probe with a 647.1 nm pump with pump/probe ratio of 100:1. This results in a set of three spectra of varying photostationary state rhodopsin, bathorhodopsin, isorhodopsin mixtures.

The sample composition of the three pump/probe experimental configurations was determined as follows. The rhodopsin, bathorhodopsin, isorhodopsin composition has been determined previously by Suzuki and Callender (1981) for singly line excitation at 488.0nm (and other frequencies). The bathorhodopsin spectrum contains unique marker bands at 856, 877, and 920 cm^{-1}. Thus the relative amount of bathorhodopsin in the 488.0/568.2 and 488.0/647.1 experiments could be determined by measuring the relative sizes of the bands to the 488.0m, probe only experiment. The rhodopsin spectrum contains a unique (but small) band at 845 cm^{-1} while that of isorhodopsin contains one at 830 cm^{-1}. The relative intensity of those two bands was used to estimate concentrations of rhodopsin and isorhodopsin. Using the approximate concentration so obtained, the appropriate spectra additions and subtractions yielded spectra which were very close to but not identical to the previously published spectra of rhodopsin, bathorhodopsin and isorhodopsin. This is probably due to the slight inaccuracies, estimated to be + 5%, in the compositional results of Suzuki and Callender (1981) and in the difficulty of determining accurately the magnitude of the 845 and 830 cm^{-1} bands. however, using this set as a trial set of compositions we then made small (up to 5%) adjustments in the composition until we obtained the spectra of rhodopsin, bathorhodopsin and isorhodopsin identical to the previously published results. The concentration of the three species, respectively, were found to be 34% (rhodopsin)/50% (bathorhodopsin)/16% (isorhodopsin) in the 488.0 experiment, 31/8/63 in the 488.0/568.2 experiment, and 58/18/26/ in the 488.0/647.1 experiment. We make the assumption that the photochemical quantum yields of interconversion between the three species is unaffected

by isotopic substitution. We thus use the same mixture ratios in calculating the isotopically labeled species spectra. Suzuki and Callender (1981) have shown that deuteration has little effect on the quantum yields.

Results

The spectral region between 1100 cm^{-1} and 1400 cm^{-1}.

This region contains the C-C stretching and H bending modes which are sensitive to the configuration of the retinal Schiff base (Callender et al., 1976; Mathies et al., 1977; Cookingham et al., 1978). The sensitivity to retinal configuration is very evident by contrasting the rhodopsin (Fig. E1-1a, 11-cis), bathorhodopsin (Fig. E1-2a, distorted all-trans), and isorhodopsin (Fig. E1-3a, 9-cis) data. Normal mode calculations have shown that for protonated Schiff bases having a C=N anti configuration the C14-C15 vibrational mode is expected to shift only a few wavenumbers upon medium deuteration, whereas for the C=N cis configuration this vibrational mode would shift to higher wavenumber by about 60 cm^{-1} (Smith et al., 1984). Our Raman spectra of regenerated pigments with ^{13}C substitute C15 retinal can be used to identify the C14-C15 mode and then the deuterated effects on this mode would enable us to determine the C=N configuration. Several lines in this region in the resonance Raman spectrum of rhodopsin are changed in the ^{13}C substitute C15 retinal pigment (Fig E1-1). The 1191 cm^{-1} band in the native rhodopsin shifts down 5 cm^{-1} to 1186 cm^{-1} in the rhodopsin spectrum of regenerated pigment. The shoulder at about 1208 cm^{-1} disappears. These two changes happen in both H_2O and D_2O suspensions. The 1240 cm^{-1} band, which appears as a shoulder in D_2O suspension shifts down 9 cm^{-1} to 1231 cm^{-1} upon ^{13}C substitution. These observations suggest that C14-C15 stretching contributes to at least 3 bands in this region. The deuteration effects in native rhodopsin is the intensity decrease of the 1240

cm^{-1} band, and the shoulder at the lower side of the 1240 cm^{-1} band becomes a major band at about 1334 cm^{-1} upon deuteration, but there is no apparent intensity increase in the other bands. The deuteration effects in ^{13}C substituted rhodopsin is the intensity increase of the 1186 cm^{-1} band, but there is no apparent intensity decrease in the other bands. These changes do not follow either the C=N cis or the C=N anti pattern. We think the reason is that C14-C15 stretching is strongly coupled with other C-C stretching and H in plane bending vibrations so that it is no longer appropriate to assign one band as a C14-C15 stretching mode. Therefore the simple pattern which worked in the case of bR and its intermediates is not valid in the case of rhodopsin.

However, in the bathorhodopsin spectrum, the change upon ^{13}C substitution at C15 is very simple (Fig 3). The band at 1209 cm^{-1} splits into two bands at 1209 cm^{-1} and 1198 cm^{-1} in both H_2O and D_2O suspensions. Therefore it can be assigned to C14-C15 stretching. Since this band does not shift upon deuteration in native and regenerated pigments, the C=N configuration should be anti. The same argument also applies to isorhodopsin (Fig 4). The C14-C15 mode mainly contributes to the 1206 cm^{-1} band because only this band shifts down to 1193 cm^{-1} in ^{13}C substitute retinal pigment. No deuteration effect observed on this band suggests that the C=N configuration in isorhodopsin should also be anti.

Another deuteration effect in isorhodopsin spectrum is the split of the 1152 cm^{-1} band into 1142 cm^{-1} and 1152 cm^{-1} bands. According to the normal mode analysis of 9-cis retinal by Curry et al (1986), the 1152 cm^{-1} band has contributions from C10-C11 stretching, C9-methyl bending and 11H bending but not from NH bending motion. So this unexpected splitting may be due to the increased coupling between the bonds in the Schiff base moiety in the opsin environment comparing to the retinal Schiff base in solution. Because of the coupling, the ND bending or N-C stretching may have

contribution to the 1142 cm^{-1} band observed in deuterated medium.

The spectral region between 1500 cm^{-1} and 1700 cm^{-1}

In this region, the C=C and C=N stretching vibrations make the largest contributions. There are five C=C and a C=N bonds in the conjugated Schiff base moiety so that a total of six bands in this region may be observed. Six bands are, in fact, observed in the Raman spectrum of rhodopsin (Fig E1-1). The 1657 cm^{-1} band has previously been assigned to the protonated Schiff base stretching mode based on its shift to 1625 cm^{-1} upon deuteration of the protonated Schiff base. This result is seen in Fig E1-1c. The 1657 cm^{-1} band moves to 1645 cm^{-1} in the $H^{13}C$ =NH+ rhodopsin given in Fig E1-1b and to 1609 cm^{-1} in the $H^{13}C$ =ND+ rhodopsin in Fig E1-1d. It is of interest that rhodopsin's 1582 cm^{-1} band (Fig E1-1a) shifts to 1572 and 1567 cm^{-1} for the -HC=ND+ and -$H^{13}C$ =ND+ substitutions respectively. This indicates that this mode either (1) contains a substantial amount of C=N stretch or N-H bend and/or (2) is strongly coupled to the Schiff base so that a substantial down shift in the 1657 cm^{-1} results in a downward shift in the 1582 cm^{-1} mode.

Table 1 summarizes the position of the Schiff base mode in rhodopsin, bathorhodopsin, and isorhodopsin for the various isotopically labeled pigments which have been mearsured, both here and ealswhere. We have included results from other studies which have examined the -DC=NH+ and the -DC=ND+ pigments, bacteriorhodopsin, and all-trans protonated Schiff base of retinal in two solvents, methyl alcohol and dichloromethane. The remarkable feature of the data in this table is the essentially identical position of the Schiff base frequency for rhodopsin and bathorhodopsin in the singly labeled derivatives. It is only the doubly labeled (-$H^{13}C$ =ND+ and DC=ND+) pigments where rhodopsin and bathorhodopsin differ in labeling

behavior. We shall show below that the band we have identified as the Schiff base mode is almost certainly very delocalized in these doubly labeled derivatives and is no longer appropriately called a 'Schiff base' band. The reason for this appears to be that the frequency of the C=N moiety is reduced to such an extent upon double labeling that a great deal of mixing with the ethylenic C=C motions occurs. We presume that the most likely reason for the differences between rhodopsin and bathorhodopsin in the doubly labeled compound results from the different C=C force constants and coupling constants in the two pigments. Such differencies can result in the different Raman or IR intensity patterns even if the two pigments have similar normal mode frequencies. Such possibility will be explored in some detail in the calculational work below.

We may contrast the data of rhodopsin and bathorhodopsin with that of the model compounds. All-trans protonated Schiff base in methanol, for example, has a Schiff base frequency at 1656 cm^{-1}, the same as rhodopsin and bathorhodopsin. However, the response of this mode for the protonated Schiff base in methanol to isotopic substitution is very different than for rhodopsin and bathorhodopsin. Moreover, there are pronounced solvent effects on the Schiff base frequency and its response to labeling when we compare the all-trans protonated Schiff base in the polar methanol and non-polar dichloromethane. Apart from the HC=NH data, the frequency of the Schiff base mode is different for the two solutions for all the other isotopes.

It is interesting to compare our resonance Raman data of bovine rhodopsin and bathorhodopsin with the FTIR data. Bagley et al (1985) obtained FTIR difference spectra of bathorhodopsin and rhodopsin for the same pigments we used. Their results showed a consistent picture with our Raman data except those with the doubly labeled $H^{13}C$ =ND+ pigment (bathorhodopsin-rhodopsin), in which there is a positive peak (due to bathorhodopsin)at 1610 cm^{-1} and a negative peak (due to rhodopsin)at 1602

cm^{-1}. Since there are no such peaks in the difference spectra from native pigments or from the $H^{13}C$=NH+ pigment, they assigned the 1610 cm^{-1} peak to the Schiff base mode for bathorhodopsin and the 1602 cm^{-1} peak to the Schiff base mode for rhodopsin. This fact was used to support the simple point charge model and raise the possibility that the charge separation may change the force constants of the molecule in such a way that the net change in Schiff base frequency in some cases could be canceled.

There is no easy assignments in our Raman spectra of $H^{13}C$=ND+ pigment for the Schiff base mode. But in the spectrum of $H^{13}C$=ND+ rhodopsin there are two bands at 1599 cm^{-1} and 1609 cm^{-1} (Fig E1-1d), whereas there is one band at 1598 cm^{-1} in the $H^{13}C$=ND+ bathorhodopsin (Fig E1-3d). If we subtract the rhodopsin spectrum from bathorhodopsin spectrum, there would be a negative peak at 1609 cm^{-1}, which is due to rhodopsin, and probably a positive peak at 1600 cm^{-1}, which is due to bathorhodopsin. Then the assignment would be just the opposite to the FTIR experiment. Our theoretical work below will hopefully provide an explanation about this apparent discrepancy.

Force field derivation

Our goal in this section is to obtain a reasonable force field that describes the rhodopsin data. We are mainly interested here in the response of the HC=NH+ stretching frequency to various isotopic substitutions. Since we expect this mode to couple with ethylenic C=C stretches, we obtain a force field which accurately describes these modes and their response to labeling.

The force constant field was obtained by adapting a set we have previously derived (Kakitani et al., 1983). This set of force constants very accurately calculates the frequency of the Schiff base in its change upon deuteration. However, in order to reproduce the ethylenic frequencies and their changes upon various isotopic

substitutions, the following modifications were made. The C=C and C-C stretching force constants were not kept all the same but were changed according to their bond orders obtained by the PPP method (Kakitani et al., 1983; 1985). The C=C,C=C and C-C,C-C coupling constants were decreased from -0.1 to -0.15mdyn/A; the C=C,C-C coupling constants were increased from 0.3 to 0.35 mdyn/A; and the C=C,C-C next next neighbors coupling were increased from 0.0 to 0.15 mdyn/A. While these minor changes could reproduce the data for native rhodopsin and ^{13}C 15 in H_2O and D_2O very well, the rather large shifts in C=C frequencies observed in cases of deuteron labeling of retinal' carbons (Eyring et al., 1982; Bagley et al., 1985) were not observed. For example, the major rhodopsin ethylenic band shifts downward by 10 cm^{-1} for 15D substituted rhodopsin; other shifts in the major ethylenic frequency are observed also in 11D, 12D, 14D rhodopsins (Eyring et al., 1982). These shifts suggest that significant couplings exist between C=C stretching and C-H in plane bending motions. We introduced these coupling constants into our force field and adjusted their values to fit the available data. The complete set of force constants and the normal mode frequencies and associated eigenvectors in the 1500-1700 cm^{-1} range are given in the supplementary material. The root mean square deviation between the calculate and observed ethylenic and Schiff base frequencies is 2.5 cm^{-1}, and the maximum deviation is 6 cm^{-1}.

Table 2 shows the experimental band positions in the 1500-1700 cm-1 region for rhodopsin and labeled derivatives, and the calculated normal mode frequencies. The table also shows the contributions to each mode by the five C=C ethylenic stretching internal coordinates and the C=N Schiff base internal coordinate. The 1636 cm^{-1} mode is little affected by any of the substitutions and is quite localized to motion of the C5=C6 bond. The other four C=C modes are delocalized to varying degrees along retinal's polyene chain. The Schiff base mode is quite localized in rhodopsin to the Schiff base moiety.

However, this mode becomes more delocalized in the isotopically labeled rhodopsins. Roughly, the mode become more delocalized as the frequency decreases. Intuitively, this behavior seems correct as coupling between a purely C=N stretch would increase as their frequencies become more equal. This behavior is demonstrated by comparing the singly and doubly labeled rhodopsins. The 'C=N mode' in the singly labeled rhodopsins have a contribution from motion extending to the C11=C12 stretch. In the doubly labeled, $H^{13}C$ =ND+ rhodopsin, the mode extense to C7=C8, very highly delocalized indeed. Moreover, all five C=C modes have a significant C=N contribution for the doubly labeled rhodopsins. Although not shown in table 2 but contained in the supplementary material, all the ethylenic and C=N modes contain significant C-H or N-H bend.

We wish to emphasize that the force field derived above is not unique. There are a larger number of internal coordinates and related force constants than independent data used for the fitting. For example, we found that a force field differing from the field defined above in the C11=C12, C13=C14, C15=N stretching force constants by about 10%, the C14-C15, C15=N and C13=C14, C15=N stretch-stretch coupling by about 75%, and the C15=N, C=N-h stretch-bend coupling by about 10% would equally well reproduce the experimentally observed frequencies. The exact values for this second force field are given in the supplementary material and the normal modes and the contributions from C=C, C=N bonds are given in table 4. the complete eigenvectors are given in the supplementary material. While these changes in the force field are not very large, the motions of the normal modes obtained from the second force field can differ substantially from the first force field in many cases. For example, the 1657 cm^{-1} Schiff base mode would be predicted to contain a significant contribution from C13=C14 (-0.13 for C13=C14 and 0.30 for C15=N) using this second force field.

Our purpose here is not to obtain an exact force field. It is unclear to us whether this

is even feasible. Our central goal here is to understand how a force field responds to closeby point charge and how, specifically, the frequency of the Schiff base would respond, if at all, upon changes in the position of close point charges. This is accomplished by using our approximate force field, derived above, as following.

Recently, Rodman and Honig (1987) have applied the MINDO/3 method (Bongham et al., 1975) to calculate scaled quantum mechanical force field for simple polyenes and protonated Schiff bases. In general, quantum mechanical calculations of force constants are not accurate enough to reproduce observed frequencies to within something like 50%. However, it has been shown that scaling of calculated force constants can lead to accurate force fields for small molecules (Pulay et al., 1983). The approach used in Rodman and Honig (1987) was to scale the force constants obtained from the MINDO/3 calculations so as to reproduce the spectra of butadiene. The same scaling factors were used for a number of polyenes, and very good fits were obtained.

Here, we use this approach in a somewhat different manner. The above empirically derived force fields for rhodopsin is assumed to correspond to the 11-cis protonated Schiff base of retinal at rhodopsin's active site including any interaction between the chromophore and the apoprotein. The active site is modeled, and the force field is calculated using MINDO/3. Changes in the chromophore=protein interaction are assumed, and the corresponding changes in the force fields are calculated. The empirically derived force fields is scaled in proportion to the calculated changes, and the new normal mode frequencies are calculated. In this way, we may assess how various changes in interaction between rhodopsin's chromophore and surrounding protein influence the observed normal modes. We consider here how charges near retinal' Schiff base moiety affect the force field and the Schiff base frequency.

Table 3 shows the results for the following calculation. A positive point charge,

presumed to be located 3.0 angstroms from the nitrogen of an 11-cis protonated Schiff base along the direction of the protonating proton, is moved to 4.5 angstroms from the nitrogen. As discussed below, this molecular arrangement is close to a specific model for light to chemical energy conversion proposed by Honig et al. (1979). The table shows how each force constant is changed, how each change (keeping all the others constant) affects the Schiff base frequency.

A number of conclusions are evident from table 3. First, movement of charges close to the Schiff base are calculated to affect the Schiff base frequency in modest but clearly measurable amounts. Also, there are only two force constants which have a major effect on the Schiff base frequency in response to charge movement. Those are the stretching force constant of the Schiff base itself, KC15=N and the bending force constant, KC15=N-H. Previous studies of the Schiff base frequency have emphasized the impotence of the Schiff base bending force constant on the position of the Schiff base frequency through a strong interaction between the stretching and bending internal degree of freedom (Aton et al., 1979; Kakitani et al., 1983). The large downward shift of the Schiff base frequency in rhodopsin upon deuteration has been explained by a much weaker coupling between those two modes when the bending frequency decreases from ca. 1350 to ca. 950 cm^{-1} upon deuteration. Indeed, the same calculations as performed above, but on a deuterated Schiff base of retinal, yield only a 4 cm^{-1} shift in the deuterated Schiff base stretching frequency when the point charge is moved from 3.0 to 4.5 angstrom due to the effect of the C15=N-H coordinate. This is in contrast to the 14 cm^{-1} change calculated for the protonated case. Finally, we find it interesting that, while both the Schiff base stretch and bending coordinates have a sizable negative effect, there is a great deal of cancellation from the effects of all the remaining internal coordinates.

We have measured the Schiff base frequency in rhodopsin and bathorhodopsin for a number of isotopically labeled analogs. Apart from doubly labeled analogs where the Schiff base mode would appear to be highly coupled to other internal coordinates, the Schiff base frequencies of both rhodopsin and bathorhodopsin are the same, within experimental error, for the analogs studied here and in other reports. This strongly suggests that the Schiff base mode is, to a larger degree, unaffected in the rhodopsin to bathorhodopsin phototransition. This intuitive conclusion is reinforced by experiments (summarized in table 1) showing that the frequency of the C=N mode of various retinal protonated Schiff bases. For example, the retinal protonated Schiff base in isorhodopsin and in different solvent types, respond differently to isotopic labeling.

While we believe that the Schiff base environments are very similar in rhodopsin and bathorhodopsin, an explanation about the different responses of the 'Schiff base' to doubly labeling in these two pigments is necessary since this fact has been used to suggest different Schiff base environment in rhodopsin and bathorhodopsin (Bragley et al., 1985). Our explanation, as discussed above, is that the C=N motion contributes to most of the bands in this region so that it is impossible to assign a single mode to the 'Schiff base' mode. Because of the strong coupling among the C=C and C=N motions very little influence of the environment will result a change in the Raman or IR intensity patterns of these modes but very little change in normal mode frequencies. In order to verify our explanation, we have used the Raman intensity calculation which was developed in Kakitani et al. (1983) and IR intensity calculation which was discussed in Person and Zerbi (1982). These calculations are not known for the accuracy of reproducing the experimental data because they require more information which is not easily available like, for example, the configuration of the molecule in its electronic excited state and the charges on each atom of the molecule. However, our task here is to

demonstrate the sensitivity of the Raman and IR intensity pattern in respond to the environments, not the exact Raman or IR intensity pattern. Therefore, it is reasonable to use such calculations.

We have done our calculations in the following manner: first we choose our first force field to simulate the environment of rhodopsin, and calculate the Raman and IR relative intensities for the 1604 and 1613 cm^{-1} bands in $H^{13}C$ =ND+ pigment, which are 0.07/0.12 and 0.20/0.12 respectively. Then we choose our second force field to simulate the environment of bathorhodopsin and again calculate the Raman and IR intensities for the 1605 and 1615 cm^{-1} bands in the same pigment. They are 0.19/0.00 and 0.18/0.19 for Raman and IR respectively. The result of our calculation reproduces the Raman and IR intensity pattern for the 'Schiff base' mode observed in the experiments. For the Raman data , there are two bands in rhodopsin at 1599 and 1609 cm^{-1} which are calculated to be 1604 and 1613 cm^{-1} respectively and there is one band in bathorhodopsin at 1599 cm^{-1} which is calculated to be 1605 cm^{-1}, the other band is too weak in Raman intensity to be observed. Similarly, in the difference spectrum of FTIR data there is a positive band at 1610 cm^{-1} which is due to bathorhodopsin and a negative band at 1602 cm^{-1} which is due to rhodopsin. If we subtract our simulated rhodopsin IR spectrum from bathorhodopsin IR spectrum, there will be a positive band at 1615 cm^{-1} and a negative band at 1604 cm^{-1}, in good agreement with experiment. Furthermore, the isomerization can also cause Raman and IR intensity pattern change. We keep the force field the same and just change the configuration of the retinal from 11-cis to a twisted all-trans (Eyring et al., 1982), the calculated Raman and IR intensities for the 1611 and 1617 cm^{-1} bands are 0.07/0.09 and 0.07/0.15 respectively, which can at least reproduce the FTIR data. The complete results of the intensity calculation are shown in tables E1-2,4 and 5.

One factor which has little influence on the Schiff base frequency is chromophore isomerization. Various isomers of Schiff bases in solution all show essentially the same Schiff base frequency (Callender and Honig, 1976). This insensitivity to isomerization would appear to result from the localization of the Schiff base mode to the Schiff base moiety.

Delocalization of the chromophore polyene backbone π electrons, which give absorption maxima red shifts, is not sufficient by it self to affect the frequency of the Schiff base. This has been quit nicely demonstrated by the experimental results of Baasov and Sheves (1985). Point charges placed near model protonated Schiff bases but relatively far from the Schiff base moiety showed large red shifts in their absorption maxima , and concommitant changes in the dominant ethylenic C=C frequency, but no measurable change in the Schiff base frequency. The shifts in absorption maxima and C=C frequency are clearly indications of π electron delocalization. Theoretically, this behavior can be understood in terms of the recent Mindo/3 calculations of Rodman and Honig (1987). As a demonstration, we carried out PPP and normal mode calculation on a twisted all-trans retinal which is suggested by Erying et al. (1982) to simulate retinal isomer in bathorhodopsin. The absorption maximum of this isomer calculated by PPP method shifts about 35 nm towards red and the major C=C mode calculated by using our first force field shifts down about 10 cm^{-1} while the C=N mode remains constant. The complete calculation of this model isomer is shown in table 5.

The charges placed quite near the Schiff base moiety appear to have significant effects of the frequency of the C=N mode. As summerized in table 2 (and also obtained in the more extensive calculations of Rodman and Honig (1987)). there are a number of calculated changes in force field by moving a charge from 3.0 to 4.5 angstroms from the Schiff base nitrogen. The effects on the C=N stretch and C=N-H bend stand out, giving

about equal contributions to the change in the Schiff base frequency. These calculations are intuitively reasonable. A charge so close to the Schiff base moiety should affect the p and s electron density of the C=N bond, and one would expect this to result in a sizable change in this force constant and Schiff base frequency for a mode reasonably localized to the C=N moiety. In fact, Baasov and Sheves (1985) have demonstrated this effect experimentally by measurements if a Schiff base analog where a positive charge located 2 angstroms from the Schiff base induced a 6 cm^{-1} change in the Schiff base frequency and a concommitant 14 cm^{-1} shift in C=C stretch and 30 nm shift in absorption maximum.

The effect of the C=N-H bend on the Schiff base frequency is also reasonable since a negative charge close to the hydrogen of C=N-H will increase the energy of C=N-H bending compared to a more distant negative charge. This is true because much of the Schiff base positive charge is located on the Schiff base hydrogen. As discussed above, there is a substantial component of C=N-H bend in the Schiff base mode. The size of this component is related to the frequency difference between the C=N-H bending and C=N stretching frequencies. As the C=N-H frequencies approach the C=N stretch from below, the frequency of the Schiff base mode is increased. Weakening the interaction of a charge with the Schiff base proton by moving the charge away from the proton weakens the interaction energy, lowers the frequency of the C=N-H bend, and thus lowers the frequency of the Schiff base mode. This is the behavior shown in the calculations. This result is borne out by the experimental studies of Sheves et al. (1986) of retinal protonated Schiff bases which show that the hydrogen bonding environment of the Schiff base moiety and/or the interaction with nearby charges (Sheves et al., 1987) markedly affect the Schiff base frequency. In fact, a measure of hydrogen bonding appears to be the frequency shift of the Schiff base bond upon deuteration of the

nitrogen. The very large 31 cm^{-1} shift in rhodopsin and bathorhodopsin suggests both these species are strongly hydrogen bonded (Sheves et al., 1987).

It is commonly believed that electrostatic interactions between the retinal and the apoprotein opsin are the primary determinants in both pigment color regulation and energy transduction. The simplest picture of energy transduction was given by Honig et al. (1979). The underlying assumption of the picture is that the positively charged chromophore in rhodopsin is stabilized by electrostatic interactions between the chromophore and apoprotein. The photoisomerization of the chromophore in the rhodopsin to bathorhodopsin transition disrupts these interactions, resulting in a high energy bathorhodopsin species. The specific model included an unspecified opsin negative charge (or arrangement of one or more stabilizing dipoles) salt-bridged to the positive Schiff base moiety. isomerization of the retinal chromophore results in weakening the salt bridge and separating these charges. It was shown that reasonable molecular parameters could result in sizable energy conversion. However, as we have shown above, it appears that the simple separation of the ion pair in the rhodopsin to bathorhodopsin photoreaction should result in a measurable effect on the Schiff base frequency, and none is observed.

In this regard, we should review the reasons to suppose that a space motion of the positively charged species against an electrostatic field is involved in the primary photochemistry. In the first place, all visual pigments known contain 11-cis chromophores of protonated Schiff bases of retinal (or very close analog like vitamin A2). This is true across many different species including vertebrates and invertebrates (reviewed in Balogh-Nair and Nakanishi, 1982; Stavenger and Schwemer, 1984). This emphasizes the special charged nature of the protonated Schiff base chromophore-opsin linkage. Moreover, an 11-cis to all-trans photoisomerization accompanies the formation

of bathoproducts, again across many different species. The protonated Schiff base in rhodopsins would certainly be expected to be energy stabilized by electrostatic mechanisms. Chromophore isomerization would certainly disrupt this stabilization.

Moreover, it is difficult to rationalize how large amounts of light energy can be converted to chemical energy by other physical effects, such as steric interactions and/or strain effects, although it is likely that some of bathorhodopsin's 35 kcal/mol energy is of this form. The reason for this is that, while visual pigment primary photochemistry is characterized by an extremely efficient and fast excited state process with little or no energy barrier between rhodopsin and bathorhodopsin is on the order of 45 kcal/mol, very large indeed (Honig et al., 1979). Strain and/or electrostatic effects do not particularly discriminate between ground and excited electronic states. On the other hand, excitation of a retinal protonated Schiff base to its excited state result in largely neutralizing the Schiff base moiety positive charge found in the ground state. Thus, rotations about retinal's C11-C12 double bond, which would be hindered in the ground state if the positively charged protonated Schiff base is electrostatically stabilized, is not particularly hindered in the excited state.

Assuming that electrostatic factors play a dominant role in the energy transduction process, how may we rationalize that the Schiff base mode is not measurably affected by the rhodopsin to bathorhodopsin photoreaction. Lacking specific structural information concerning the local protein environment of the chromophore it is not possible to work out detailed models. There are, however, a number of possibilities. In the first place, the data strongly suggest that the Schiff bases of both rhodopsin and bathorhodopsin are strongly hydrogen bonded. The frequency of both Schiff base bands are high and both exhibit large frequency shifts upon Schiff base deuteration. As mentioned above, this behavior strongly correlated with strong hydrogen bonding.

Given this, there are two possibilities, broadly speaking, for the electrostatic interaction between chromophore and apoprotein stabilizing rhodopsin relative to bathorhodopsin. In the first case, it is possible that he Schiff bases of both rhodopsin and bathorhodopsin are hydrogen bonded but that the apoprotein superimposed on additional electrostatic fields. For example, it has been proposed (Rodman and Honig, 1987) that a large electric field in the vicinity of the Schiff base could be produced by a a-helix dipoles. Models of rhodopsin's tertiary structure based on sequence data suggest that the helix containing the retinal may be disrupted, and this can lead to large local fields. This the local hydrogen bonding environment remains the same so that the Schiff base mode is not measurably affected rhodopsin to bathorhodopsin photoreaction while the positive Schiff base moves against a substantial, but relatively constant field. Motion through a relatively constant fields would have little effect on the Schiff base frequency as is implied in the experimental and theoretical work described above.

Another model which is consistent with the data is that the counterion of rhodopsin's protonated Schiff base is some charged species which forms a salt bridge. Upon photoisomerization, the salt bridge is disrupted, and the Schiff base of bathorhodopsin forms a hydrogen bond with some neutral group. In both rhodopsin and bathorhodopsin, the C=N-H bending mode frequency would be increased because of the local interaction between the Schiff base proton and either the charged protein moiety in rhodopsin or the dipole groups in bathorhodopsin. As described above, this leads to a higher C=N frequency and large deuteration effect which could mask effects on the C=N frequency brought about by movement against an electrostatic field. It is clear that many specific possibilities exist and that further studies, particularly protein structure work, is needed before any detailed understanding of chromophore-apoprotein interaction is possible.

2. Proton-deuteron exchange of the retinal Schiff-base in purple membrane (Bacteriorhodopsin)

Bacteriorhodopsin (bR), the purple membrane protein of *Halobacterium halobium*, uses light to actively transport protons from the inside to the outside of the cell membrane. The chromophore of bR is all-trans retinal bound in the form of a protonated Schiff base to the ε-amino group of lysine 216 in the protein. The Schiff base deprotonates and then reprotonates during the course of the light-driven photocycle of bR, and it is likely that these events are associated with the proton pumping mechanism (See reviews by Stoeckenius and Bogomolni, 1983; Ebrey,1982). It is known from Raman studies that the Schiff base proton exchanges for a deuteron, resulting in a downward frequency shift of about 16 cm^{-1} in the 1640 cm^{-1} C=NH protonated Schiff base stretching vibration (Lewis et al, 1974).

The rate of exchange can, in principle, provide important information about the proton pumping mechanism, since it depends on the accessibility of the Schiff base to water molecules and to protons in solution. Two groups have previously measured the proton-deuteron exchange half time, One (Ehrenberg et al, 1980) reported a 4.7 msec exchange half time at pH7 and pH2 while a second (Doukas et al, 1981) suggested an exchange half time of shorter than 3 msec over a pH range of 4-10. We have extended these experiments by improving the apparatus resolution to about 1 msec, performing measurements over an extended pH range and with varying ionic strength, and on both light and dark-adapted bR samples.

Methods

Cultures of *H. halobium* were grown and the purple membrane purified according to the procedures of Becher and Cassim (1975). This sample was provided by T.

Ebrey's group in University of Illinois. Deuterated samples were prepared by subsequent centrifugation and resuspension in D_2O. deuteration of the Schiff base was confirmed by the appearance of the C==N stretch mode at 1624 cm^{-1}. No buffer was used in our experiments.

Continuous-flow experiment were carried out by rapidly mixing the deuterated bR sample with double distilled water solution at pH2, pH6.5, pH12, with or without 4M NaCl, in a 1:20 ratio. The mixing chamber was constructed with two jets meeting with an angle of about 160 degree, and with a cross section ratio of 1:20. The mixed sample exited through a 0.5 mm diameter glass capillary, with 100 degree angle to both incoming jets, at a flow rate of 60ml per minute. The Raman spectra was measured along various positions of the exiting capillary by a 530.9 nm line from a krypton ion laser. The laser beam, at a power level of 50 mW at sample, was focused by a cylindrical lens. Under these conditions, less than 15% of sample undergoes photolysis (Callender et al, 1976).

The dead time of the mixing chamber, 0.9 ms $\pm$ 0.3 ms, was calculated from the measured flow rates and the volume of the flow cell. The completion of mixing was verified by a transmission experiment performed on the same mixing chamber as following. A focused laser beam transmitting through the exit capillary was collected by a power meter (Keithley Instruments, model 150B). The reading of the power meter with only water coming through the capillary was recorded as relative 100% transmission. The reading of water rapidly mixed with 2,6-dichlorophenolindophenol (DCIP) was recorded as relative 0% transmission. DCIP has an absorption maximum of 600nm at pH7 which shifts to about 510 nm instantaneously when pH changes to 2.5. When DCIP at pH2.5 is reduced by 20 mM L-ascorbic acid, its absorption disappears with a half time of 0.66 ms. The reaction of DCIP at pH7 with 20 fold excess of 20mM

L-ascorbic acid at pH2.5 was used for this check-up experiment. When 647.1 nm line from a krypton ion laser was used to probe the reaction, the recorded transmission was already 100% at the shortest possibly time. This result indicated that the mixing was complete within the dead time. When 530.9 nm line from the same laser was used, the recorded transmission was 60% at 0.9ms and >90% at 2 ms This result suggested that the half time of the reaction was about 0.7 ms, in good agreement with the reported value. Thus the dead time of the mixing chamber was verified.

Resonance Raman spectra were obtained with a spex 1877 triplemate spectrometer, a water cooled EG & G 1420-2 solid state detecter and a 1218 multi channel detecter controller. This system has been described in more detail elsewhere(Deng et al, 1984). The spectral resolution was 8 cm^{-1}.

Results and Discussion

Fig E2-1 shows a series of runs where light adapted bR, suspended in D_2O, is rapidly mixed with water, in a 1:20 ratio. The Raman spectrum of the mixed solution in the vicinity of the C=NH stretching mode is measured downstream from the mixing chamber at various positions, which can be translated to the time after mixing by measuring the fluid flow velocity. It is clear from Fig E2-1 that the deuterated C=ND band at 1624 cm^{-1} converts to the protonated band at 1640 cm^{-1} on the millisecond time scale. Fig E2-2 plots the decrease of the 1624 cm^{-1} band and the increase of the 1640 cm^{-1}band. They appear to have similar kinetics, as expected.

In order to determine the exchange half time, a separate Raman experiment was performed on the light adapted bR in 50% H_2O and 50% D_2O (v/v) mixture. Under this condition, the 1624 cm^{-1} band appears higher than 1640 cm^{-1} band, in agreement with the result obtained by Hildebrandt and Stockburger (1984). We also obtained the Raman

spectra of light adapted bR in 75% H_2O, 25% D_2O and 25% H_2O, 75% D_2O mixtures in order to determine the relative amount of C=NH and C=ND along the exchange reaction.

In the tables 6-9, we show the exchange half time dependence on various conditions. It can be seen from these tables that variation of pH from 2.4 to 10.7 has little effect on the exchange kinetics. Ionic strength does not influence the reaction until the salt concentration is raised above 1M. At this salt concentration, the exchange time increases to about 1.5 msec, and increases further to 2.7 msec when the salt concentration is raised to 4M. The most drastic change of the kinetics comes from the serious aggregation of bR in 4M NaCl at pH3. Under this condition, the exchange half time becomes 10 msec. Dark-adaptation does not influence the exchange half time much in high salt concentration but does increase the time to 2.7 msec in absence of salt. We have also observed that papain treated bR, with the C-terminal end clipped off, which shows little change in the exchange half time.

We believe our results can rationalize the two different exchange half times reported by two different groups in their previous works. The two bR samples may have different degree of aggregation. Our data also suggest that the C-terminal end of bR as well as the surface charge, which can be neutralized in 0.5M ionic strength (Ehrenberg and Meiri, 1983), are not involved in the exchange mechanism. .

The standard mechanism for hydrogen-deuteron exchange involves a base catalyzed dissociation followed by a reprotonation of the Schiff base. We (Doukas et al, 1981) previously considered reactions where the base catalyzing the reaction was either OH^- or H_2O. We calculated that either reaction, under conditions where the resulting exchange half times were derived from diffusion controlled rate constants found in water, were in the order of 100 sec, at least four orders of magnitude longer than measured here. The reasons for this are:

(1) Considering OH^- as the base, at low pH there are not enough OH^- ions to deprotonate on the millisecond scale and (2) Considering H_2O as the base, the pK=13.3 of bR's Schiff base (Sheves et al, 1986) is too high to permit a millisecond deprotonation.

In order to account for such a fast exchange half time, we proposed previously an exchange mechanism where by the Schiff base and a nearby water molecule simultaneously exchange a hydrogen. This suggested scheme is given in Fig E2-3. In this scheme, the hydrogen-deuteron exchange rate in bR's Schiff base is determined by the diffusion of water to the retinal binding site, followed by the reaction of water with the Schiff base. According to Fig E2-3, our data do not unambiguously show which of these two steps is rate limiting. However, the fact that the exchange half time increases significantly with aggregation suggests that the rate limiting step is the diffusion of water to the binding site.

3. Resonance Raman Study of Deionized Blue membrane

Bacteriorhodopsin (bR), the only protein present in the purple membrane of *H.halobium*, consists of a molecule of retinal covalently bound to the protein by a Schiff base linkage to the ε-animo group of lysine 216. The dark-adapted bR contains retinal in both the all-trans and the 13-cis conformations of about equimolar. On absorbing light, the 13-cis retinal form converts to all-trans, and the absorption maximum of bR changes from 558nm in dark adapted bR to 568nm. The light-adapted bR contains only all-trans retinal which isomerizes upon illumination to initiate the proton pump mechanism (see reviews by Stockenius and Bogomolni 1982; Ebrey 1982).

The blue membrane is formed from dark adapted bR upon removal of Ca^{++} and Mg^{++} ions by any of a variety of methods (Kimura et al., 1984; Chen et al., 1984; Chang et al., 1985). Like dark adapted bR, blue membrane also has chromophore retinal covalently bound to the protein via a protonated Schiff base linkage, which is supported by the observation of a shift of the C=N stretch mode from 1634 cm^{-1} in H2O to 1616 cm^{-1} in D2O. It also consists of a heterogeneous pigment population, with the chromophore retinal in the all-trans and 13-cis isomeric forms, as suggested in the previous studies (Smith et al., 1985; Pande et al., 1985).

In a previous study (Pande et al., 1985), based on the low temperature resonance study of dark and light adapted blue membrane, we suggested that in the blue membrane, the 13-cis isomer has an absorption maximum higher than the all-trans isomer, which is contrary to the case in dark adapted bR. In order to verify this hypothesis, we have used resonance Raman spectroscopy to study the photoproducts of blue membrane at room temperature. It is believed that the all-trans chromophore isomer in dark adapted bR has the absorption maximum 568 nm and the 13-cis chromophore isomer of dark adapted bR has a absorption maximum of 548nm from the reconstitution studies of the

bacterio-opsin + all-trans and 13-cis retinal respectively (Sperling et al, 1977). Therefore it is reasonable to assume that the two different chromophore isomers in blue membrane also have different absorption maxima. In this work, we used the assumptions that the photoproducts from 13-cis and all-trans isomers should be different, and the photoproducts similar to the photointermediates of light adapted bR should be from the all-trans isomer in blue membrane.

Chromophore extraction studies on the blue membrane reveal that it contains about 35% 13-cis and 65% all-trans retinal isomers. By using these percentages, and assuming the all-trans isomer has a lower absorption maximum similar to the light adapted bR, we can simulate the absorption spectrum of the 13-cis isomer in blue membrane by subtracting properiate amount of light adapted bR spectrum from the blue membrane spectrum as the first order approximation. The result is shown in Fig E3-1. From the Fig we can see that the 568.2nm or 514.5nm light will basically only excite the all-trans isomer, while 676.4nm light will only excite 13-cis isomer. Therefore, a study of the photoproducts from each pigment is possiblesince we may excite one but not the other. Our data indicate that the photoproducts excited by 568.2nm light are very similar to the intermediates from light adapted bR while the photoproducts excited by 676.4nm light have features from 9-cis isomer which is not observed in the photocycles of light adapted bR. This result strongly suggest our hypothesis about the absorption maxima of the all-trans and 13-cis isomers in blue membrane is correct.

Methods

Blue membrane was prepared from purple membrane by the method of Chang et al. (1985). The purple membrane sheets were incubated with papain/EDTA (Sigma) for 3.5 hrs at 37 C. Then washed with deionized water five times. All water used in the

experiment was double distilled and then passed through a Water-I system (Gelman Sciences). D_2O used in the experiment was also deionized by the water-I system and was above 90% pure. The absorption maximum at about 600nm confirms the formation of blue membrane. The deuterated form of the blue membrane was prepared by suspending the pelleted blue membrane in deionized D_2O . The concentration of the sample for Raman study was about 35 mM.

Resonance Raman spectra of the blue membrane and its photoproducts were measured at room temperature by a spinning cell set up and the pump and probe technique, which were described elsewhere (Deng et al., 1985), except a cylindrical lens with a focal length of 6cm was used for the probe beam. There were several laser lines used in the experiment: the 676.4 nm, 568.2 nm lines from a krypton ion laser and the 496.5 nm, 514.5 nm lines from an argon ion laser. The intensity of the probe beam and the angular velocity of the spinning call were adjusted such that less than 10% of the pigments photoisomerized after a single pass through the probe beam and more than 90% of the blue shifted intermediates relaxed back after a complete cycle as discussed before (Callender et al., 1976; Deng et al., 1985).

A triplemate spectrometer (Spex model 1877), connected to an LSI-11 computer interfaced solid state detector (EG&G Princeton Applied Research Model 1420-2/1218), was used to collect the Raman spectra (Deng et al., 1985). The spectra resolution for 496.5 nm probe is 9 cm^{-1} and for the 514.5 nm probe is 8 cm^{-1} . The wavenumber scale of the spectra are calibrated against the Raman lines of toluene.

Absorption measurements made before and after the Raman experiments were in a G. C. McPhearson spectrophotometer which was interfaced to a PDP-8 computer system for data collection and storage.

Results and discussion

Fig E3-2 shows the resonance Raman spectra of blue membrane in D_2O (a) and in H2O (b) suspension. The C=N stretching mode, which shifts from 1634 cm^{-1} in H2O suspension to 1616 cm^{-1} in D_2O , suggests that the Schiff base is protonated. The similarities between the Raman spectra of blue membrane and dark adapted bR as well as the extraction studies led to the conclusion that blue membrane consists of a mixture of all-trans and 13-cis chromophore (Smith et al., 1985; Pande et al., 1985). The appearance of the 1208 cm^{-1} shoulder and the decrease of the 1170 cm^{-1} peak upon deuteration of dark adapted bR have been used to determine the C=N cis configuration of the 13-cis isomer in the dark adapted bR (Smith et al 1984). Although the deuteration effects are much less in blue membrane than that in dark adapted bR, they are still clear. Since the population ratio of the 13-cis to all-trans chromophore isomer in blue membrane is also less than that in dark adapted bR, the deuteration effects of blue membrane suggest that the 13-cis chromophore in blue membrane remains the same as in the dark-adapted bR.

Fig E3-3 shows the resonance Raman spectra of (a) Blue membrane probed by 496.5nm laser line. (b) Mixture of blue membrane + its photoproducts excited by 676.4nm light, 1.5msec upstream of the probe beam. (c) Photoproducts excited by 676.4nm light, obtained from subtracting proper amount of (a) from (b).

Fig E3-4 shows the resonance Raman spectra of (a) Same as (a) in Fig E3-3. (b) Blue membrane + its photoproducts excited by 568.2nm light, 1.5msec upstream from the probe beam. (c)Photoproducts excited by 568.2nm light, obtained from subtracting proper amount of (a) from (b).

These two resonance Raman spectra of the photoproducts from blue membrane look very complicated, because they are from heterogeneous species. However, useful

information can be derived by using the correlation between the ethylenic stretching frequency and the absorption maximum observed in bR and the visual pigments (Rimai et al., 1971; Aton et al., 1977). According to this corralation, the two isomers in the blue membrane should have corralations betwee ethylenic band and absorption band as follows: The 1520cm^{-1} band in Raman spectrum should be from the isomer which has an absoption maximum 610nm and vise versa; The same ralation applies to 1530cm^{-1} Raman band and 570nm absorption maximum.

We can assign the 1532 cm^{-1} band in the resonance Raman spectrum of the protoproducts excited by 676.4nm light (Fig E3-3 (c)) to the low absorption isomer in blue membrane. Because part of the high absorption isomer is converted into its photoproducts by 676.4nm light (conf. Fig E4-1), the intensity ratio of the 1520 cm^{-1} band from high absorption isomer to the 1530 cm^{-1} band from low absorption isomer in Fig E3-3 (b) should be less than that in Fig E3-3 (a). Therefore when we subtract Fig E3-3 (a) from Fig E3-3 (b) just enough to get rid of the 1520 cm^{-1} band contributed from the high absorption isomer in blue membrane, the 1530 cm^{-1} band from low absorption isomer in blue membrane would be left over. The 1141 cm^{-1} band in Fig E3-3 (c) indicates that the phtoproducts of the blue membrane excited by 676.4nm light contains 9-cis isomer, because this band is unique for 9-cis protonated Schiff base (Pande et al,1986; Oseroff and Callender,1974). Since none of the phtointermediates of the light adapted bR contains this chromophore isomer, it implies that these protoproducts could not be from all-trans isomer in blue membrane, therefore the high absorption isomer in blue membrane is not all-trans.

The resonance Raman spectrum of the photoproducts of blue membrane excited by 568.2nm light (Fig E3-4 (c)) shows very different features. There is very little 1141 cm^{-1} band indicating that no contributions from 9-cis isomer in the spectrum.

Furthermore, it has features similar to the resonance Raman spectrum of the photointermediates L from light adapted bR. For example the 1548 cm^{-1} band and the 1644 cm^{-1} band like the corresponding bands in L. In the finger print region, it is also similar to the L. The similarity between the photointermediate L of the light adapted bR and the photoproducts of blue membrane excited by 568.2nm light strongly suggests that these photoproducts are from the all-trans isomer in blue membrane, therefore the low absorption isomer is all-trans in blue membrane.

Although our assumptions about the isomer absorption maxima agree with the experimental results well, there are two questions should be answered. The first question is about the validity to use spinning cell set up to study the 676.4nm excited photoproducts from blue membrane, because it is known that under the illumination of this light, the blue membrane would slowly be converted to species absorbing at about 496nm which has been called 'pink' membrane, and studied in detail elsewhere (Pande et al 1986). Therefore instead of observing the mixture of the photointermediates and blue membrane in Fig E3-3 (b), the spectrum may result from the that 496nm species and blue membrane since in the spinning cell these two species would be expected to reach a certain equilibrium. However, in the previous studies we have found that it takes at least 2 hours to convert about 80% of blue membrane to 'pink' membrane by irradiation with deep red light, whereas the 'pink' membrane converts back to blue membrane instantly upon irradiation of blue light (Pande et al 1986). These observations suggest that although the 13-cis isomer in blue membrane can reach an excited state which will lead a small portion of it to the 'pink' membrane, the majority of isomers on the excited state would fall back to blue membrane. Thus this problem can be greatly reduced by taking the spectrum in Fig E3-3 (a) and the spectrum in Fig E3-3 (b) alternatively in short time period to avoid the accumulation of the 'pink' membrane. The

difference between the spectrum in Fig E3-3(c) and 'pink' membrane suggests that our statement is true. There are more bands like 1214 cm^{-1},1098 cm^{-1} and 1022 cm^{-1} in Fig E3-3(c) which are not present in the Raman spectrum of 'pink' membrane. Moreover, the absence of the first two bands mentioned above in the spectrum of the photoproducts excited by 568.2nm light also suggests that the these two kind of photoproducts, excited by 568.2nm and 676.4nm respectively, are not from the same chromophore isomer in blue membrane.

The second question is the influeunce of the remaining cations in blue membrane. In the early studies of the blue membrane, it was found that no matter which method was used, there was still about 10% cations left in the blue membrane (Chang et al 1984). Therefore the observed photoproducts in the spectrum Fig E3-4(c) could be from the remaining purple membrane caused by these cations rather than from blue membrane itself. This is possible because at present, there is no method available to find out wether the remained cations are at the same binding site as in purple membrane or at different binding site. Thus it can not be ruled out that the 1564cm^{-1} band in Fig E3-4(c) may be due to M which is the photointermediate of light adapted purple membrane.

However, we believe that the spectrum shown in Fig 3E-4(c) we discussed earlier are not from L intermediate of light adapted purple membrane based on two reasons. The first reason is that the L species from purple membrane has different kinetics than this species from blue membrane. In an earlier flashphotolysis studies, it was found that two photointermediates of blue membrane, with the absorption maxima at about 400nm and 500nm respectively, arised from and relaxed back to blue membrane at about the same time with a millisecond scale when blue membrane was excited by the actinic light flash >540nm (Chang et al., 1984). This kinetics was also observed in acid blue membrane (Mowery et al., 1979), which has the virtually identical Raman spectrum compared with

deionized blue membrane (Smith et al., 1985). In contrast, the photointermediate M arises after another intermediate L in the photoreaction of bR and only M has life time in millisecond scale.

This kinetics was also verified in the Raman studies. The L spectrum could be obtained by using the same method of obtaining Fig E3-4(c) but with pump-probe time separation of 20 μsec when purple membrane was used. At a time separation of 1.5 msec, which was the condition used in the study of intermediates from blue membrane, the spectrum, obtained by the same method, showed very little L and mainly M spectrum (data not shown). Although there were many reports about the kinetic changes of the purple membrane photocycle under various conditions (for a list of papers, see Deng et al., 1984), none of conditions changed the life time of L by two orders of magnitute except in the Acid blue membrane, which, in many aspects, was considered the same as deionized blue membrane. If the remained cations in blue membrane behave like the cations in purple membrane, we would expect that the L intermediate from the remained bR residues have the same kinetics as the L from normal bR, and the L like species with the life time of msec should be from blue membrane. If the remained cations in blue membrane have different function from those which could be removed by various methods, we would have the same conclution.

The second reason is that the quantum yield of the L like species from blue membrane are similar to that of L from purple membrane. In the 496.5 nm probe and 568.2 nm pump Raman measurements, we found that the ratio of the 1548 cm^{-1} band to 1530 cm^{-1} band in blue membrane(Fig. 3E-4(a)) was about 30%; wheares in purple membrane the ratio was about 20% (data not shown). Even the broadness of the ethylenic band in blue membrane and the possible resonance discremination are considered, the two ratios can not be different by a factor of 10. Thus if the spectrum in

Fig. 3E-4(c) was from the remaining bR in blue membrane, the quantum yield should be 10 times less than that in purple membrane because only 10% cations remaining in the blue membrane. Based on these two reasons we conclude that the spectrum shown in Fig. 3E-4(c) is not from L.

To prevent contaminations of blue membrane from cations during our Raman experiment, we have used spinning cell set up. The blue membrane remained unchanged in the cells for at least several days. The absorption spectra taken before and after the Raman studies insured that there was no contamination from cations during the Raman experiments.

Since the 13-cis isomer has an absorption maximum 548nm in dark adapted bR, which is lower than the absorption maximum of all-trans isomer, but has an absorption maximum above 600nm in blue membrane, which is higher than that of all-trans, it is then obvious that the protein environment of the 13-cis isomer in dark adapted bR undergoes much larger change than that of the all-trans isomer when the cations are removed from purple membrane. We can reveal part of the change by studying the resonance Raman spectra of blue membrane and dark adapted bR in some detail.

In the low frequency region of the resonance Raman spectrum of dark adapted bR there is a sharp peak at about 800 cm^{-1}, which is due to 13-cis isomer (Smith et al 1984, Massig et al 1985 and our unpublished result). In the deionized blue membrane, this peak is greatly reduced(Smith et al 1984, and our unpublished result). The disappearance of this band by double substitution of hydrogens with deuterons at C12 and C14 positions (Smith et al, 1984) suggests that this band is mainly due to hydrogen out of plane bending vibration. Because such band is Raman active only when the retinal chromophore is twisted (Brainman and Mathies, 1981), it is possible that the removal of the cations from dark adapted bR relaxes its 13-cis chromophore isomeric form, Since

in solution both all-trans and 13-cis retinal protonated schiff base have the same absorption maximum. This possibility is also supported by employing the semiempirical π- electron PPP calculations based on the external charge model which has been successfully used on both purple membrane and visual pigment (Kakitani et al, 1983, 1985). If the counter ion is kept at the same distance from the nitrogen of the Schiff base, then there is only 1-2nm absorption maximum down shift from all-trans to 13-cis according to the calculation. However, when the C13-C14 single bond of the retinal is twisted 30 degrees, the absorption maximum down shift from all-trans to 13-cis is more than 10nm. Therefore it is possible that the twist around C13-C14 is responsible for the appearance of the 800 cm^{-1} peak as well as the lower absorption maximum of the 13-cis isomer in dark adapted bR. The most simple assumption for the higher absorption maximum of the 13-cis chromophore in blue membrane is that the counter ion is far apart from the 13-cis isomer but at about the same distance from all-trans isomer as in dark adapted bR. However, at present time, there is not enough experimental evidence to support this statement.

4. M412

Light adapted becteriothodopsin, bR570, contains retinal in the all-trans conformation. On absorbing light, bR570 undergoes the a photocycle shown in Fig 3. Of all the known intermediates in the photocycle, M412 is the only species which contains an unprotonated Schiff base linkage to the protein. The conversion from L to M species has also been associated with the pumping of proton(s)(Lozier et al., 1975; Li et al., 1984). Due to this unique structure and the implication of its direct participation in the proton pumping, the M412 species has been the subject of extensive structural and mechanistic investigations.

Flash photolysis studies of bacteriothodopsin have shown that the decay of M412 is biphasic and the two rate processes are depend on pH, temperature, ionic strength (Korenstein and Hess, 1979; Lam and Packer, 1983; Einsenbach et al., 1976; Li et al.,1984). These data suggest the presence of two forms of M412, which decay at different rates and whose relative amounts are sensitive to the above mentioned conditions. It has also been reported that the formation rate of M412 is also described by the sum of two rate processes (Ort and Parson, 1978; Fukumoto et al., 1984; Hanamoto et al., 1984). These data suggest that the formation of M412 proceeds via two distinct forms of L.

In a recent report, Li et al., (1984) have shown that the slow decaying form of M412 is associated with proton transport while the more repidly decaying form is not. One purpose of our experiments was to see if some difference in chromophore conformation, as revealed by their vibrational spectra, could help in determining why these spectrally similar intermediates may have such different physiological roles. Additionally, based on their calculations, Schulten and Tavan (1978) have postulated two forms of M412 with the chromophore in 14-s-cis and 14-s-trans conformations. If these correspond to the

two forms of M412 observed by the decay-kinetics measurements, then a difference in their vibrational spectrum is expected (cf. Cookingham and Lews, 1978). Finally, Hanamoto et al., (1984) have suggested that the two forms of M412 seen in the formation-kinetics of M412 may be due to the ionization state of a nearby tyrosin. It is conceivable that resonance Raman spectroscopy may detect this difference.

Methods

The triplemate spectrometer multichannel detector were used to obtain the Raman spectra. Raman measurements were made in a plexglass spinning cell which could be rotated at variable speeds. In the experiment, a spectrum was taken with the sample irradiated by two laser beams of different wavelengths: a pump beam to initiate the photocycle and a probe beam down stream from it. The distance between the two beams could be varied. A spectrum taken with probe beam only constituted the control for the first spectrum. The 568 nm line and the 413 nm line from two Krypton ion lasers were used as the pump and the probe beams, respectively. The photo-conversion probabilities, P413 due to the probe beam irradiation and P568 due to the pump beam irradiation, were calculated according to Callender et al. (1976):

$$P = \pi^{-1/2} I_0 \sigma_A \psi r_0^{-1} R^{-1} \omega^{-1}$$

where $\sigma = 3.824\ 10^{-21}\varepsilon$ is the absorption cross section, ε is the molar extinction coefficient, I_0 is the laser intensity, ψ is the quantum yield, r_0 is the laser beam radius at the sample, and R and ω represent the radius and the angular velocity, respectively, of the spinning cell. Assuming quantum yield of 0.3 for bR and 0.7 for M412 (Becher and Ebrey, 1977), the laser intensities, I_0, and the angular velocity, ω, were adjusted so that the rotatiion period was at least three times longer than the lifetime of M412. This was

verified experimentally.

Results and discusion

Fig E4-1 shows the formation and the decay profile of M412 in 20mM imidazole, pH9.1. The intensity of the 1568 cm-1 band which is proportional to the amount of M412 has been plotted as a function of the time separation, Δt, between the pump beam, which initiates the photocycle, and the probe beam. The decay kinetics of the M412 species obtained in this manner agree well with the flash photolysis results using absorption spectroscopy. Similar studies in 100 mM potassium phosphate at pH9.5 (data not shown) showed that the formation kinetics was faster and the decay was significantly slower than in imidazole at pH9.1. This is consistant with the previous results (Becher and Ebrey, 1977; Lam and Packer,1983).

The resonance Raman spectra of the two decaying forms of M412, were obtained for bR samples in 20mM imidazole, pH9.1. Flash photolysis studies under these conditions (Li et al., 1984; Tsuda and Ebrey to be published) yield a biphasic decay kinetics. The fast decaying form, Mfd, has a lifetime, t, of 2 ms and intial amplitude of 60%, whereas the slow decaying form, Msd, has a lifetime of 13 ms and an amplitude of 40%. Raman measurements were made at Δt = 0.5 ms (Fig E4-2a) where the composition is 60% and 40% of Mfd and Msd, respectively, and at Δt = 5 ms (Fig E4-2b) where their respective amounts were calculated to be 20% and 80%, These compositions were used to calculate the spectra of the pure Mfd (Fig E4-2c) and Msd (Fig E4-2d) forms of M412. Identical Raman cross sections were assumed for the two forms of M412 in these calculations and the data wew normalized with respect to the ethylenic peak intensity before subtraction.

The sample was suspended in 100mM potassium phosphate to obtain the resonance

Rman spectra of the two forms of the M412 that are formed from the two decaying forms of L550 (Hanamoto et al., 1984). Under these conditions the ratio of the two types of M formed depends on the pH; at pH7, the composition is 10% of the fast forming M (Mff) and 90% of the slow forming M(Msf), whereas at pH9.5 their respective amounts are about 50% each. FigE4-3a and E4-3b show the Raman spectra of the M412 species at pH9.5 and pH7 respectively. The data were obtained at a Δt of 0.2 ms, which corresponds to the plateau in the M412 formation profile. Fig E4-3c and E4-3d represent, respectively, the resonance Raman spectra of Msf and Mff species, calculated from the spectra in Figs. E4-3a and -3b.

It seems clear from Fig E4-2 and 3 that the spectra of M412 species obtained under various conditions as well as the spectra that were calculated from these, namely Mff, Msf, Mfd and Msd are not significantly different from each other. Since resonance Raman spectroscopy is sensitive to the chromophore structure, identical spectra of all the above forms of M412 imply identical chromophore structures in them. This suggests that the difference in the M412 species must, therefore, lie in the protein structure.

5. SERS Studies Of Purple Membrane

Electromagnetic theory predicts that the SERS profile has a maximum at about 390 nm for an isolated spherical silver particle system in aqueous solution, which is corresponding to the absorption center of the Ag sol. However, all previous SERS profiles observed in the experiments have a maximum at about 500 nm or higher. Since aggregations were generally found in those SERS active samples, this red shifted SERS profile was believed to be due to the silver particle aggregation, and several models to simulate the aggregated silver particle system have been suggested (Aravid et al., 1981; Kerker et al., 1984). Nevertheless, the effort to find a SERS profile with peak at about 400 nm failed (Kerker et al., 1984). This has lead to the general belief that the SERS effect always has contributions other than electromagnetic enhancement, for example, enhancement due to charge transfer (for a recent review see Moskovits 1985). The argument for other enhancement effects is that one often sees only the 390 nm peak in the absorption spectrum of a colloid/ adsorbate system, yet the SERS excitation profile achieves a maximum at a frequency in the red that does not appear to correspond to any discernable absorption peak, the implication being that the excitation profile maximum corresponds to an absorption, perhaps an adsorbate-metal charge transfer absorption, whose absorption strength is too low to be detected.

Our experiments on the SERS studies of retinaloxime in free solution and on membrane, as well as that of purple membrane showed that at least in some cases, the enhancement can be due to an electromagnetic effect only.

Methods

Retinaloxime was prepared according to the method of Groenendijk et al. (1979). All-trans retinal (Eastman Organic Chemicals) was mixed with 50 fold molar excess of

hydroxyamine bicarbonate (pH6.5)to the retinal in methanol (final methanol concentration 70% by volume). The retinaloxime formed had a absorption band at 360nm. The membrane bound all trans retinaloxime was prepared by bleaching the purple membrane, which was prepared according to the procedure of Becher and Cassim (1979). The bleaching was performed by mixing purple membrane with 1M NH_2OH at pH7 and then illuminating by a 150W projector lamp with a cut off filter at 530nm for about 15 hours . The sample was stirred and bathed by tap water to prevent heating. The retinal chromophore of the purple membrane reacts with NH_2OH to form retinaloxime which is bound to the membrane. The color of the pruple membrane is thus bleached since retinaloxime absorbs in the U. V.. The bleached purple membrane was then washed by the double distilled water a few times to remove the excess NH_2OH.The pure bacterio-opsin was prepared by lyophilizing the bleached membrane and then washing it several times with n-hexane until the absorption band at 360nm disappears.

Ag hydrosol (i.e., colloidal silver metal particles) was prepared by mixing aqueous equivolumetric amount of 0.5 mM $AgNO_3$ (Alfa) and 1.0 mM $NaBH_4$ (Baker) bathed in ice water. The resulting sol had a symmetric absorption peak at about 390nm with full half width of 45 nm.

The resonance Raman profile of the retinaloxime was measured according to the procedure of Doukas et al (1978). The surface enhanced resonance Raman spectra of the retinaloxime in solution and membrane bound were measured at room temperature. In order to reduce the possible isomerization of the retinaloxime, the spinning cell (made of optical glass) method of measurement was used with a cylindrical lens arrangement. The SERS spectra of purple membrane were also obtained by this set up. The concentration of the retinaloxime in the final solution for both cases and for bR was 20μM.The Raman spectra were obtained with a Spex 1401 double monochrometer and a cooled RCA

31034 photomultiplier, both interfaced with a LSI-11 computer for data collection, storage and analysis. Several laser lines were used in the experiment. The 514.5 nm, 501.7 nm, 496.5 nm, 488.0 nm, 476.5 nm, 472.7 nm, 465.8 nm, 457.9 nm, 454.5 nm lines were from a argon ion laser (Spectra Physics model 165), and 568.2nm, 530.1 nm, 520.8 nm, 415.4 nm, 413.1 nm, 406.7 nm, 356.4 nm and 350.7 nm line from a krypton ion laser (Coherent Radiation model CR2000). The typical laser power at sample was 10 mW. The resolution of the spectra was about 10 cm^{-1}.

Absorption measurements were made in a G. C. McPhearson spectrophotometer which was interfaced to a PDP-8 computer system for data collection and storage. The data were then transferred to a Vax computer for analysis.

Results

Fig E5-1a shows the resonance Raman scattering (RRS) excitation profile of the 1572 cm^{-1} peak of retinaloxime. The relative intensities at each laser excitation is compared with the solvent Raman lines, so that the effect of the optics aligment would not influence the result.

Fig E5-1b shows the surface enhanced resonance Raman scattering (SERRS) profile of the 1572 cm^{-1} peak of retinaloxime in free solution. The Ag particles aggregated considerably, and there was an distinct shoulder in its absorption spectrum at about 430 nm. Fig E5-1c shows the SERRS profile of the 1572 cm^{-1} peak of the retinaloxime on membrane. In this case the absorption spectrum of this solution was almost identical to the summation of the absorption spectra of the retinaloxime and Ag sol, that was an indication that very little aggregation occurred in this case. During the experiments we found that to measure the absolute Raman intensities at each laser frequency by adjusting laser power would easily introduce 50% error. Therefore we used the 3500 cm^{-1} H_2O

Raman band as our internal reference for the Raman intensity of the retinaloxime peaks because this band does not show SERS effect under normal conditions (Macomber et al., 1982). Since this band is rather far from the 1572 cm^{-1} band of the retinaloxime, it would introduce some error due to the frequency dependent quantum yield of the photomultiplier tube and diffraction grating. We have estimated that this error was less than 10%, which is much less using an external reference.

It has been assumed that resonance Raman and SERS effect are independent of each other (Siiman et al., 1983; Hildebrandt & Stockburger 1984). Therefore, the SERS profile of the retinaloxime can be obtained by dividing Fig E5-1b or 1c with Fig E5-1a. Fig E5-2a shows the SERS profile of the retinaloxime in Ag hydrosol, Fig E5-2b shows the SERS profile of the retinaloxime on membrane (bleached purple membrane) in Ag hydrosol. These SERS profiles are good demonstrations of the effect of aggregation on the maximum of SERS profile peak. When retinaloxime is free, it interacts with Ag particles and Ag particle aggregation occurs. Apparently, the aggregation then causes the red shift of the SERS peak so that it appears at 500 nm or above. When retinaloxime is bound to membrane, no serious aggregation occurs because the membrane separates Ag particles. Thus, SERS peak appears near the position predicted by electromagnetic theory , in this case, at about 430nm. This SERS peak is still a little red shifted because the retinaloxime may not be stuck on the membrane firmly so that Ag particles aggregate slightly. This is confirmed by the SERS experiment on purple membrane. Fig E5-2c shows the the SERS profile of the 1370 cm^{-1} Raman peak of purple membrane in Ag hydrosol, and it can be seen that the SERS peak position is much closer to the theoretical predicted value comparing with previous experiments. The reason is that the interaction between certain animo residues of bR in membrane and Ag spheres keeps membrane sheets attached on Ag spheres so that Ag spheres are well separated. Therefore this

system is close to the ideal situation of isolated silver sphere systems used in the electromagnetic theory of SERS. Fig E5-3 shows a SERS spectrum of purple membrane in hydrosol excited by 407 nm laser line.

However, in order to conclude that the SERS effect in this case is due to electromagnetic effect only, we need to compare the experimental result and theory in some more detail. One apparent discrepancy is that the SERS peak width obtained in the experiments is much broader than the value calculated, which is also true in the case of absorption spectrum. Furthermore, electromagnetic theory predicts that the SERS excitation profile has two features, one associated with the incident resonance, the other with the scattered resonance. However there is no definite reports of doublet in any SERS excitation profiles.

One explanation about this discrepancy was suggested by Kreibig and Fragstein (1969) in their study of absorption spectra of small silver spheres. The basic idea is that when the silver particle size is smaller than the conduction electron free path length, which is about 300 angstroms in case of silver, the dielectric constant ε obtained in the bulk silver has to be modified.

According to extended Drude theory (Frohlich, 1936) the dielectric constant ε consists of the additive contributions from conduction electrons A1, A2 and bound electrons B1, B2.

$\varepsilon = A1 + B1 + i(A2 + B2)$

The contribution from conduction electrons are:

$$A1 = 1 - \frac{\omega_p^2 \tau^2}{1 + \omega^2 \tau^2}$$

$$A2 = \frac{\omega_p^2 \tau}{\omega (1 + \omega^2 \tau^2)}$$

where

$$\tau^{-1} = \sum \tau_i^{-1}$$

are collision times caused by phonons, impurities and defects. When $\tau * v_F$ (Fermi velocity of the conduction electron) > R (the radius of sphere), the collision of the conduction electron with the particle surface become important as an additional collision process and the collision time is then less than that in the bulk metal. It has been proved that the mean free path of collisions of conduction electrons with the spherical particle surfaces is R (Euler, 1954). Therefore

$$\tau(R)^{-1} = \tau^{-1} + v_F/R$$

In order to obtain size dependent dielectric constant $\varepsilon(\omega,R)$, A1 and A2 have been calculated with the bulk value of τ_s and ω_p (Johnson and Christy, 1972) and then subtracted from the measured bulk values to obtain the bound electron contribution B1 and B2. By using the size dependent $\tau(R)$, the corresponding quantities A1(R) and A2(R) were found. Then

$$\varepsilon(\omega,R) = A1(R) + B1 + i\,[A2(R) + B2]$$

is the size dependent dielectric constant. The absorption spectrum calculated with this $\varepsilon(\omega,R)$ was in good agreement with the experiment in the photosensitive glass (Kreibig and Fragstein, 1969). The free path effect was suggested to be the major factor which influences the shape and the band width of the absorption spectrum for small silver spheres. Therefore it is reasonable to extend the usage of $\varepsilon(\omega,R)$ in the calculation of SERS profile.

Fig E5-4a shows the calculated SERS profile of a 1400 cm^{-1} Raman band by using the bulk $\varepsilon(\omega)$. Fig E5-4b shows the calculated SERS profile of a 1400 cm^{-1} Raman

band by using size dependent $\varepsilon(\omega,R)$ with the average radius of 50 angstroms and a Guassian distribution half width 30 angstroms. These two parameters, the average radius and half width of the distribution used for the calculation of the SERS profile, were obtained by fitting the absorption spectrum of the Ag sol. Fig E5-4c is the SERS profile of 1370 cm^{-1} band from purple membrane. In this figure, the molecular dipole was supposed to be parallel to the silver surface. The result for the molecular dipole perpendicular to the surface was similar. Although there were not enough experimental data points to determine its real shape, they set the limit on the SERS peak width which was much narrower than any of the previously observed SERS peak in aggregated Ag hydrosols and closer to our calculated value.Thus, both the SERS profile maxmum and width are in very good agreement with the prediction of the electromagnetic theory. Therefore, we believe that electromagnetic effect in our SERS experiment is the predominant factor.

Our calculation on the distance dependence of SERS enhancement factor G shows that it drops two orders of magnitude in the first 25 angstroms when the molecular dipole is moved away from the surface of the Ag sphere. This means that no decent Raman signal of those amino acid residues of purple membrane will be detected if Ag sphere are not in contact with them.One possible application of the SERS to the purple membrane is to identify certain amino acid residues in bacteriorhodopsin. It has been found that certain amino acid residues of bR can be chemically modified and the success of the modification can be easily verified by absorption spectroscopy. For example, four tyrosine residues, 26, 64, 131, and 133 can be nitrated by treating purple membrane with tetranitromethane to form nitrotyrosine. The chemical study shows that three out of these four residues are on the surface of the membrane (Lemke and Oesterhelt, 1981). Since the nitrated purple membrane changes its absorption maximum from 570 nm to

530 nm, it is easy to monitor the nitration of the purple membrane. The SERS spectrum of the nitrated purple membrane is shown in Fig. E5-5c. For a comparison, Fig E5-5a, b, d show the Raman spectra of nitrotyrosine, SERS of nitrotyrosine, and SERS of purple membrane, respectively. The new band appeared at 1336 cm^{-1} in nitrated purple membrane SERS spectrum comparing with the SERS spectrum of purple membrane, as well as the similar band appeared in the SERS spectrum of nitrotyrosine, indicate that some of the nitrated tyrosines are indeed on the surface of the membrane, which verifies the conclusion of the chemical study by Lemke and Oesterhelt (1981).

Some residues with COO- group can be labeled with ANTS and subsequent wash changes its absorption maximum to 600 nm, same as deionized blue membrane (Chang et al., 1985). Thus, the success of the labeling is easy to verify. Fig.E5-6 shows the Raman spectrum of ANTS. However, the SERS study of the ANTS labeled purple membrane does not show any difference with the unlabeled purple membrane. An interpretation of the above SERS study of the purple membrane is that the silver particles only attached to one surface of the purple membrane, on this surface, the tyrosine residues 64, 131, and 133 are located. The residues which can be labeled by ANTS is on the other side of the membrane, therefore, the Raman bands of the ANTS can not be enhanced by SERS effect because the 45 angstroms thickness of the membrane prevents the effective enhancement of the Raman scattering from ANTS . This picture of the purple membrane is consistent with various models of bR suggested by the chemical studies (Ovichinnikov, 1982; Wallace, 1982). According to those models, tyrosines which can be nitrated are located at the outer surface of the membrane. The residues with carboxyl group are mostly located at the inner surface of the membrane. In the future,by modifying selected amino residues and using this SERS technique, more detailed informations about the structure of bR should be revealed.

Table 1. C=N band positions (cm-1) for varies protonated and deuterated Schiff bases.

Species	C=NH	C=ND	^{13}C=NH	^{13}C=ND	DC=NH	DC=ND
Rhodopsin	1656	1625	1645	1609(a)	1648(b)	1610(c)
Bathorhodopsin	1656	1625	1645	1600?	1648(b)	1602(c)
Isorhodopsin	1656	1631	1647	-	1648(b)	1614(c)
bR(d)	1640	1624	1623	1607	-	-
L(d)	1644	1620	1626	1603	-	-
PBS in MeOH(c)	1656	1632	1637	1614	1641	1618
PBS in CH2Cl2(c)	1653	1632	1632	1612	1639	1618

(a): See text for discussion.

(b): Data from Raman spectra in Eyring et al.(1982).

(c): Data from IR spectra in Bagley et al.(1985).

(d): Data from our unpublished results.

Others are from our Raman spectra in this work.

Table 2. The normal modes calculated for rhodopsin.

Table 2a

HC=NH									
Exp	Cal	C5=C6	C7=C8	C9=C10	C11=C12	C13=C14	C15=N	RamanI	IRI
1549	1549		-0.24	-0.21	-0.15			1.00	0.61
1582	1583		0.14		-0.10	-0.30		0.41	0.32
1599	1598		-0.11	0.28	-0.20			0.11	0.74
1609s	1606		0.22	-0.11	-0.20	0.17		0.38	0.77
1636	1635	-0.38		0.084				0.00	0.02
1657	1657						0.31	0.10	0.93

Table 2b

HC=ND									
Exp	Cal	C5=C6	C7=C8	C9=C10	C11=C12	C13=C14	C15=N	RamanI	IRI
1547	1548		-0.23	-0.20	-0.17			1.00	0.90
1572	1577		0.15	0.11	-0.11	-0.22	-0.16	0.41	0.82
1598	1595		0.10	-0.24	0.17	-0.20	0.10	0.06	0.82
	1605		-0.23	0.17	0.13	-0.18		0.20	0.50
1625	1625				-0.19		0.27	0.00	0.19
1635s	1637	-0.38		0.08				0.00	0.01

Table 2c

$H^{13}C$=NH									
Exp	Cal	C5=C6	C7=C8	C9=C10	C11=C12	C13=C14	C15=N	RamanI	IRI
1547	1549		-0.24	-0.21	-0.15			1.00	0.66
1580	1582		0.13		-0.09	-0.29		0.43	0.44
1598	1597		-0.10	0.28	-0.20	0.10		0.12	0.88
1609s	1606		-0.23	0.12	0.19	-0.17		0.37	0.78
1635	1636	-0.37						0.01	0.13
1645	1640				-0.12		0.27	0.04	0.79

Table 2d

$H^{13}C$=ND									
Exp	Cal	C5=C6	C7=C8	C9=C10	C11=C12	C13=C14	C15=N	RamanI	IRI
1546	1546		-0.21	-0.19	-0.17		-0.11	1.00	1.00
1567s	1570		0.16	0.14		-0.15	-0.21	0.25	0.89
1599	1593		0.10	-0.19	0.12	-0.27	0.12	0.01	0.54
	1604		-0.21	0.22		-0.18	0.09	0.07	0.20
1609	1613		-0.10		0.27		-0.18	0.12	0.12
1634	1636	-0.38		0.09				0.00	0.00

Table 2e

DC=NH									
Exp	Cal	C5=C6	C7=C8	C9=C10	C11=C12	C13=C14	C15=N	RamanI	IRI
1537	1538		-0.13	-0.13	-0.16	-0.25		1.00	0.85
	1559		-0.23	-0.18		0.24		0.03	0.03
1585									
1599	1597		0.09	-0.28	0.22	-0.09		0.12	0.91
	1605		-0.25	0.12	0.21	-0.12		0.39	0.86
1634	1637	-0.39						0.00	0.02
1548	1655				-0.10		0.30	0.05	0.86

Symbols used: HC=NH, native rhodopsin in H2O suspension; HC=ND native rhodopsin in D2O suspension; etc; Exp, experimental data from the Raman spectra; s, shoulder; Cal, Calculated normal modes by using the model rhodopsin described in the text; C=Cs and C=Ns, the contribution by these double bonds in the vectors corresponding to normal modes; RamanI, relative Raman intensities calculated by the method in Kakitani et al(1983); IRI, relative IR intensities calculated by the method given in text.

rms for this fitting is 2.48; the maximum deviation is 7 cm^{-1}.

Table 3. The effects on the C=N mode by changing each force constant or coupling constant.

Constant changed		C=NH Band(cm-1)		C15=ND Band(cm-1)	
K or C	Change	Position	change	Position	Change
Tatol Change	3.0-4.5 angstroms	1658->1639		-19	
C15=N	8.88 -> 8.48	1640	-18	1614	-11
C14-C15	6.7 -> 6.9	1660	+2	1627	+2
C13=C14	8.7 -> 8.35	1657	-1	1624	-1
C15=N-H	0.5 -> 0.41	1644	-14	1621	-4
C15=N,C14-C15	0.5 -> 0.6	1654	-4	1622	-3
C15=N,C13=C14	-0.15 -> -0.25	1660	+2	1628	+3
C15=N,C12-C13	0.15 -> 0.25	1662	+4	1630	+5
C14-C15,C13=C14	-0.15 -> -0.30	1660	+2	1628	+3
C14-C15,C12-C13	0.15 -> 0.25	1659	+1	1628	+3
C15=N,C14-C15=N	0.7 -> 1.05	1663	+5	1629	+4
C15=N,C15=N-H	-0.15 -> -0.13	1654	-4	1623	-2

The model rhodopsin configuration and the set of constants are the same as in table 2. The changes were calculated by the methods given in text. Symbols used: K, force constant, mdyn/angstrom in stretching(two atoms), mdyn angstrom/rad^2 in bending(three atoms); C, coupling constant, mdyn/angstrom in stretch-stretch, mdyn/rad in stretch-bend; Position, the calculated C=N band position after the constant is changed; Change, the change with respect to the original C=N band.

Table 4. The normal modes calculated by an alternative set of force constants.

Table 4a

HC=NH									
Exp	Cal	C5=C6	C7=C8	C9=C10	C11=C12	C13=C14	C15=N	RamanI	IRI
1549	1548		-0.23	-0.20	-0.17			1.00	0.74
1582	1581		0.15	0.10	-0.13	-0.24	-0.11	0.45	0.75
1599	1597		-0.12	0.28	-0.18	0.13		0.02	0.39
1609s	1606		0.22	-0.12	-0.19	0.19		0.20	0.38
1636	1636	-0.38		0.075				0.00	0.01
1657	1657					-0.13	0.30	0.08	1.00

Table 4b

HC=ND									
Exp	Cal	C5=C6	C7=C8	C9=C10	C11=C12	C13=C14	C15=N	RamanI	IRI
1547	1544		-0.20	-0.17	-0.18		-0.11	1.00	1.00
1572	1569		-0.18	-0.15		0.17	0.19	0.16	0.57
1598	1597		-0.14	0.27	-0.17	0.15		0.01	0.27
	1606		-0.23	0.10	0.21	-0.15		0.17	0.31
1625	1625				-0.22		0.26	0.00	0.33
1635s	1637	-0.38		0.08				0.00	0.00

Table 4c

$H^{13}C$=NH									
Exp	Cal	C5=C6	C7=C8	C9=C10	C11=C12	C13=C14	C15=N	RamanI	IRI
1547	1548		-0.23	-0.20	-0.17			1.00	0.84
1580	1579		0.15	0.10	-0.11	-0.24	-0.13	0.42	0.91
1598	1597		-0.11	0.27	-0.19	0.13		0.03	0.45
1609s	1606		-0.23	0.12	0.20	-0.16		0.20	0.36
1635	1636	-0.37						0.00	0.08
1645	1641				-0.16		0.27	0.04	1.00

Table 4d

$H^{13}C$=ND									
Exp	Cal	C5=C6	C7=C8	C9=C10	C11=C12	C13=C14	C15=N	RamanI	IRI
1546	1541		-0.16	-0.14	-0.18	-0.09	-0.17	1.00	1.00
1567s	1561		-0.20	-0.18		0.13	0.19	0.02	0.26
1599	1598		-0.12	0.27	-0.18	0.15		0.01	0.20
	1605		-0.23		0.23	0.09	0.06	0.19	0.18
1609	1615			0.09		-0.27	0.20	0.00	0.19
1634	1636	-0.38						0.00	0.00

Table 4e

DC=NH									
Exp	Cal	C5=C6	C7=C8	C9=C10	C11=C12	C13=C14	C15=N	RamanI	IRI
1537	1535		-0.13	-0.12	-0.17	-0.23	-0.10	1.00	1.00
	1559		-0.23	-0.18		0.22		0.02	0.01
1585									
1599	1596		0.06	-0.26	0.24	-0.11		0.10	0.73
	1605		-0.26	0.15	0.18	-0.11		0.25	0.40
1634	1636	-0.39						0.00	0.01
1548	1654				-0.07	-0.13	0.29	0.05	0.85

The configuration of this model rhodopsin is the same as that used in table 2. The changes in the set of force constants are given in the text. Symbols used: HC=NH, native rhodopsin in H2O suspension; HC=ND native rhodopsin in D2O suspension; etc; Exp, experimental data from the Raman spectra; s, shoulder; Cal, Calculated normal modes by using the model rhodopsin described in the text; C=Cs and C=Ns, the contribution by these double bonds in the vectors corresponding to normal modes; RamanI, relative Raman intensities calculated by the method in Kakitani et al(1983); IRI, relative IR intensities calculated by the method given in text.

rms for this fitting is 2.49; the maximum deviation is 6 cm^{-1}.

Table 5. The effects on the C=N mode by changing the configuration of the model Schiff base.

Table 5a

HC=NH								
Cal	C5=C6	C7=C8	C9=C10	C11=C12	C13=C14	C15=N	RamanI	IRI
1538		-0.18	-0.20	-0.20	-0.12		1.00	0.85
1580		-0.25			0.24		0.01	0.06
1602			0.24	-0.25	0.12		0.05	0.57
1614		0.21	-0.18	-0.13	0.19		0.13	0.13
1640	0.38						0.00	0.02
1658						0.31	0.07	0.81

Table 5b

HC=ND								
Cal	C5=C6	C7=C8	C9=C10	C11=C12	C13=C14	C15=N	RamanI	IRI
1536		-0.17	-0.19	-0.20	-0.12		1.00	1.00
1577		0.24	0.09		-0.20	-0.12	0.01	0.21
1596		-0.09	0.22	-0.16	0.18	-0.17	0.04	0.70
1614		0.20	-0.13	-0.18	0.19		0.13	0.13
1625			0.15	0.14	-0.09	0.25	0.03	0.34
1641	-0.38		-0.09				0.00	0.01

Table 5c

$H^{13}C$=NH								
Cal	C5=C6	C7=C8	C9=C10	C11=C12	C13=C14	C15=N	RamanI	IRI
1538		-0.18	-0.20	-0.20	-0.12		1.00	0.88
1579		0.25			-0.24		0.01	0.09
1602			-0.24	0.23	-0.12		0.06	0.67
1614		-0.21	0.17	0.14	-0.19		0.12	0.11
1637	0.26					0.23	0.04	0.53
1642	0.27		-0.11			-0.18	0.02	0.30

Table 5d

$H^{13}C$=ND								
Cal	C5=C6	C7=C8	C9=C10	C11=C12	C13=C14	C15=N	RamanI	IRI
1535		0.17	0.18	0.20	0.12	0.09	1.00	1.00
1571		-0.21	-0.13		0.13	0.20	0.01	0.43
1590		-0.16	0.15		0.23	-0.19	0.01	0.45
1611		0.14		-0.28	0.12	0.12	0.07	0.07
1617	-0.10	-0.15	0.24		0.16	-0.11	0.09	0.15
1640	0.38						0.00	0.00

Table 6. pH dependence.

bR in	mixed with	halftime(ms)
D2O(D) pD6	4M NaCl pH6.5	2.7
D2O(D) pD6	4M NaCl pH10.7	2.3
D2O(D) pD6	4M NaCl pH2.4	2.5
D2O(L) pD6	4M NaCl pH6.5	2.7
D2O(L) pD6	4M NaCl pH10.7	2.8
D2O(L) pD6	4M NaCl pH2.4	2.3

L stands for light adapted bR and D stands for dark adapted bR.

Table 7. Dark adaptation effect.

bR in	mixed with	halftime(ms)
D2O(L)pD6	H2O pH6.5	1.3
D2O(D)pD6	H2O pH6.5	2.8
D2O(L)pD10	H2O pH10.5	1.2
D2O(D)pD10	H2O pH10.5	2.6

L stands for light adapted bR and D stands for dark adapted bR.

Table 8. Ionic strength dependence.

bR in	mixed with	halftime(ms)
4M NaCl(L) pD6	4M NaCl pH6.5	2.5
1M NaCl(L) pD6	1M NaCl pH6.5	1.5
D2O(L) pD6	H2O pH6.5	1.3
4M NaCl(L) pD10	4M NaCl pH10.5	2.3
1M NaCl(L) pD10	1M NaCl pH10.5	1.5
D2O(L) pD10	H2O pH10.5	1.2

L stands for light adapted bR

Table 9. Aggregation effect.

bR in	mixed with	halftime(ms)
4M NaCl pD2.5	4M NaCl pH3	10*
1M NaCl pD2.5	1M NaCl pH3	4

* bR under this condition aggregates and shows little tendency of light adaptation.

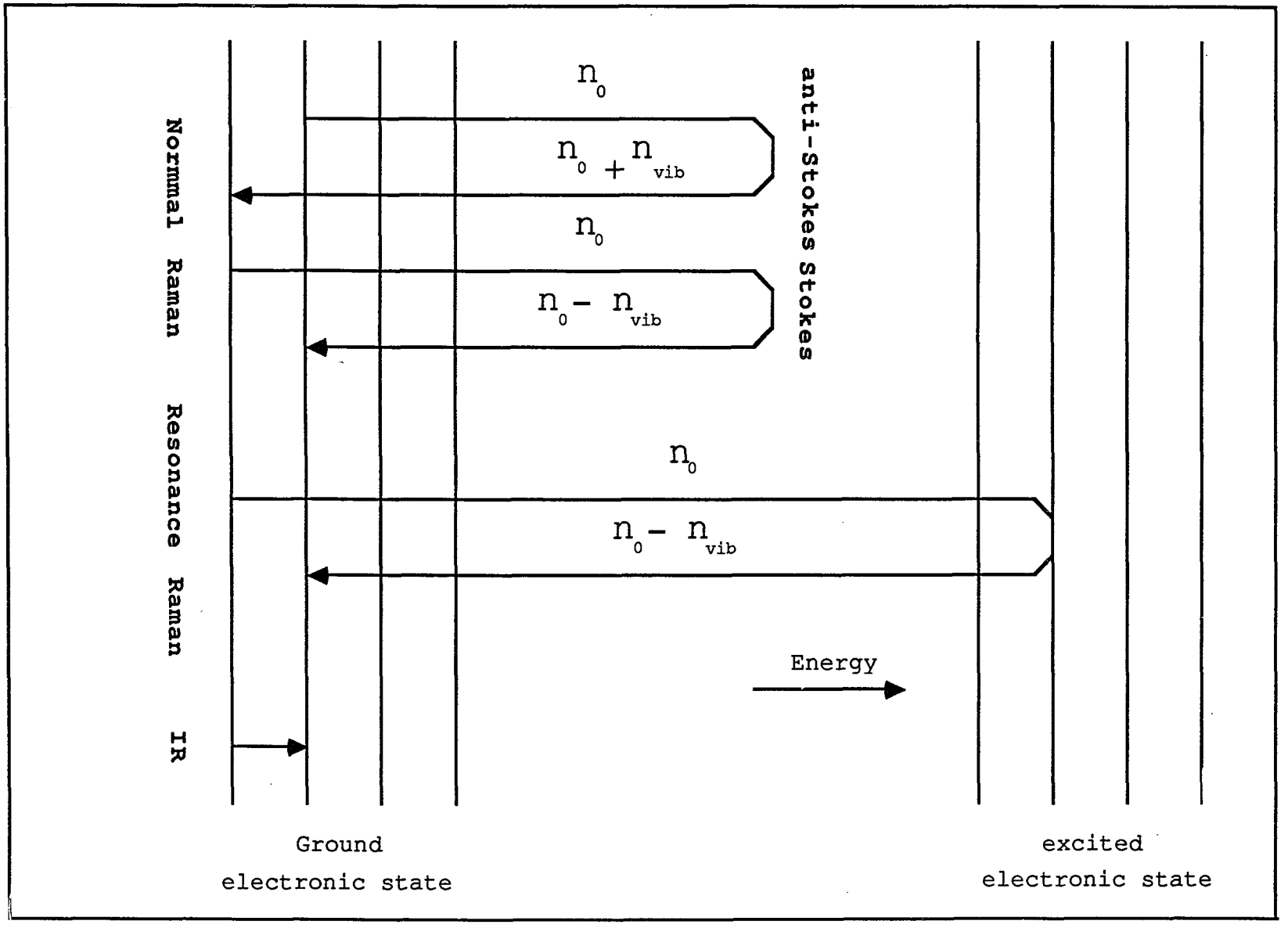
Normmal Raman
Resonance Raman
IR
anti-Stokes Stokes
n_0
$n_0 + n_{vib}$
n_0
$n_0 - n_{vib}$
n_0
$n_0 - n_{vib}$
Energy
Ground
electronic state
excited
electronic state

a

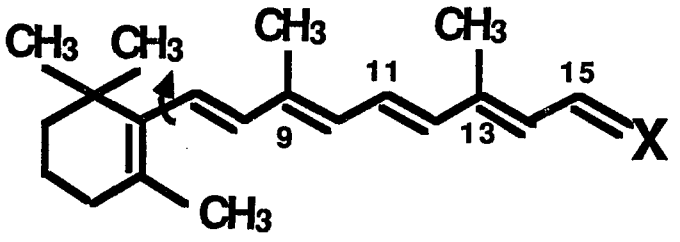
CH3
CH3
CH3
CH3
11
15
9
13
X
CH3

b

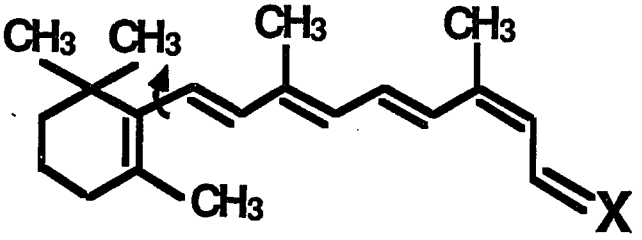
CH3
CH3
CH3
CH3
CH3
X

c

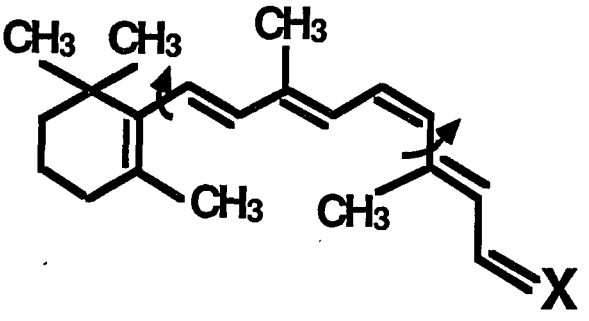
CH3
CH3
CH3
CH3
CH3
X

d

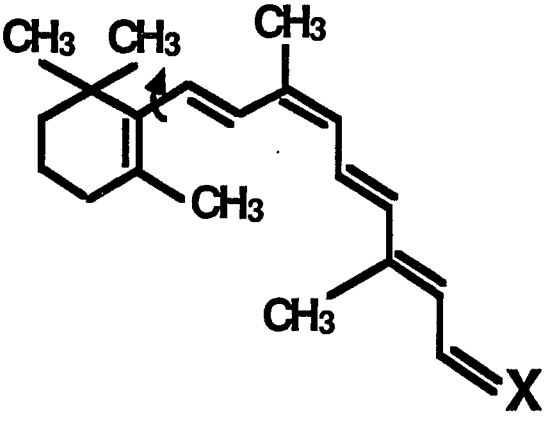
CH3
CH3
CH3
CH3
CH3
X

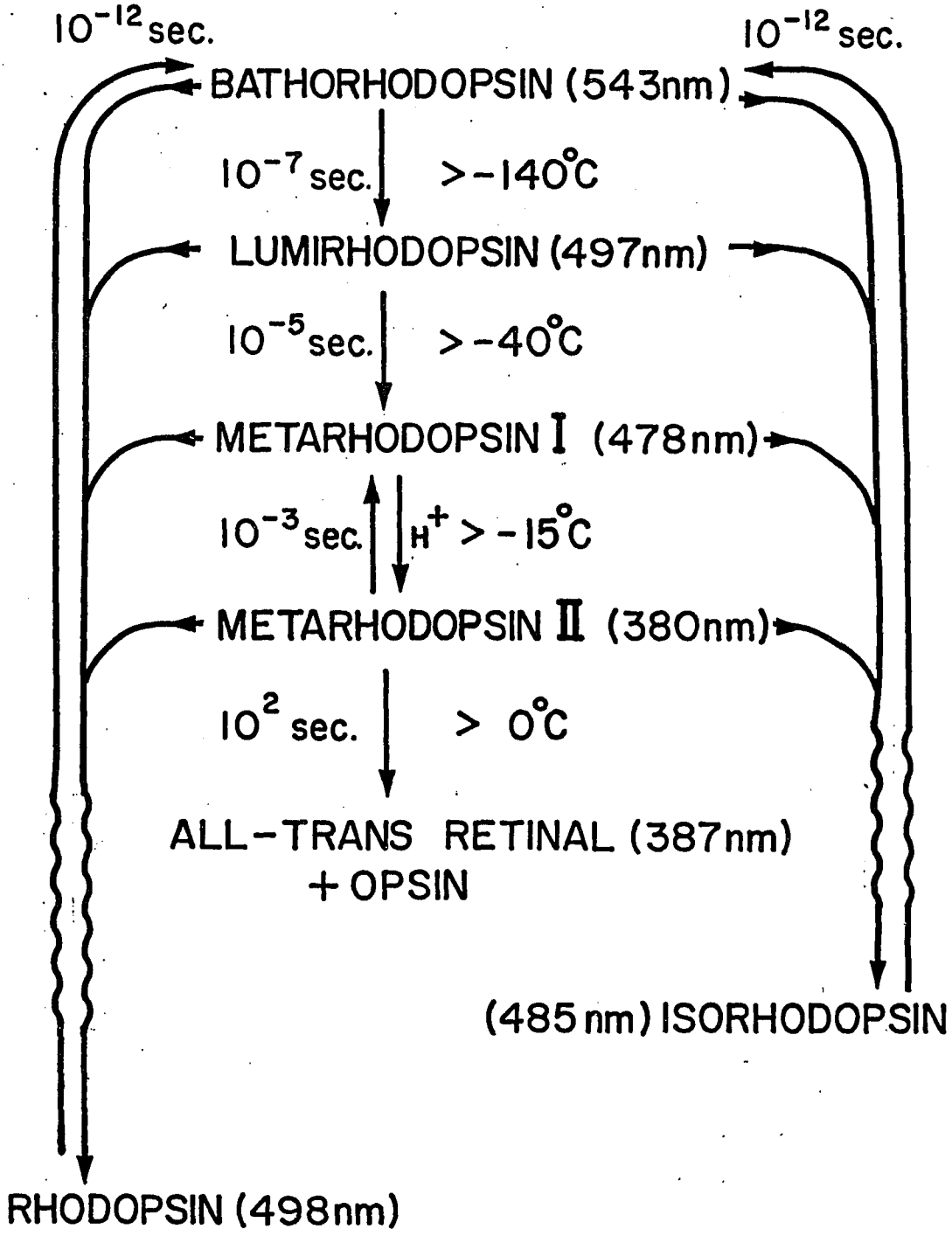
10^{-12} sec.
10^{-12} sec.
BATHORHODOPSIN (543nm)
10^{-7} sec.
>-140°C
LUMIRHODOPSIN (497nm)
10^{-5} sec.
>-40°C
METARHODOPSIN I (478nm)
10^{-3} sec.
H^+ > -15°C
METARHODOPSIN II (380nm)
10^{2} sec.
> 0°C
ALL-TRANS RETINAL (387nm)
+ OPSIN
(485 nm) ISORHODOPSIN
RHODOPSIN (498nm)

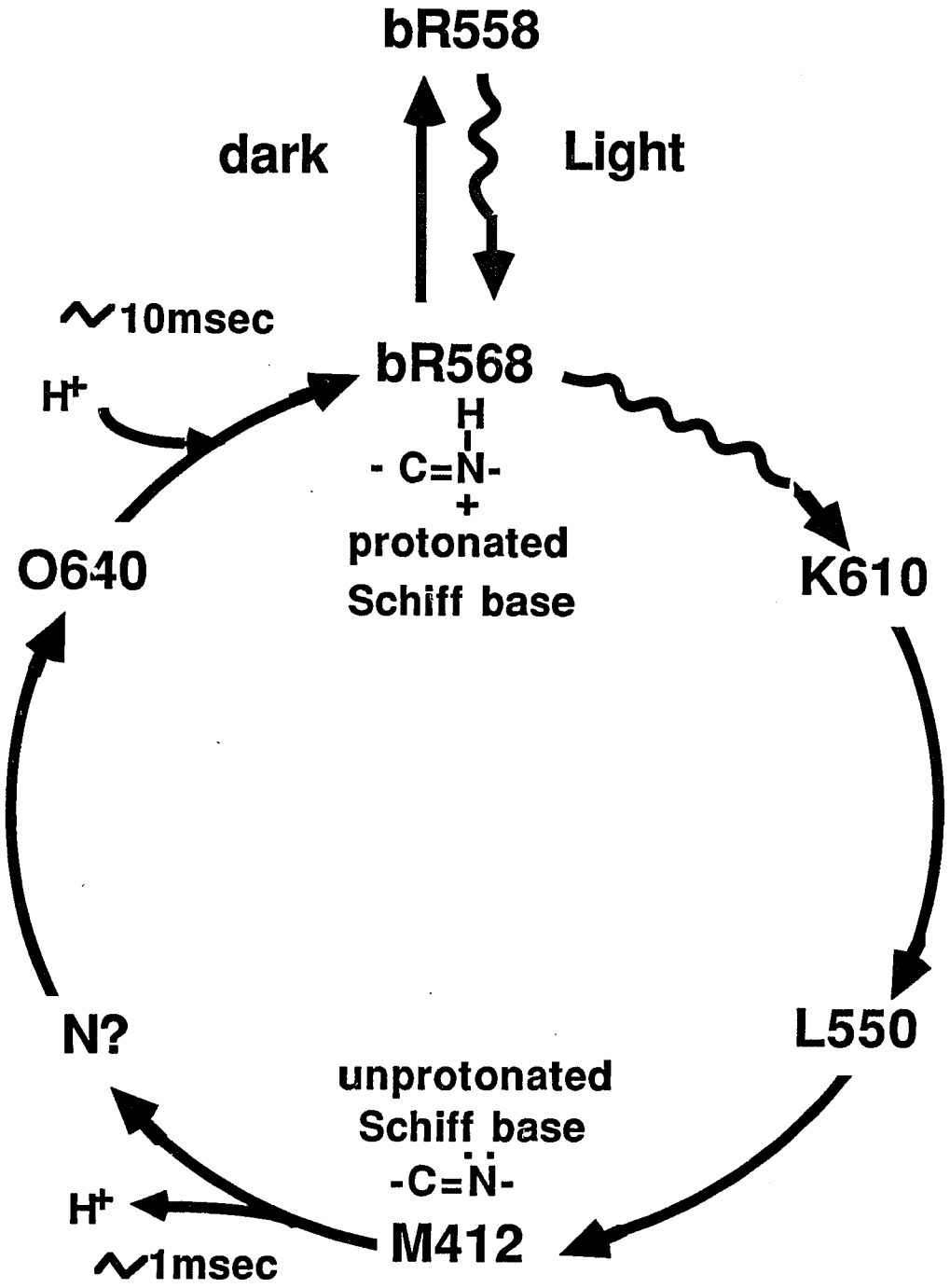
bR558
dark
Light
~10msec
H+
bR568
H
- C=N-
+
protonated
Schiff base
K610
L550
O640
N?
unprotonated
Schiff base
-C=N-
H+
~1msec
M412

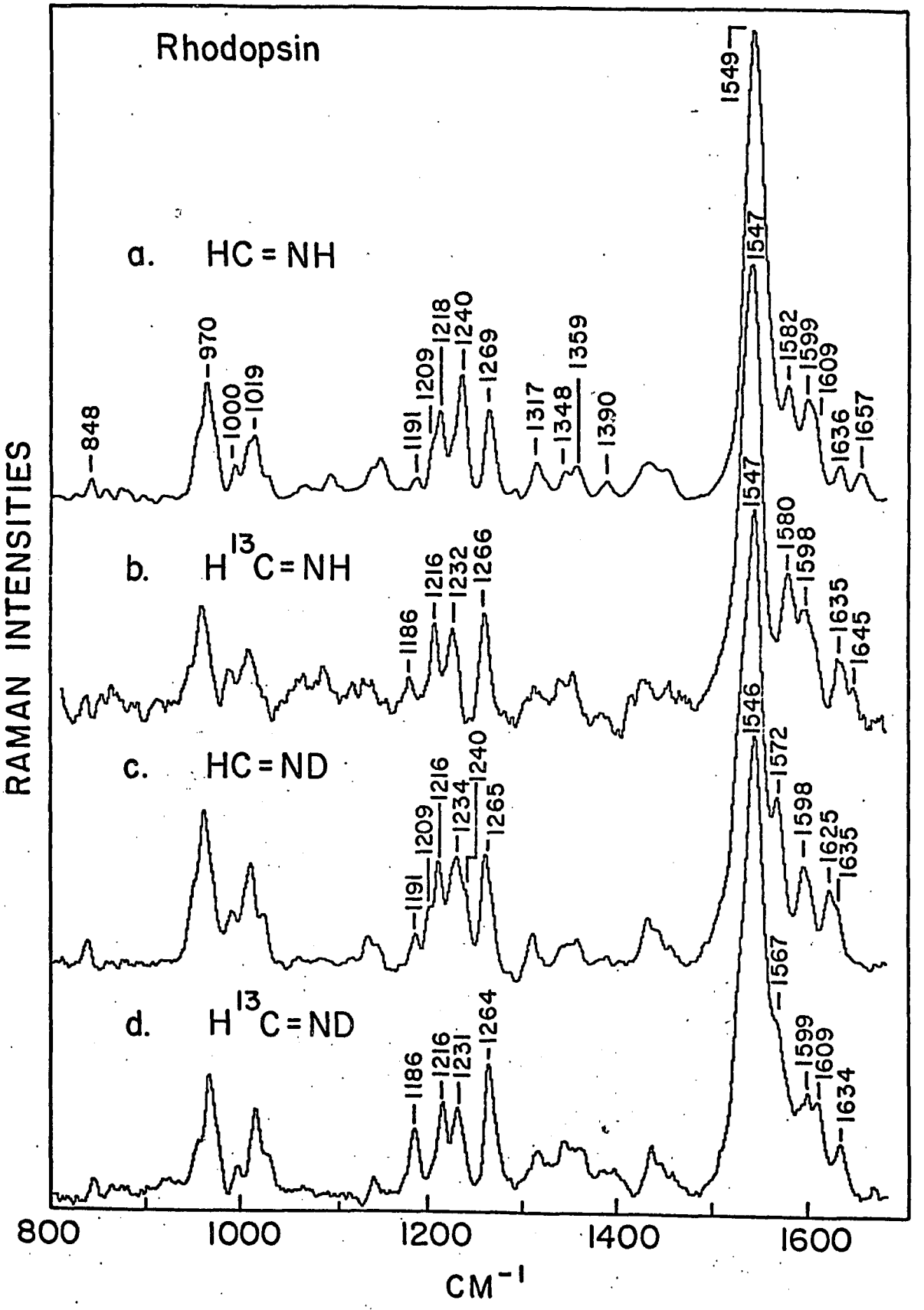
Rhodopsin
a. HC = NH
b. H13C = NH
c. HC = ND
d. H13C = ND
RAMAN INTENSITIES
800
1000
1200
1400
1600
CM-1
848
970
1000
1019
1191
1209
1218
1240
1269
1317
1348
1359
1390
1549
1547
1582
1599
1609
1636
1657
1186
1216
1232
1266
1580
1598
1635
1645
1546
1572
1191
1209
1216
1234
1240
1265
1598
1625
1635
1567
1186
1216
1231
1264
1599
1609
1634

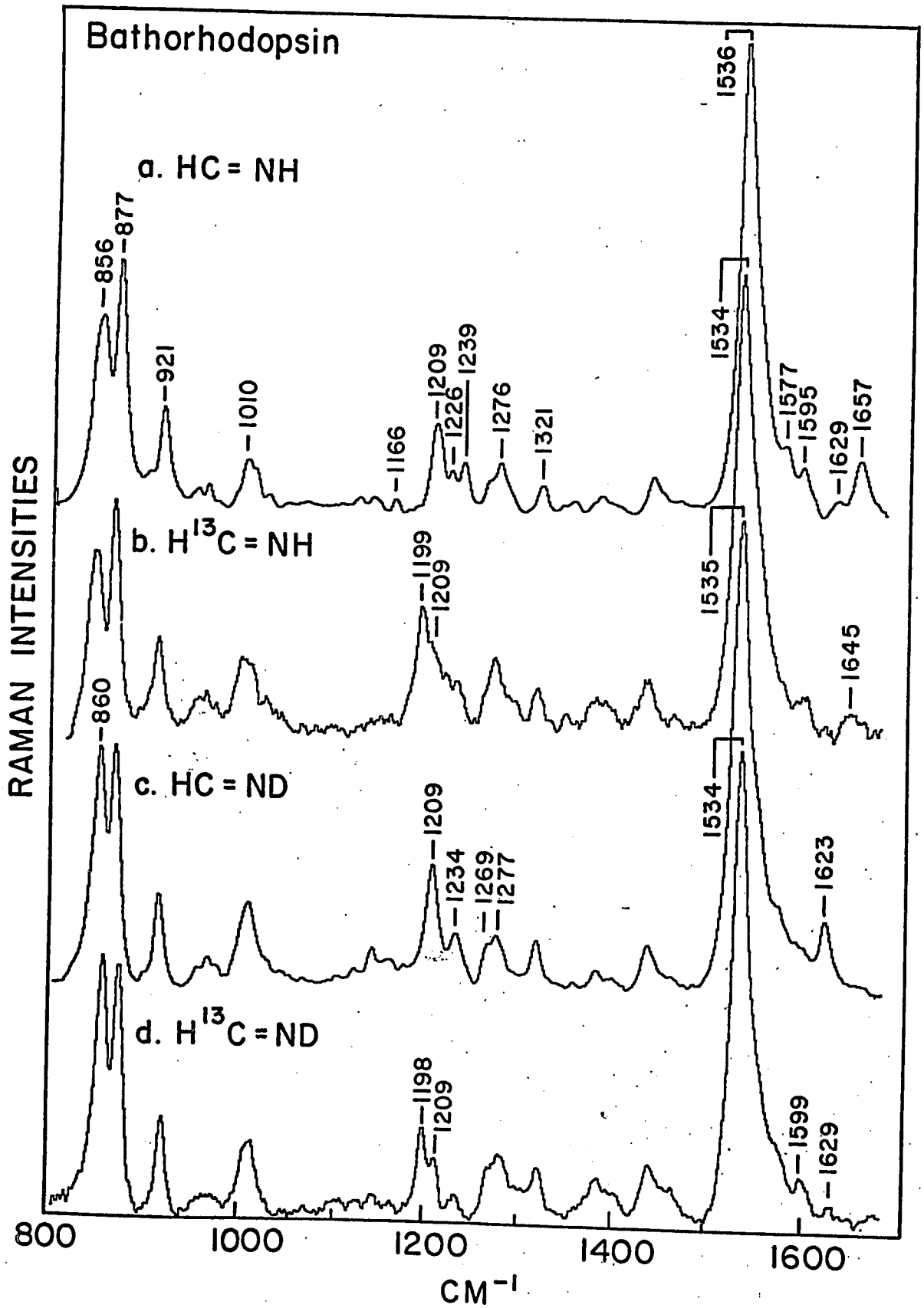
Bathorhodopsin
a. HC = NH
b. H13C = NH
c. HC = ND
d. H13C = ND
RAMAN INTENSITIES
800
1000
1200
1400
1600
CM-1
856
877
921
1010
1166
1209
1226
1239
1276
1321
1534
1536
1577
1595
1629
1657
860
1199
1209
1535
1645
1209
1234
1269
1277
1534
1623
1198
1209
1599
1629

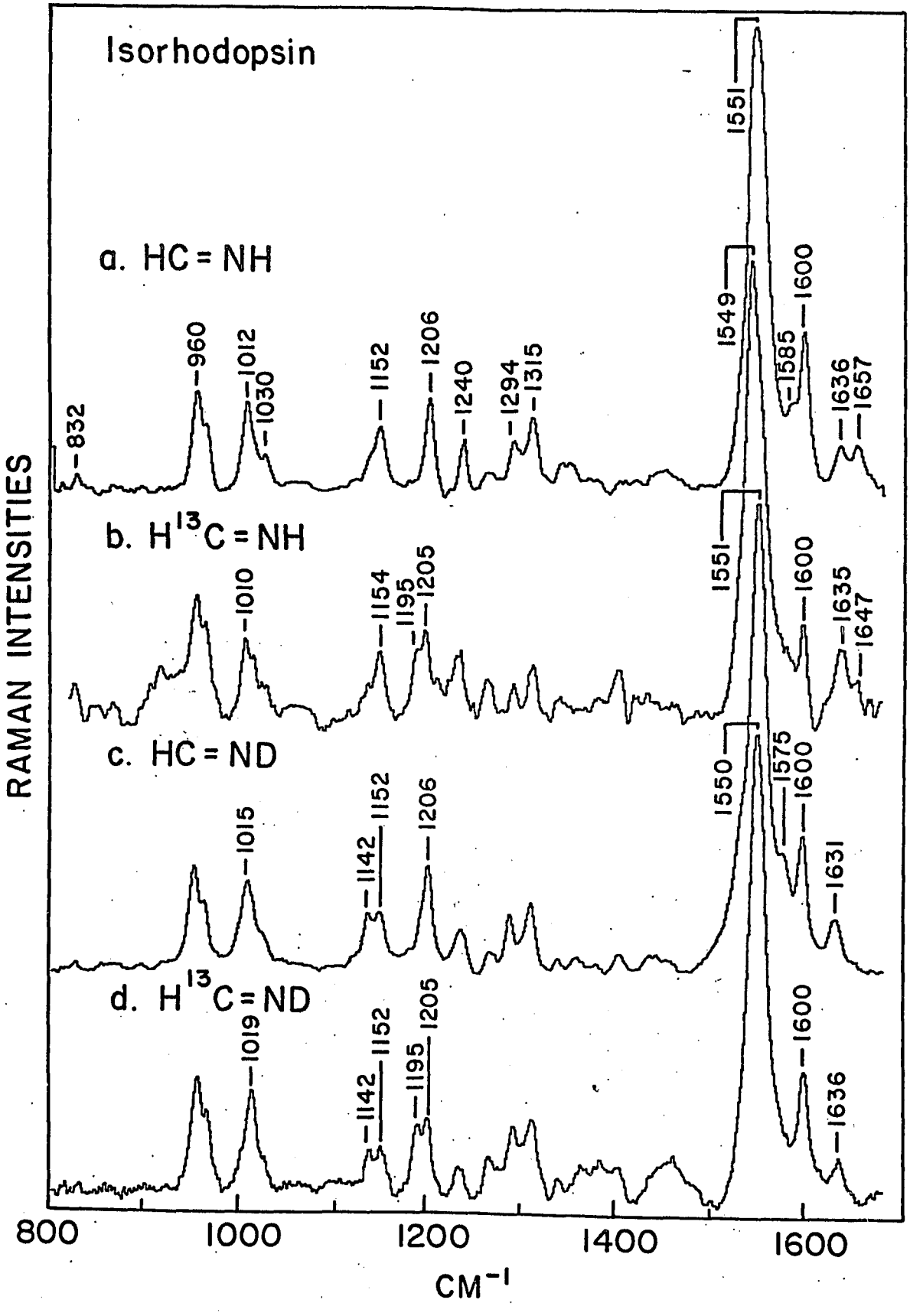
Isorhodopsin
a. HC = NH
b. H13C = NH
c. HC = ND
d. H13C = ND
RAMAN INTENSITIES
832
960
1012
1030
1152
1206
1240
1294
1315
1549
1551
1585
1600
1636
1657
1010
1154
1195
1205
1551
1600
1635
1647
1015
1142
1152
1206
1550
1575
1600
1631
1019
1142
1152
1195
1205
1600
1636
800
1000
1200
1400
1600
CM-1

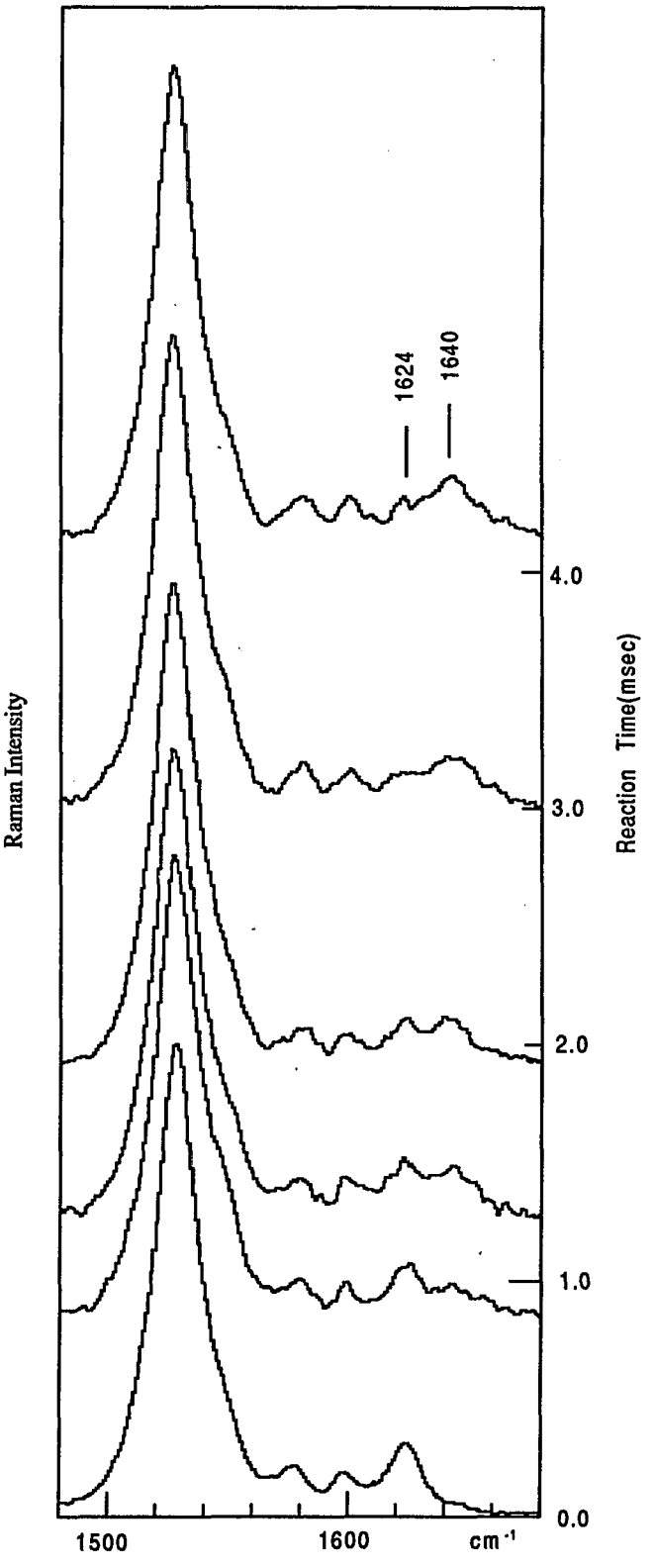
1624
1640
4.0
3.0
2.0
1.0
0.0
Raman Intensity
Reaction Time(msec)
1500
1600
cm⁻¹

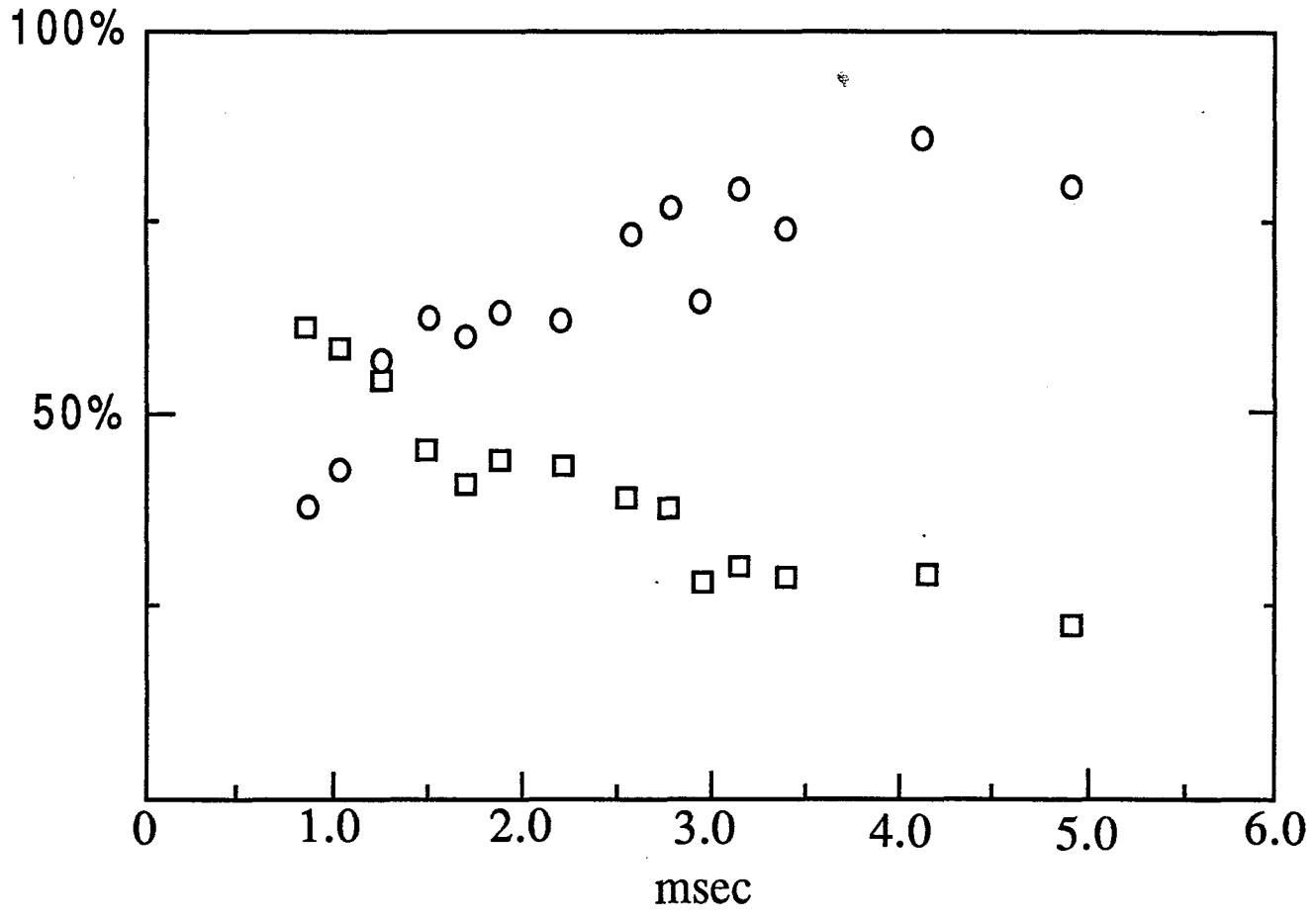
100%
50%
0
1.0
2.0
3.0
4.0
5.0
6.0
msec

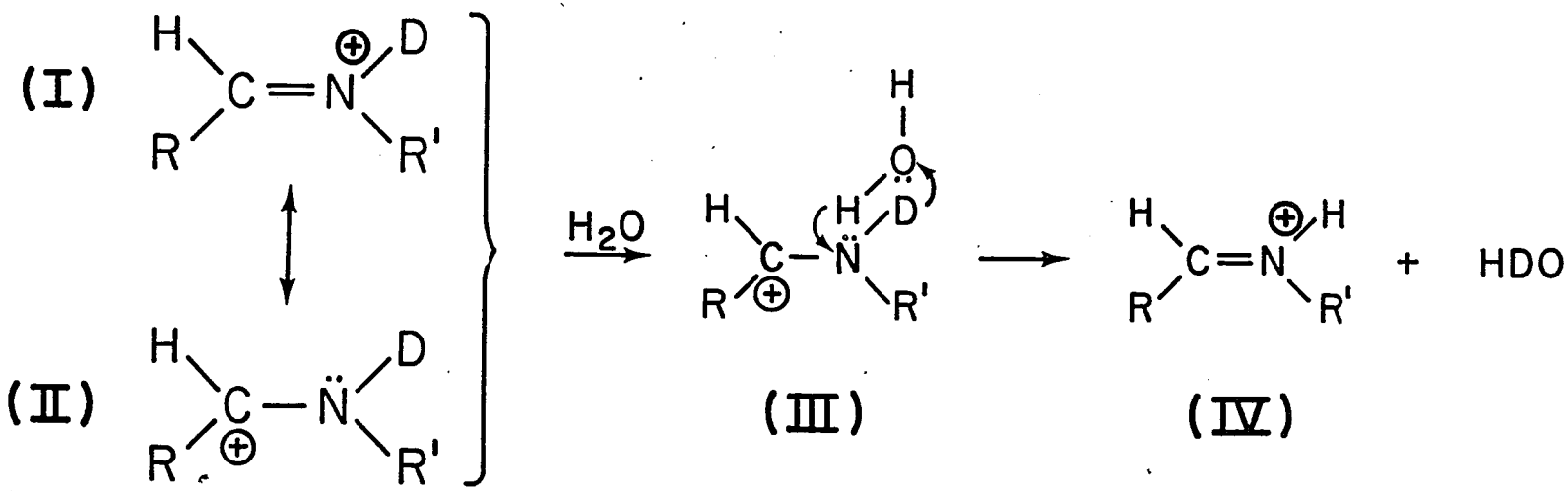
(I)
(II)
H2O
(III)
(IV)
+ HDO

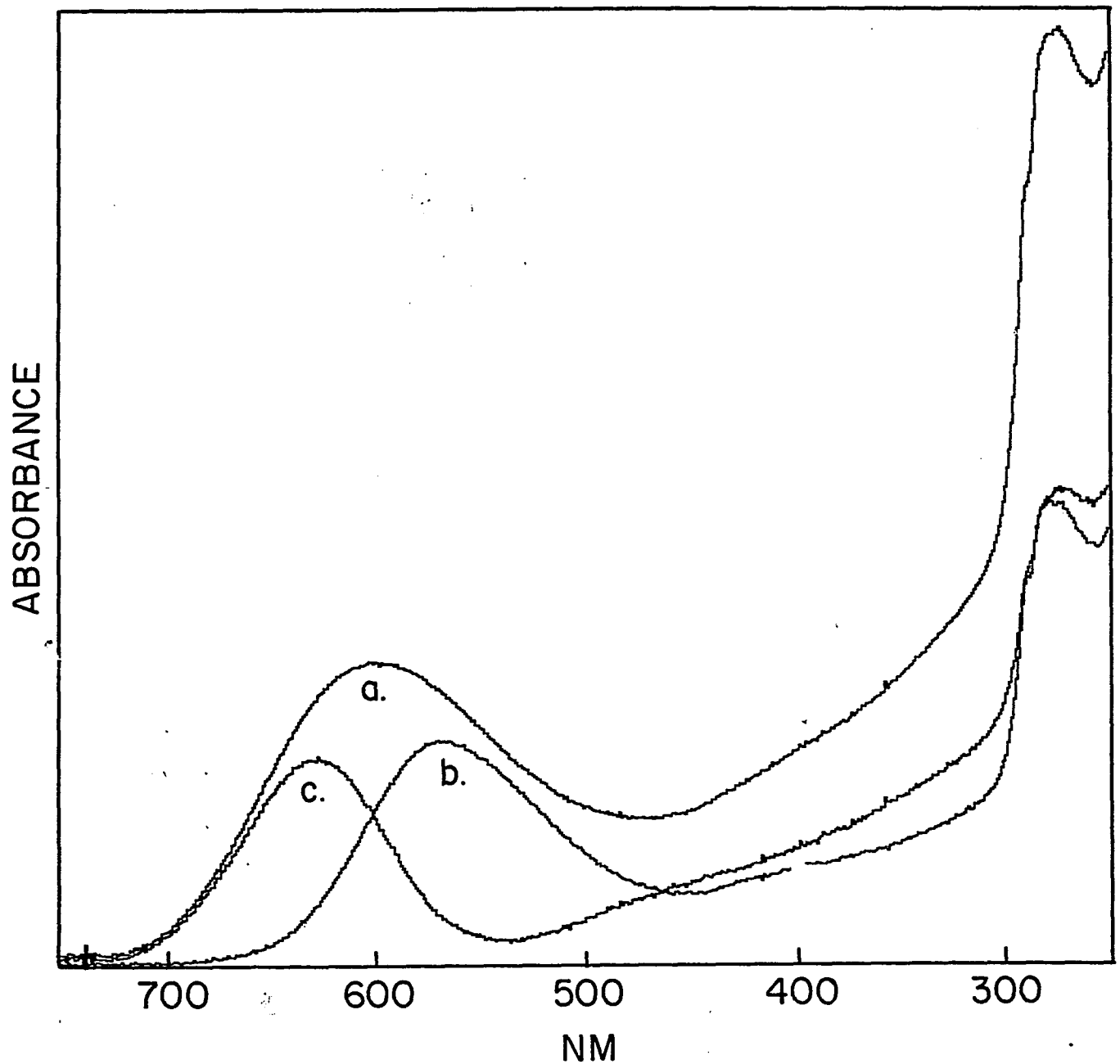
ABSORBANCE
a.
b.
c.
700
600
500
400
300
NM

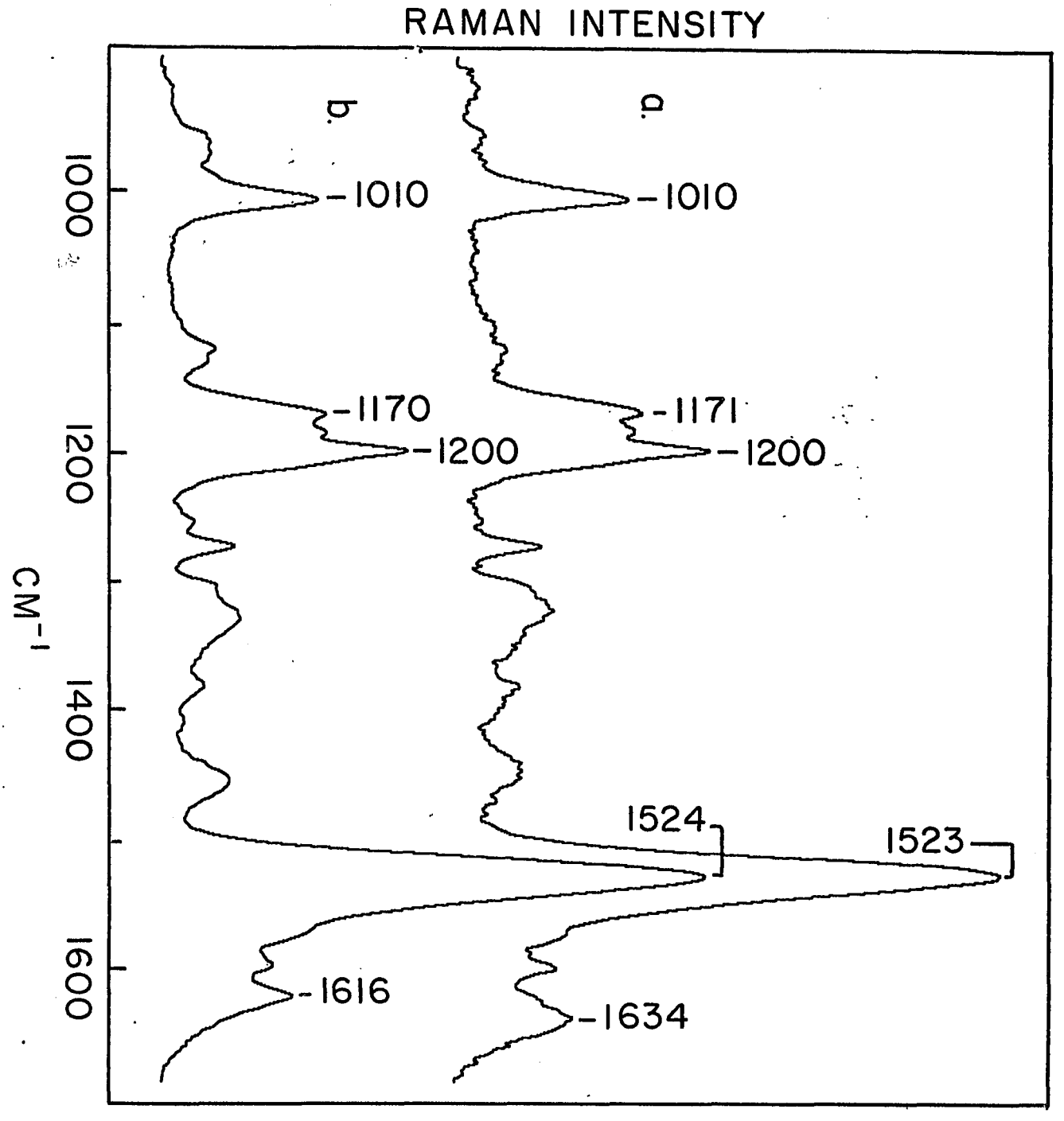
RAMAN INTENSITY
b
a
1010
1010
1170
1171
1200
1200
1524
1523
1616
1634
1000
1200
1400
1600
CM-1

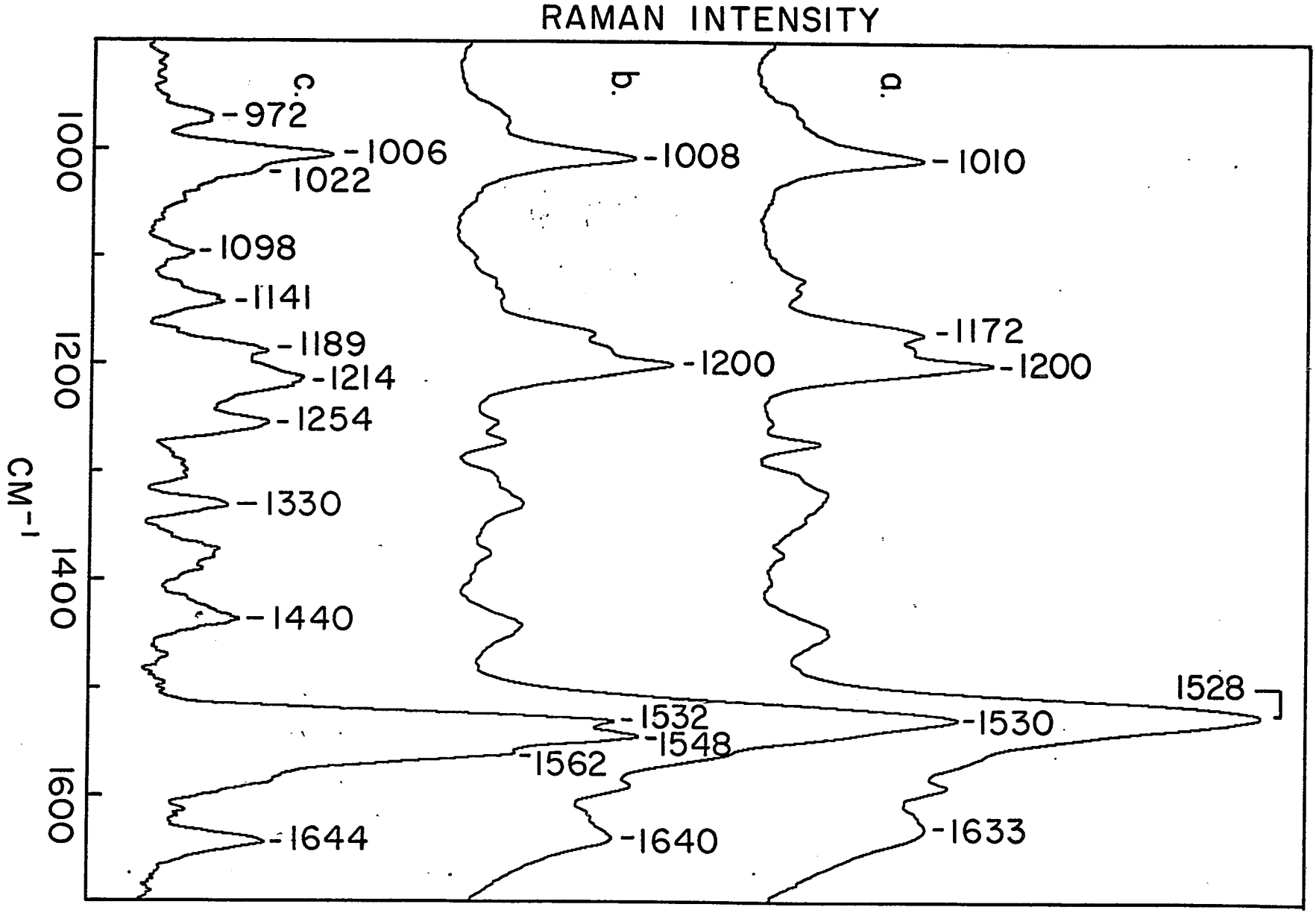
RAMAN INTENSITY
c
b
a
-972
-1006
-1022
-1098
-1141
-1189
-1214
-1254
-1330
-1440
-1532
-1548
-1562
-1644
-1008
-1200
-1640
-1010
-1172
-1200
1528
-1530
-1633
1000
1200
1400
1600
CM-1

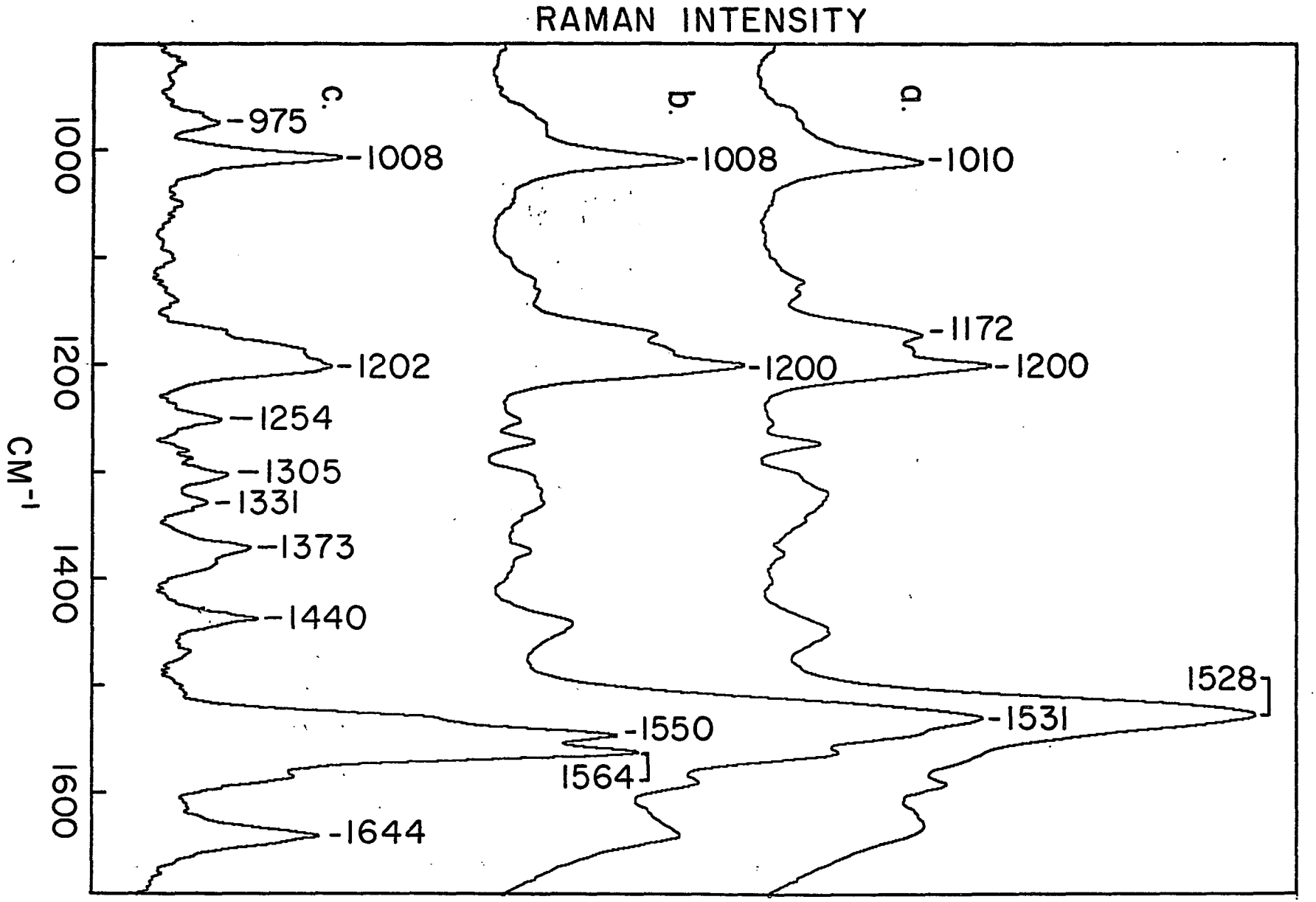
RAMAN INTENSITY
c
b
a
-975
-1008
-1008
-1010
-1172
-1202
-1200
-1200
-1254
-1305
-1331
-1373
-1440
1528
-1531
-1550
1564
-1644
1000
1200
1400
1600
CM-1

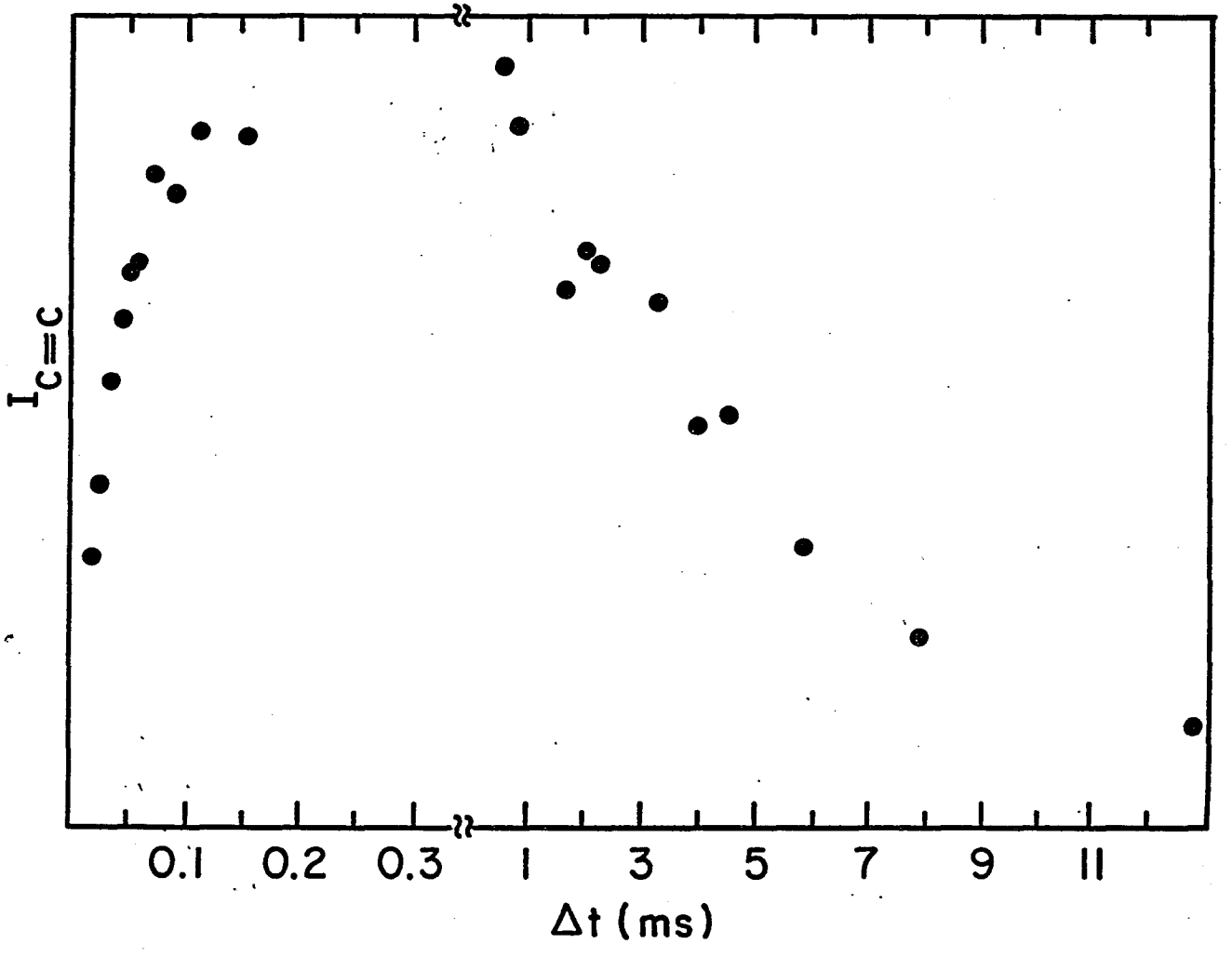
$I_{C=C}$
0.1
0.2
0.3
1
3
5
7
9
11
Δt (ms)

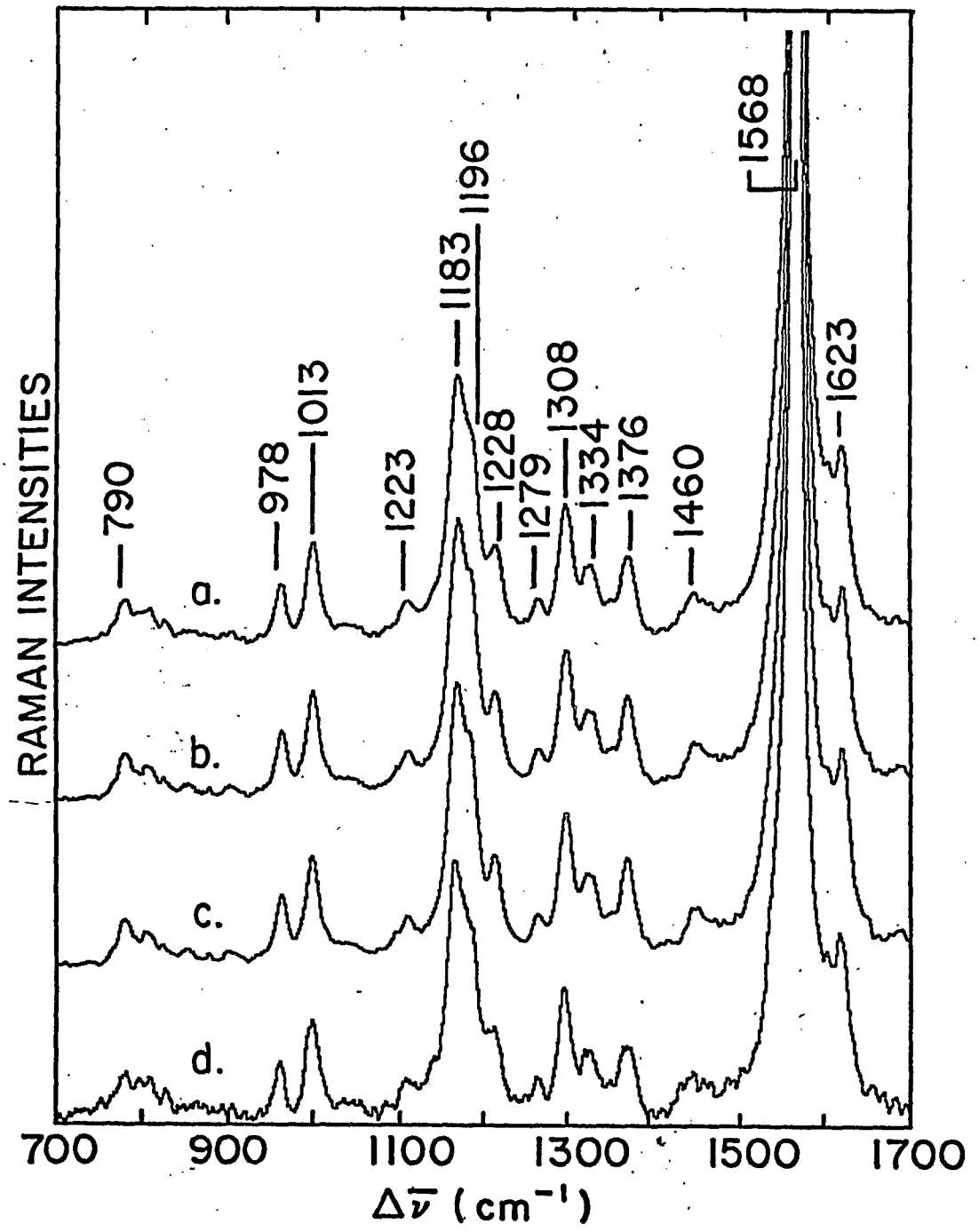
RAMAN INTENSITIES
790
978
1013
1223
1183
1196
1228
1279
1308
1334
1376
1460
1568
1623
a.
b.
c.
d.
700
900
1100
1300
1500
1700
Δν̄ (cm⁻¹)

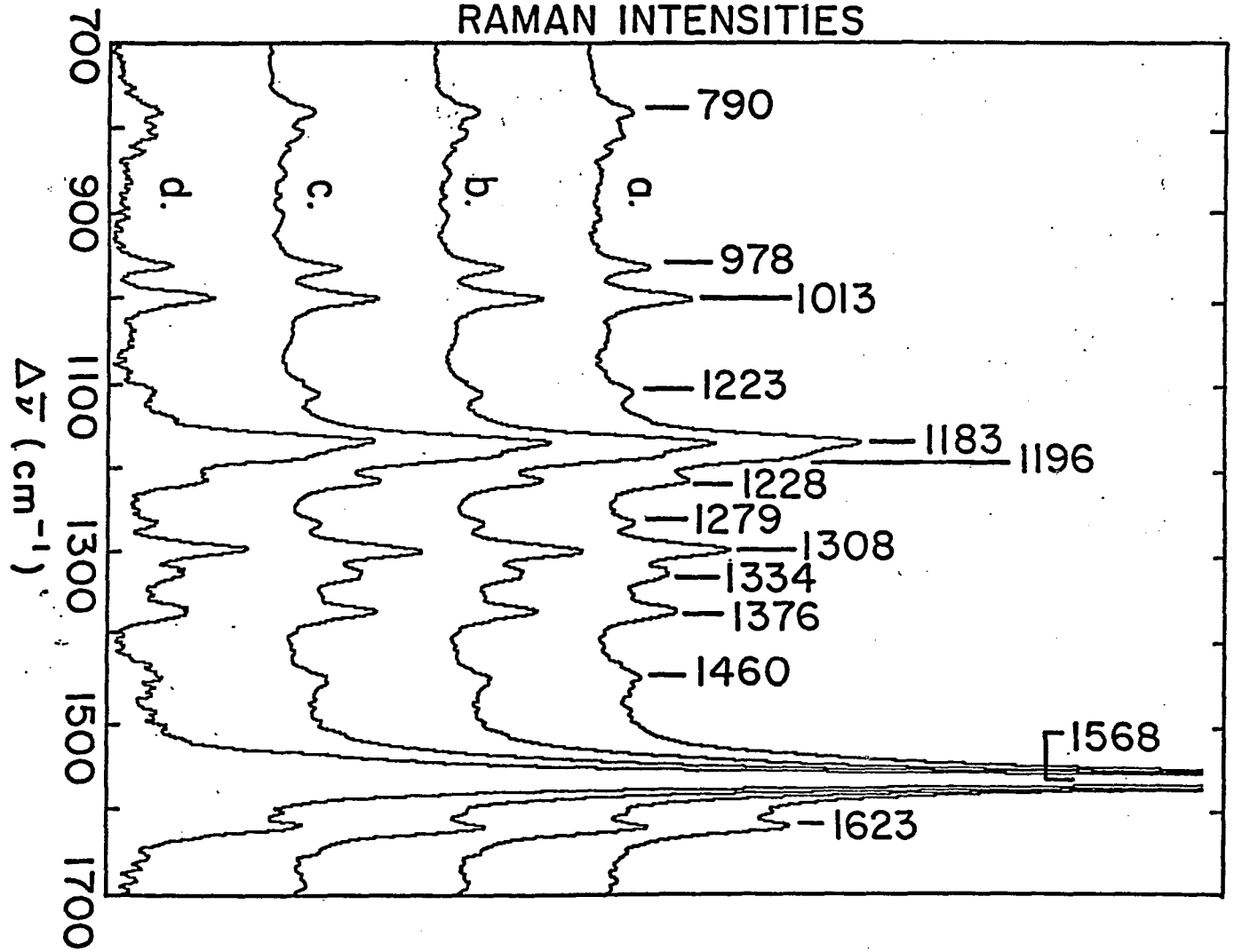
RAMAN INTENSITIES
700
900
1100
1300
1500
1700
Δν̄ (cm⁻¹)
d.
c.
b.
a.
790
978
1013
1223
1183
1196
1228
1279
1308
1334
1376
1460
1568
1623

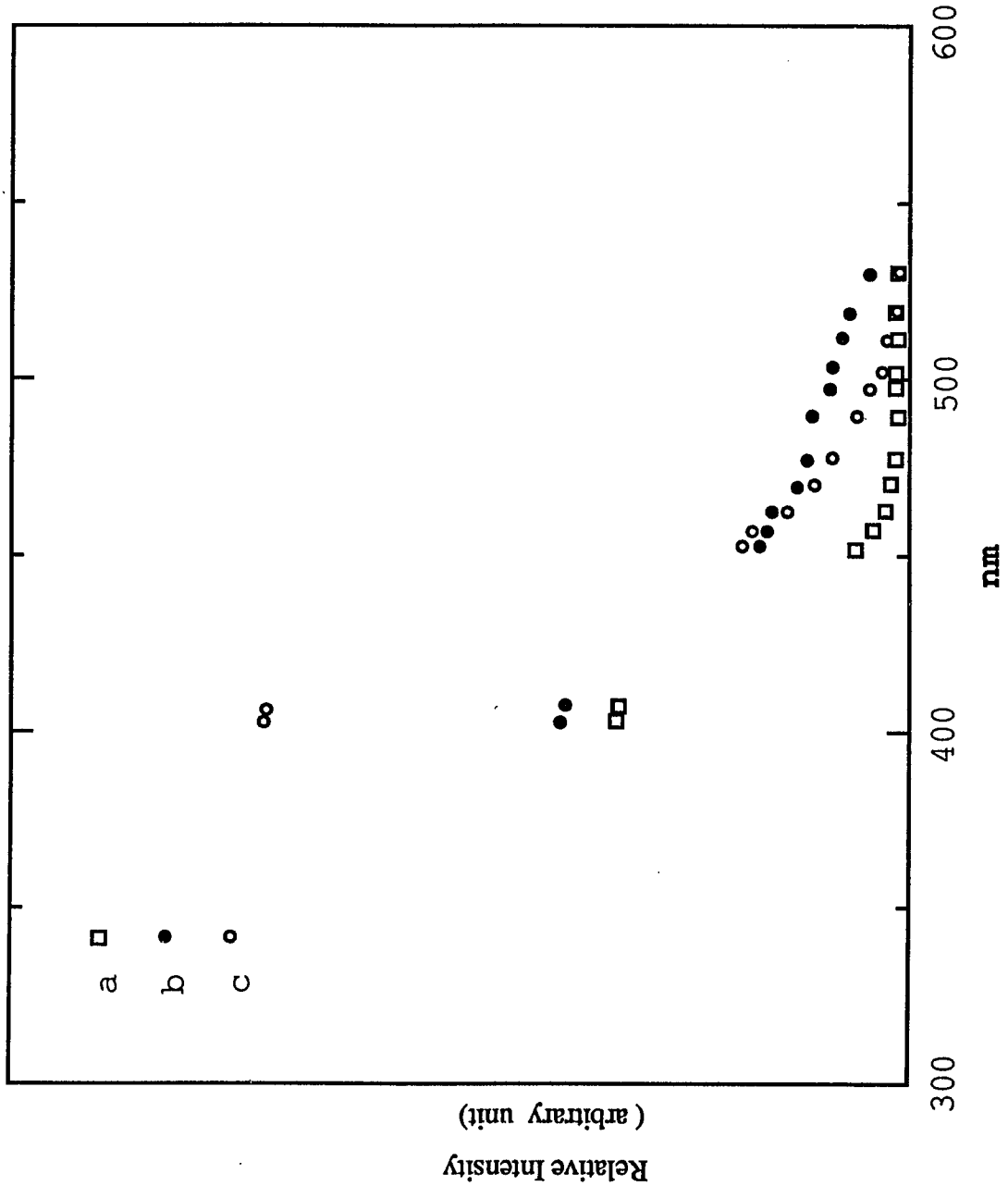
Relative Intensity
(arbitrary unit)
300
400
500
600
nm
a
b
c

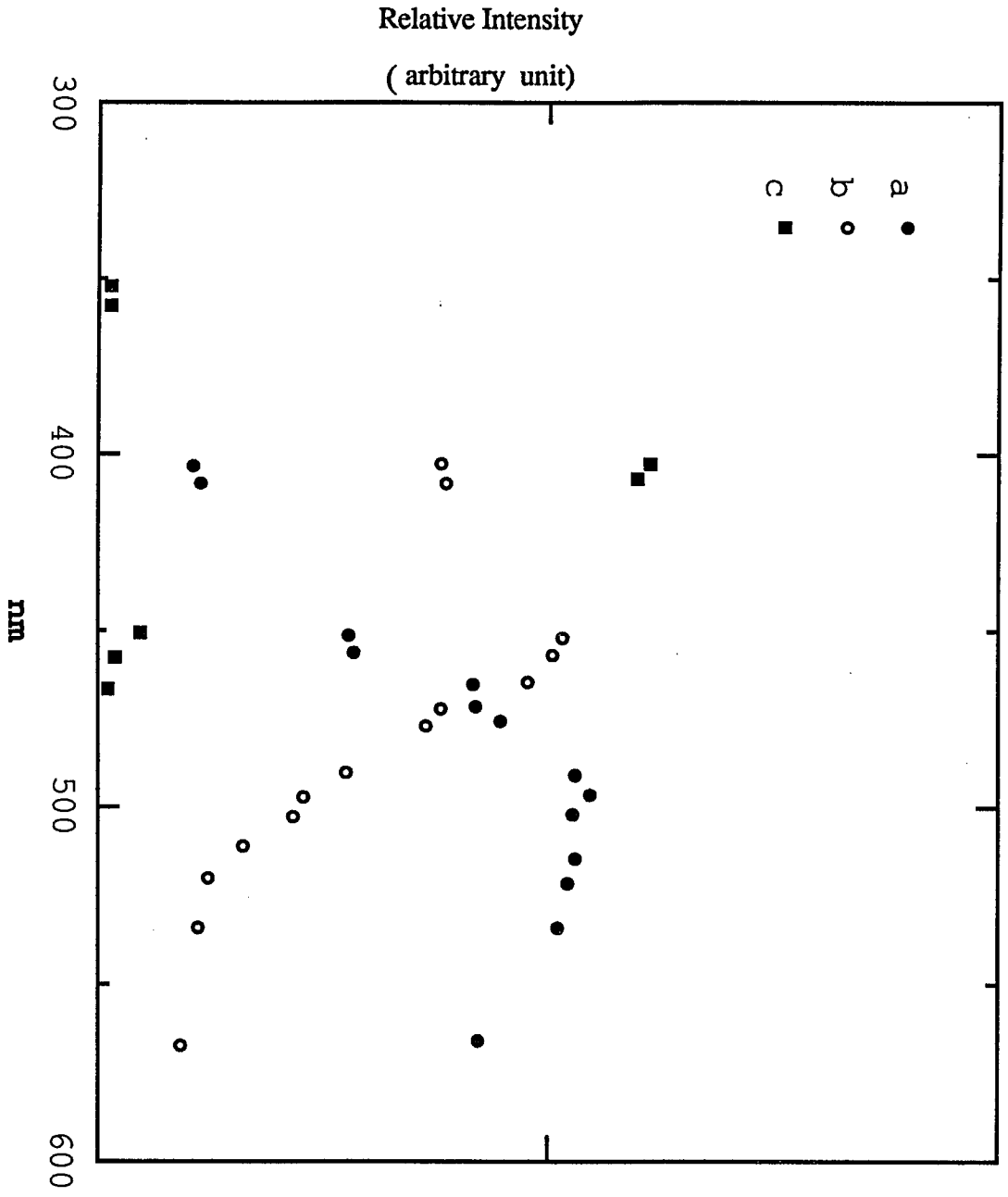
Relative Intensity
(arbitrary unit)
300
400
500
600
nm
a
b
c

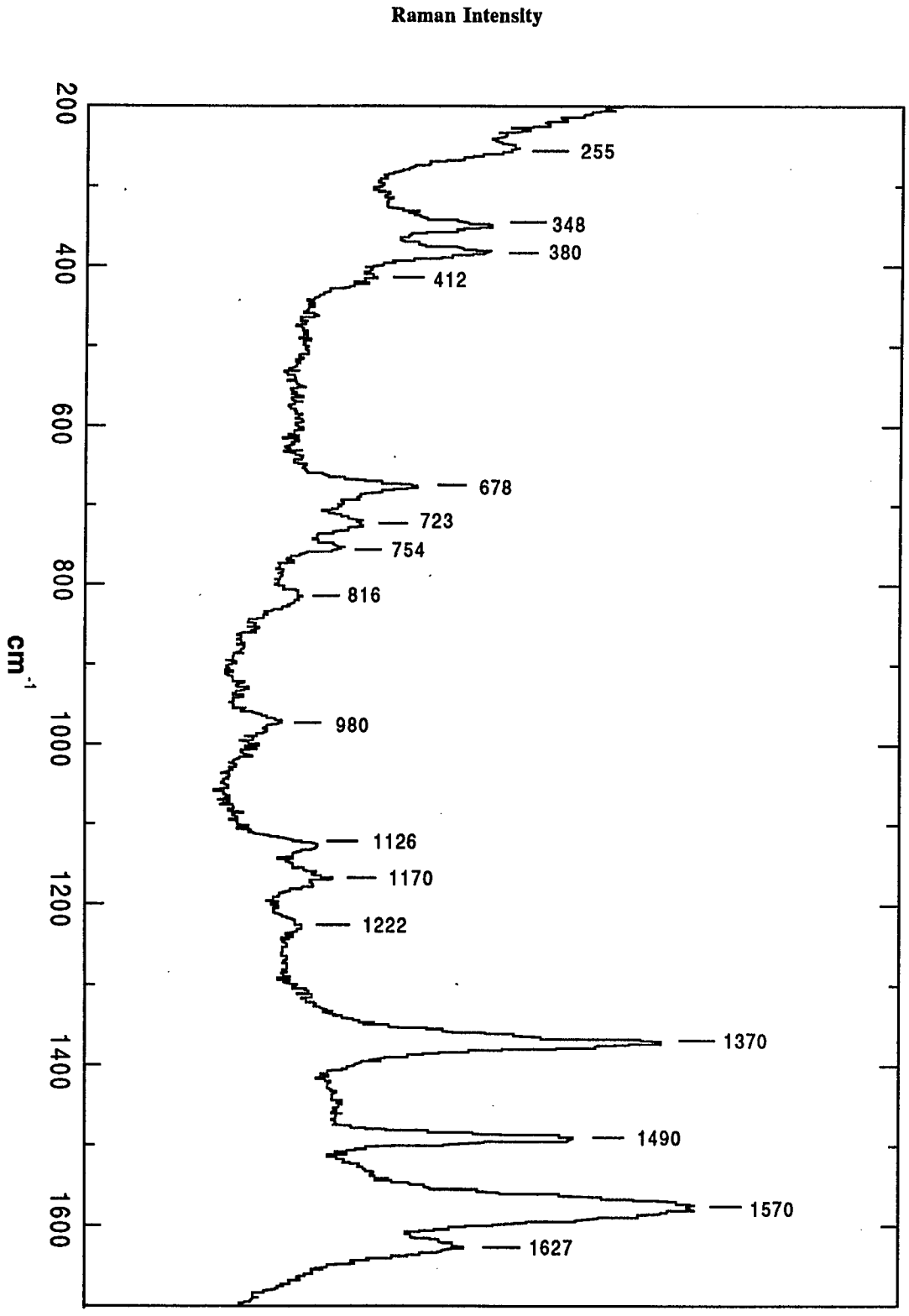
Raman Intensity
200
400
600
800
1000
1200
1400
1600
cm-1
255
348
380
412
678
723
754
816
980
1126
1170
1222
1370
1490
1570
1627

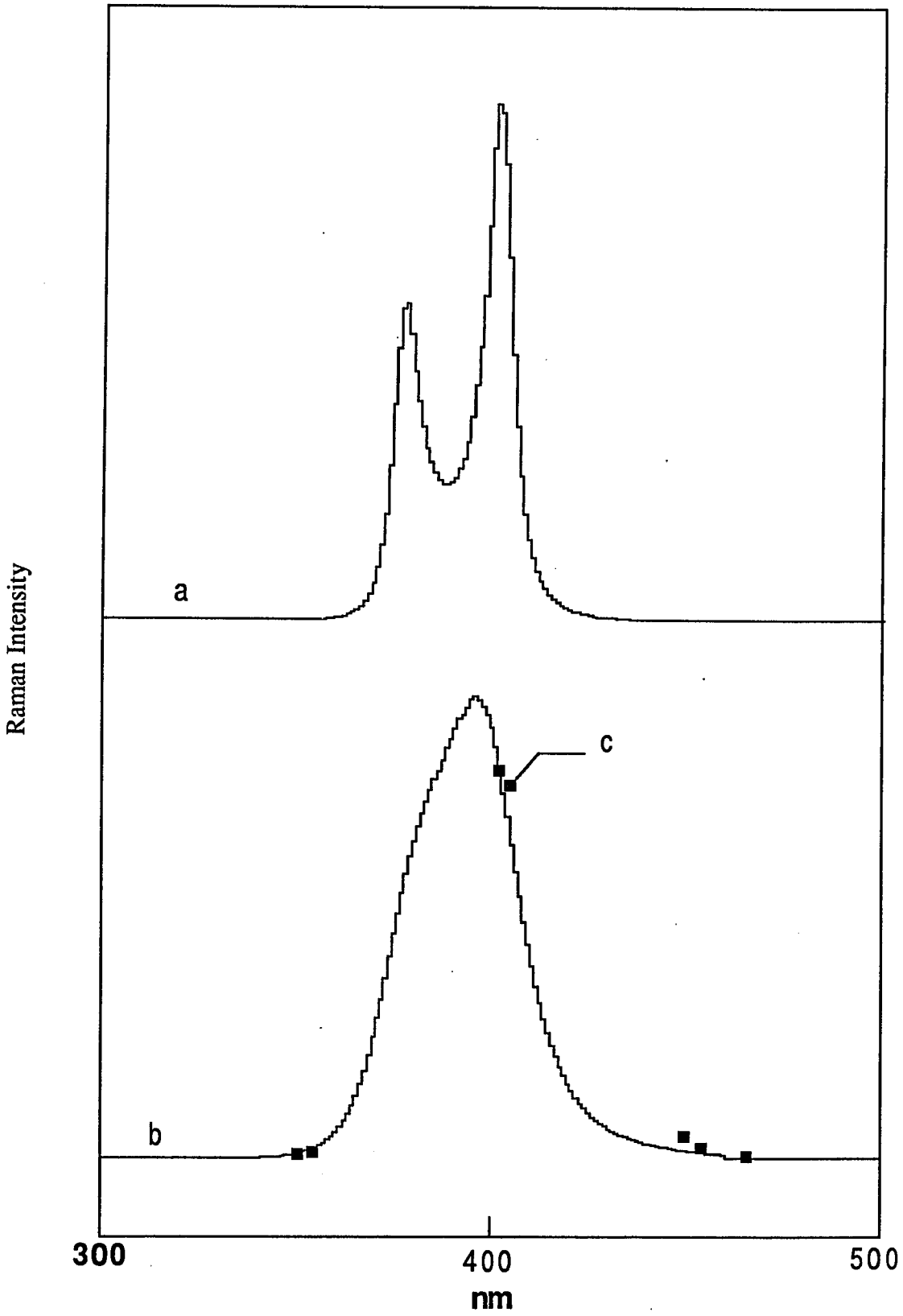
Raman Intensity
a
b
c
300
400
500
nm

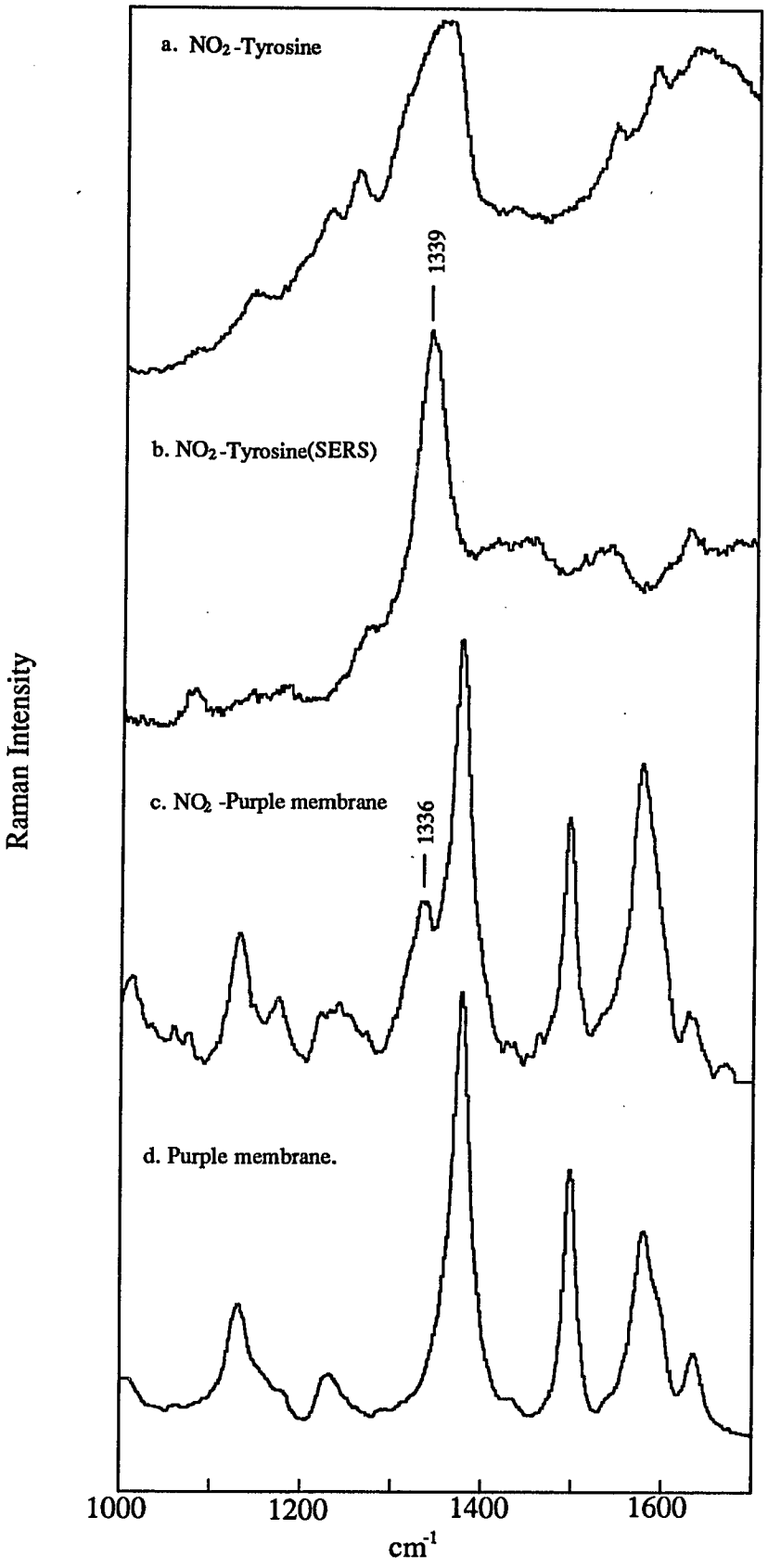
a. NO_2-Tyrosine
1339
b. NO_2-Tyrosine(SERS)
c. NO_2 -Purple membrane
1336
d. Purple membrane.
Raman Intensity
1000
1200
1400
1600
cm^{-1}

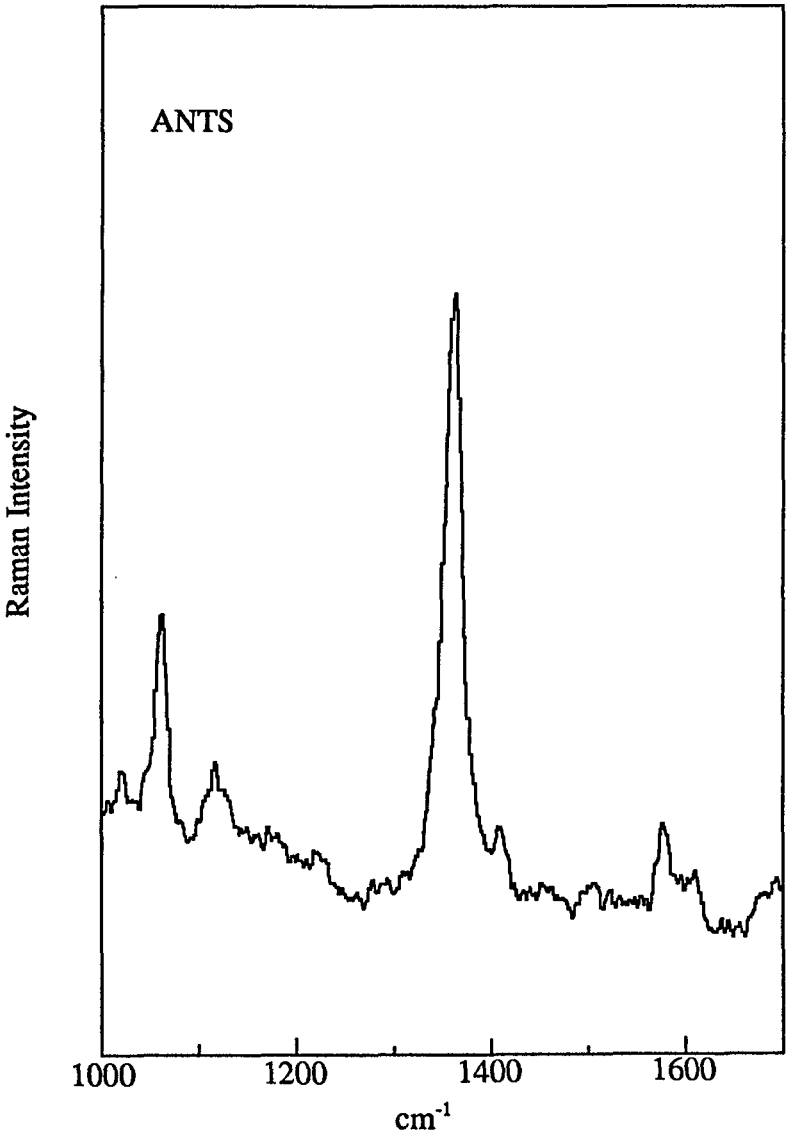
ANTS
Raman Intensity
1000
1200
1400
1600
cm-1

References

Adrian, F., *J. Chem. Phys., 77,* 5302 (1982).

Aravid, P., A. Nitzan and H. Metiu, *Surf. Sci., 110,* 189 (1981).

Argade, P. and K. Rothschild, *Biochemistry 22,* 3460 (1983).

Arya, K. and R. Zeyher, *Phys. Rev., B24,* 1852 (1981).

Aton, B., A. Doukas, R. Callender, B. Becher and T. Ebrey, *Biochem. 16* , 2955 (1977).

Aton, B., A. Doukas, D. Narva, R. Callender, U. Dinur and B. Honig. *Biophys. J. 29,* 79-94 (1980).

Bagley K., V. Balogh-Nair, A. Croteau, G. Dollinger, T. Ebrey, L. Eisenstein, M. Hong, K. Nakanishi and J. Vittitow. *Biochem. 24* , 6055-6071 (1985).

Balogh-Nair, V. and K. Nakanishi. *"New Comprehensive Biochemistry". C. Tamm ed. Vol3* Elsevier Biomedical Press, Amsterdam.

Becher, B. and Y. Cassim *Prep. Biochem. 5,* 161(1975).

Blasie, J. and C. worthington *J. Mol. Biol. 39,* 417(1969).

Blaurock, A and W. Stoeckenius. *Nature 233,* 152(1971).

Braiman, M and R. Mathies. *PNAS. USA.79,* 403-407 (1982).

Brown, P. *Nature 236,* 35(1972).

Busch, G., M. Applenbury, A. Lamola and P. Rentzepis. *PNAS USA 69,* 2802(1972).

Callender, R., A. Doukas, R. Crouch and K. Nakanisi. *Biochem. 15,* 1621-1629 (1976).

Callender, R. and B. Honig. (1977) *Ann.Rev. Biophys. Bioeng. 6,* 33-55.

Callender, R., A. Doukas, R. Crouch and K. Nakanisi. (1976) *Biochem. 15,* 1621-1629.

Chang, C.-H., J. G. Chen, R. Govindjee and T. Ebrey. (1985) *PNAS. USA. 82,* 396-400.

Chang, R. and T. Furtak, *Eds Surface Enhanced Raman Scattering,* Plenum Press, New York, 1982.

Chen, J. G., C.-H. Chang, R. Govindjee and T. Ebrey. (1984) *Biophys. J. 45,* 214a.

Cone, R. *Nature 236,* 39(1972).

Cookingham, R., and A. Lewis and A. Lemley. (1978) *Biochem. 17,* 4699-4711.

Cooper, A.. (1979) *Nature(London) 282,* 531-533.

Cormeli,C., A. Quinlanilha and L. Packer *PNAS 77* , 4707 (1980).

Curry, B., A. Broek, J. Lugtenburg and R. Mathies. *J. Am. Chem. Soc. 104* , 5274 (1982).

Curry, B., I. Pallings, A. Broek, J. Pardoen, J. Lugtenburg and R. Mathies. *Advances in Infrared and Raman Spectroscopy Vol12.* 1986.

Daemen, F. *Biochem. Biophys. Acta 300,* 255(1973).

Danon, A., and W, Stoeckenius. *PNAS USA 71,* 1234(1974).

Deng, H., C. Pande, R. Callender and T. Ebrey. (1985) *Photochem. Photobiol. 41,* 467-470.

Doukas, A. B. Aton, R. Callender and T. Ebrey. *Biochem.17,* 2430(1978).

Doukas, A., B. Aton, R. Callender and B. Honig, *Chem. Phys. Lett., 56,* 248 (1978).

Doukas, A., J. Pande, A. Pande, H. Suzuki, R. Callender, B. Honig and M. Ottolenghi.*Biophy. J. 33* , 275 (1981).

Druckmann,S., M. Ottolenghi, J. Pande and R. Callender. *Biochem. 21,* 4953 (1982).

Ebrey, T. (1982) *Methods Enzymol. 88,* 516-528.

Ebrey, T. 1982. Light Energy Transduction in *H. Halobium* In *membranes and Transport* (A. Martonosi, ed) Plenum press, New York, 323-330.

Ehrenberg, B., A. Lewis, J. Porta, J. Nagle and W. Stoeckenius. *PNAS 77* , 6571 (1980).

Ehrenberg, B., and Meiri *FEBS Lett 164* , 63 (1983).

Euler, J.. *J. Physik 137,* 318 (1954).

Eyring, G. and R. Mathies. *PNAS USA 76,* 33-37 (1979).

Eyring, G., B. Curry, R. Mathies, R. Fransen, I. Palings and J. Lugtenburg. *Biochem. 19*, 2410(1980).

Eyring, G., B. Curry, A. Broek, J. Lugtenburg and R. Mathies. (1982) *Biochem. 21*, 384-393.

Fischer, U. C., P. Towner and D. Oesterhelt. (1981) *Photochem. Photobiol. 33*, 529-537.

Fleischmann, M., P. Hendra and A. McQuillan. Chem. Phys. Lett. 26, 163(1974).

Frohlich *Elektronentheorie der Metalle.* Berlin: Springer (1936).

Gersten, J., R. Birke and J. Lombardi, *Phys. Rev. Lett., 43*, 147 (1979).

Gersten, J., *J. Chem. Phys., 72*, 5779 (1980).

Gersten, J. and A. Nitzan,*J. Chem. Phys., 73*, 3023 (1980).

Gersten, J., D. Weitz, T. Gramila and A. Genack, *Phys. Rev., B22*, 4562 (1980).

Gersten, J. and A. Nitzan, *Surf. Sci., 158*, 165 (1985).

Grocnendijk, G., W. Grip and F. Daemen, *Anal. Biochem., 99*, 304 (1979).

Gvindjee,K. Ohno and T. Ebrey. *Biophy. J. 38* , 85 (1982).

Herderson, R. *J. Mol. Biol. 93*, 123(1975).

Herderson, R. and P. Unwin. *Nature 257*, 28(1975).

Hilderbrandt, D. and M. Stockburger. *M. J. Phys. Chem. 88*, 5935 (1984).

Honig, B., A. Greenburg, U. Dinur and T. Ebrey. *Biochemistry 15* , 4953 (1976).

Honig, B., T. Ebrey, R. Callender, U. Dinur and M. Ottolenghi. (1979) *PNAS USA 76*, 2503-2508.

Hess, B., and D. Kuschmitz. *FEBS Lett. 100* , 334 (1979).

Hubbard, R. *J. Biol. Chem. 241*, 1814(1960).

Hubbard, R. and A. Kropf. *J. Gen. Physiol. 49*, 381(1965).

Johnson, P. B. and R. W. Christy. *Phys. Rev. B6*, 4370 (1972).

Kakitani, T.and H. Kakitani.(1975)*J. Phys. Soc. Jpn. 38*, 1455.

Kakitani, H., T. Kakitani, H. Rodman, B. Honig, and R. Callender. (1983) *J. of Phys. Chem. 87*, 3620-3628.

Kakitani, H., T. Kakitani, H. Rodman, and B. Honig. (1985) *Photochem. Photobiol. 41,* 471-479.

Kerker, M., D-S. Wang and H. Chew. *Appl. Opt. 19*, 4159(1980).

Kerker, M., O. Siiman and D-S. Wang, *J. Phys. Chem. 88*, 3168 (1984).

Khorana, H. G., G. Gerber, W. Herlihy, C. Grey, R. Anderegg, K. Nihei and K. Biemann *PNAS USA 76,* 5046(1979).

Kimura, Y., A. Ikegami and W. Stoeckenius. (1984) *Photochem. Photobiol. 40,* 641-646.

Kouyama, T., K. Kinosita and A. Ikegami. *J. MOl. Biol. 165*, 91(1983).

Kreibig, U. and C. Fragstein. *Z. Physik 224*, 307-323 (1969).

Laor, U. and G. Schatz, *Chem. Phys. Lett., 37,* 923 (1981).

Lemke, D. and D. Oesterhelt. *Biochemistry 115,* 595 (1981).

Lewis, A. R. Fager and E. Abrahamson. *J. Raman Spectr.* 1, 145(1973).

Lews, A., J. Spoonhower, R. Bogomolni, R. Lozier and W. Stoeckenius, *PNAS USA 71*, 4462(1974).

Li, Q., R. Govindjee and T. Ebrey *PNAS 81,* 7079 (1984).

Liver, N., A. Nitzan and J. Gersten, *Chem. Phys. Lett., 111,* 449 (1984).

Lombardi, J., R. Birke, L. Sanchez, I. Bernard and S. Sun, *Chem. Phys. Lett., 104,* 240 (1984).

Lopez-Garriga, J., S. Hanton, G. Babcock and J. Harrison. *JACS* 1986.

Lozier, R., R. Bogomolni and W. Stoeckenius. *Biophys. J. 15,* 955(1975).

Macomber, S., T. Furtak and T. Devine, *Surf. Sci.,* (Martonosi, ed) Plenum press, New York, 323-330.

Maeda, A., T. Iwasa and T. Yoshizawa. *J. Biochem. 82,* 1599(1977).

Maeda, A.,T. Iwasa and T. Yoshizawa .*Photochem. Photobiol. 33* , 559 (1981).

Massig, G., M. Stockburger and T. Alshuth. (1985) *Can. J. Chem. 63,* 2012-2017.

Mathies, R., A. R. Oseroff, T. B. Freedman and L. Stryer (1976) In *Turnable Lasers Applications, Ed.* T. Jaeger, P. Stokseth, A. Mooradian. New York:

Springer-Verlag(1976).

McCall, S., P. Platzman and P. Wolff. *Phys. Lett. 77A,* 381(1980).

Monger, T. R. Alfano and R. Callender. *Biophys. J. 27,* 427(1979).

Moskovits, M.,*Reviews of Modern Physics, 57,* 783 (1985).

Mowery, P. C., R. Lozier, Q. Chae, Y-W Tseng, Mary Taylor, and W. Stoeckenius. *Biochemistry 18,* 4100-4107 (1979).

Nakanishi and J. Vittitow. (1985) *Biochem. 24* , 6055-6071.

Narva, D. and R. Callender. (1980) *Photochem. and Photobiol. 32,* 273-276.

Oesterhelt, D. *Hoppe-Seyler's Z. Physiol. Chem. 353,* 1554(1972).

Oesterhelt, D. and W. Stoeckenius *Nature 233,* 149(1971).

Oseroff, A. R., and R. Callender. (1974) *Biochemistry 13,* 4243-4248.

Ohno, K., Y. Takeuchi and M. Yoshida. *Biochem. Biophys. Acta 462,* 575(1977).

Ovchinnikov, Y., N. Abdulaev, Y. Feigina, A. Kisilerand Lobanov. *FEBS Lett. 84,* 1(1977).

Ovchinnikov, Y., N. Abdulaev, Y. Feigina, A. Kisilerand Lobanov. *FEBS Lett. 97,* 15(1979).

Ovchinnikov, Y. *FEBS Lett. 148,* 179(1982).

Pande, C., R. Callender, C. -H. Chang and T. Ebrey. (1985) *Photochem. Photobiol. 42,* 545-548.

Pande, C., R. Callender, C. -H. Chang and T. Ebrey. (1986) In press

Pande, J., R. Callender and T. Ebrey. *PNAS 78,* 7379 (1981).

Papermaster, S., and J. Dreyer. (1974) *Biochem. 13,* 2438-2444.

Pauling, L. and E. Wilson Jr., *'Introduction to Quantum Mechanics'* McGraw-Hill, New York, (1935).

Person, W. B. and G. Zerbi Eds., 'Vibrational Intensities in Infrared and Raman Spectroscopy' Elsevier. Amsterdam. (1982).

Poo, M. and R. Cone. *Nature (London) '247,* 438(1974).

Rosenfeld, T., B. Honig, M. Ottolenghi, J. Hurley and T Ebrey.(1977) *Pure Appl. Chem. 49, 341.*

Rothschild, K., P. Argade, T. Earnest, K. Huang, E. londeon, M. Liao, H. Bayley, H. Khorana and J. Herzfeld. *J. Biol. Chem. 257*, 8592(1982).

Ruppin, R.,*Solid State Commun., 39*, 903 (1981).

Schulten, K. and P. Tovan. *Nature 278* , 85 (1978).

Seltzer, S. and R. Zuckermann. (1985) *J. Am. Chem. Soc. 107*, 5523-5525.

Sheves, M., T. Baasovand N. Friedman. *Biochem.* in press.

Siebert, Mantele and Gerwert. *Eur. J. Biochem. 136* , 119 (1983).

Siiman, O., L. Bumm, R. Callaghan, C. Blatchford and M. Kerker. *J. Phys. Chem. 87*, 1014 (1983).

Smith, S., J. Pardeon, P. Mulder, B. Curry, J. Lugtenburg and R. Mathies. *Biochem. 23* , 3141(1983).

Smith, S. O., A.Myers, J. Pardeon, C. Winkel, P. Mulder, J. Lutenburg and R. Mathies (1984) *PNAS. USA. 81*, 2055-2059.

Smith, S. O., A.Myers, R. Mathies, J. Pardeon, C. Winkel, E. Berg and J. Lutenburg (1985) *Biophys. J. 47*, 653-664.

Smith, S. O., and R. Mathies (1985) *Biophys. J. 47*, 251-254.

Sperling, W., P. Carl, C. Rafferty and N. Dencher. *Biophys. Struct. Mech. 3*, 79-94 (1977).

Stavenger, D. G. and J. Schwemer. *"Photoreception and Vision in Invertebrates" M. A. Ali ed.* Plenum Publishing Corporation, New York(1984).

Stockburger, M., W. Klusman, H. Gattermann, G. Massig and R. Peters. *Biochem. 18* , 4886 (1979).

Stoeckenius, W., R. Lozier and R. Bogomolni. *Biochem. Biophys. Acta 505*, 215 (1979).

Stoeckenius, W., and R. Bogomolni. (1982) *Ann. rev. biochem. 52*, 587-616.

Suzuki, T. and R. Callender (1981) *Biophys. J. 34*, 261-265.

Terner, J.,C. Hsieh, A. Burns and M. El-Sayed. *PNAS 76* , 3046 (1979).

Tavan, P., K. Schulten and D. Oesterhelt. *Biophy. J. 47*, 415-430, (1985).

Wald, G. *Science 162*, 230(1968).

Wang, D., H. Chew and M. Kerker. *Appl. Opt. 19*, 2256(1980).

Wang, D. and M. Kerker, *Phys. Rev., B24*, 1777 (1981).

Wang, D. and M. Kerker, *Phys. Rev., B25*, 2433 (1982).

Warshel, A., *Nature 260,* 679, (1976).

Warshel, A. *Ann. Rev.Biophys. Bioeng. 6* , 87 (1977).

Warshel, A. and P. Dauber, *J. Chem. Phys. 62*, 1074, (1977).

Wilson, E., J. Decius and P. Cross. *'Molecular Vibration'* McGraw-Hill New York. 1955.

Yoshizawa, T. and G. Wald. *Nature 197,* 1279, (1963).